No.

TR－A－0036

ゲシュタルト心理学の流れを汲む最近の視知覚研究

川津　茂生

Shigeo　Kawazu

1988. 11. 14

ＡＴＲ視聴覚機構研究所

CONTENTS

Introduction

このレポートは,現代の視知覚研究の中でゲシュタルト学派の伝統に関連したものを,いくつか紹介するために作成された. 全体の構成は,三つの章から成りたっている. 第一章では, Stephen Palmerと彼の協力者達の研究を,第二章ではE. Leeuwenbergによって始められたcoding theoryと,その応用研究を,そして第三章ではAnne Treismanと彼女の協力者達の研究を扱っている.

初めに,全体のあらましを述べておこう.Palmerはゲシュタルト学派の流れを汲む,アメリカのすぐれた研究者である. 彼の関心は,大別して二つに分類されるであろう. 一つは,ゲシュタルト学派に固有のpattern goodnessという概念に関するものであり,もう一つは,古典的なゲショタルト学派にはみられないが, Gestalt-like-effectと形容される, reference frame selectionに関するものである. Reference frameとは,たとえば,正三角形をみるときに,それが三つの可能な向きのうちの,どの向きを向いているように見えるかが視覚系で決定されるのであるが,その際に,基準とされる方向性をもった枠組みのことである. 正三角形が,一つぽつんと視野の中にあるとき,その枠組みは不安定であり,三つの可能な向きのいずれにもみえる[1].しかし,さまざまなcontextを与えると,枠組みの選択に偏りが生ずるのである.Palmerはcontextのreference frame selectionに与えるglobalな(あるいはholisticな)影響を調べたのである.

上に述べた, Palmerの二つの関心に共通しているのは,対称性へのこだわりであろう. 対称性は, pattern goodnessの理論では変換の上での不変性という側面から取り入れられ, reference frame selectionの理論では,contextによって現出するグローバルな線対称(reflectional symmetry)という面から取り入れられている. (しかし, Palmerが,最近の研究で,グローバルな対称性だけではreference frame selectionを説明し切れないとしている点を指摘しておこう. pp.18-20 参照)

対称性は, 自然界にも人工物においても無数に存在している. そのこと

からしても，対称性がパターン認知において持つ意義の重要性を推し量ることができる．しかし，Palmerのreference frame selectionにおける対称性の理論が必ずしも成功しているとは言い切れないように，対称性の知覚の研究は，まだまだ緒に就いたばかりなのである．そのこととは別に，Palmerがゲシュタルト的現象としてreference frame selectionに注目していることは重要である．工学的には，正三角形がどちらを向いているか，などということは，むしろ捨象されるべき余分な情報ではないであろうか．その余分な情報が，人間の知覚においては基本的な情報の一つなのである．

Coding theory (あるいは，structural information theory)はLeeuwenberg(1967)によって提唱された．Coding theoryの基本は，図形を要素の羅列としてとらえ，さらにその要素をシンボルで置き換えた上で，その図形をシンボルの列，すなわちcode，で表現するところにある．Coding theoryには"syntactic rules"も具わっている．Syntactic rulesは，上に述べた方法で得られたcode (primitive code)を，それが持っているさまざまなredundancy(たとえば対称性)を利用して，短縮することにより，与えられた図形の簡略化されたcode (end code)を作ることに用いられる．そして，その簡略化されたend codeの持っているシンボルの数とsyntacticな要素の数の和を，図形の複雑さ，あるいは情報量(information load)，とするのである．Coding theoryは，与えられた図形の解釈が二つ以上ありうる場合，上に述べたような方法でそれらの解釈の複雑さを計算し，より単純な解釈が視覚系によって選択されるであろうと予測する．このように，Coding theoryの特徴は，ゲシュタルト学派の提唱した単純さや対称性の概念を，codeとsyntaxを用いて情報理論化し，数量化した点にある．この数量化という点にだけ注目すれば，Garner (1974)の理論の一部分(R & R subset size)と共通しているともいえる．しかし，coding theoryが最も成功しているのは，上に述べたような図形における応用よりも，Restle(1979)の運動知覚への応用であろう(pp.28-35参照)．

Coding theoryは情報理論化，数量化という点で，ある程度の型式性を持っている．しかし，実際にprimitive codeを作ったり，syntactic rulesを用い

てend codeを作ったりする際には，研究者の主観がかなり入り込むのである．したがって，coding theoryが工学的に応用されるためには，まず理論の完ぺきな型式化がなされねばならないであろう．

Palmerの立場とcoding theoryの立場は，それぞれ全く違った仕方ではあるが，ゲシュタルト学派の伝統の側に立っている．これに反して，Treismanの立場はゲシュタルト学派の伝統と対立している．ゲシュタルト学派が，形態の知覚は全体的(holistic)だとするのに対して，Treismanは，対象の知覚処理過程は，その初期の段階では分析的(analytic)である，とするのである．Treismanのfeature integration theoryは，知覚処理過程の前注意的(preattentive)段階では，対象の持つさまざまな特徴がそれぞれ独立に並行して処理され，その後，対象の位置にattentionを注ぐことによって，それらの特徴が統合されると主張する．この理論は，彼女が行なったさまざまなパラダイムを用いた実験によってconverging evidenceが提出されているので，かなりの説得力を持つ．

それらのパラダイムの中で，最近Treismanが最も頻繁に用いているのが，いわゆるsearch paradigmである．Search paradigmでは，被験者が複数のdistractorの中に隠れているtargetをできる限り早く捜し，その反応時間を計るのである．Search paradigmを用いたfeature integration theoryの実験では，targetがdistractorと単一の特徴において異なるとき(たとえば，targetが赤かOで，distractorが青いT)，targetはdistractorの数にほとんど影響されずに"飛び出し(pop out)"てくるのに，targetが二つの特徴の結合としてしか定義され得ないとき(たとえば，targetが赤いOで，distractorが赤いTや青いO)は，searchがserialになって，反応時間がdistractorの数のほぼlinearな関数になるのであった．Search paradigmを用いた最近の研究(Treisman & Souther,1985; Treisman & Gormican, 1988)は，search asymmetryという特異な現象を発見している．Search asymmetryとは，二つの異なる図形が，targetとdistractorの役割を交代すると，searchの早さが変わるということである．Treismanと

Gormican(1988)は,さまざまな組の図形でsearch asymmetryが生じることを示している.

Search asymmetryは,工学的見地からは一見無用の長物と映ずるかもしれない. Targetとdistractorが役割を交代するだけで,searchの早さが変わるような工学的メカニズムは,不必要な複雑さを取り込んだものと考えられるであろう.しかし,TreismanとGormican(1988)は,pooled response modelというきわめて単純なモデルとWeberの法則という人間の知覚にとって基本的な法則を組み合わせた,非常に単純な理論でsearch asymmetryを説明しているのである(pp.46-47; 51-52). 一見不必要に見えるsearch asymmetryという知覚特性が単純な理論で説明され得るということは,パターン認知の研究に携わる工学者にも重要な示唆を与えるのではないであろうか.

Treismanの立場に関して注意すべき点は,彼女がゲシュタルト学派の伝統と対立しているとはいえ,初期視覚処理過程におけるholistic processingを完全に否定しているのではないということである.たとえば,texture segregationでfigureとgroundが一つの属性でのみ異なっているとき(たとえば,figureが赤で,groundが緑とか,figureが○で,groundがT),そのsegregationはholisticであると,Treismanは認めるであろう.しかし,このような文脈でholisticという語を用いると,"holistic"の意味が,"holistic"が"analytic"と対比されたときの意味とずれてきてしまうのである.そこでTreismanは,上のような場合でもholisticという語の使用はなるべく避け(その代わりにparallel processingという表現を用いる),自分の立場はanalyticだと主張するのである.

現代の認知心理学の特徴の一つは,研究者の思想的背景が分かり易いということではないだろうか. Palmerがゲシュタルト学派の影響を受けているのは容易に分かるし,coding theoryがゲシュタルト学派と思想としての情報理論に影響されているのも明白である.そして,Treismanのfeature integration theoryも,明確な科学的仮設であると同時に,強い思想的立場の表明であると見ることはできないであろうか.どの科学にも思想的背景

はあるであろう. とくに, 科学の発達段階の初期において, それは顕著に現われる. しかし, 認知心理学において思想性が顕らかなのは, 認知心理学が, いまだその揺らん期にあるということだけでなく, それが心の科学であるという, この科学特有の事情にもよるのではないであろうか.

最後に, このレポートに関する注意事項を述べておこう. このレポートの本文の大半は, 原論文から直接取られたものである. これは, このレポートの目的が, それらの論文をできるだけ忠実に読者に伝えるところにあるからである. (ただし, coding theoryの序に当たる部分は, 分かり易くするために筆者が大幅に手を加えた.) 読者は原論文を読む労力の数分の一で, その論文の内容の大筋をつかむことができるであろう. しかし, 原論文を短縮したのであるから, 筆者の独断で割愛したところも多い. したがって, もしある論文に強い関心をもつならば, 原論文を直接手にとって読まれるのがよいと思う. このことは, 特に最後に掲載した論文, Treisman & Gormican (1988), についていえる. この論文は非常にち密に書かれていて, 数多くの重要な議論を展開しているが, このレポートはそれらの議論の中で最も基本的なものをいくつか取り上げただけである.

本文中の図(Figure)の番号は, 図の左下に手書きで添えたものに照合している. 表(Table)の番号は, 表の左上にやはり手書きで記されている.

注1. これは, gravitational frameとretinal frameを度外視すればということである.

I. Palmer and his associates

Measures of figural goodness

Palmer, S. E. (1983). On goodness, Gestalt, groups, and Garner. Paper presented at annual meeting of Psychonomic Society, Sandiego, California.

Gestalt psychologists claimed that figural goodness is the determinant of perceptual segregation. They suggested that qualitative aspects of a figure such as good continuation and symmetry are the factors of figural goodness. However, they did not provide the precise measure of figural goodness.

Garner(1974) suggested such a precise measure of figural goodness which is called the R & R subset size. He proposed that figural goodness is the decreasing function of the R & R subset size (i.e., the number of different patterns produced by rotating and reflecting a given pattern about the vertical, horizontal, and two diagonal axes).

Palmer (1983) proposed another measure of figural goodness based on the mathematical concept of symmetry subgroups. In mathematics, the transformations over which an object is invariant is called its symmetry subgroup(Weyl, 1952). Palmer focused on the group of transformations over which the figure is invariant rather than focussing on the figures generated by the group of transformations (the latter is the case of R & R subset).

The size of symmetry subgroups is isomorphic to the size of the R & R subset. However, there is an advantage of symmetry subgroup over R & R subset; that is, it is possible to compare symmetry subgroups across figures for the *identity* of their elements in addition to the number of their elements. So, the question is, Does it help to know the identities of the transformations to predict subjective figural goodness? Palmer found that it does. There were many significant differences between classes of figures whose subset sizes are the same , but whose symmetry subgroups contain different transformations. For example, figures with vertical symmetry were rated "better" than ones with horizontal symmetry, and both of these were rated "better" than figures with diagonal symmetry or figures with 180° rotational symmetry (Figure 1).

Palmer mentions another problem with the R & R subset analysis: All figures with no symmetries are predicted to be equally "bad", even though some seem to contain a great deal more structure than others. The problem here is that only global symmetries were considered in the R & R subset analysis. Palmer argues that local symmetries within the figure should be taken into account also. In an *experiment* he probed different positions within figures for the goodness of their relationship to the figure to see

whether local symmetry structure would emerge from the subjects' ratings. For example, a rectangle has two axes of global symmetry plus four prominent axes of local symmetry along the bisectors of its angles (Figure 2). 35 stimuli, each containing a single small circle representing for a position within the rectangle were prepared. Subjects rated each one for the "goodness" of the relation between the circle and the rectangle; that is to rate how well the circle "fit" into the context provided by the outer figure. The *results* (Figure 3) showed that the highest rating was given to the center where the two global symmetries coincide. The next highest was the vertical axis followed by the horizontal axis. Of particular interest was that the ratings were also elevated along the local symmetries on the angle bisecters. Similar results were found for other figures like trapezoid. A further study showed that the Ss were not mistaking the figures diagonal with the angle's bisectors.

Global vs. Local Processing of Ambiguous Triangles

Palmer, S, E. (1980). What makes triangles point: Local and global effects in configurations of ambiguous triangles. *Cognitive Psychology, 12,* 285-305.

Palmer(1980) examined how global and local aspects of different configurations affect the perceived pointing of equilateral triangles.

A basic tenet of Gestalt theories of perception is that the perception of a whole is different from the sum of its perceptual parts(Koffka,1935; Wertheimer,1923). A natural corollary is that a given stimulus may be perceived differently when it is seen as part of some larger configuration than when it is seen as a whole figure and that it may be perceived differently in different configurations.

Two hypotheses can explain such configural effects. One hypothesis is the global-to-local hypothesis which says that the whole form is analyzed first and that its holistic perceptual characteristics then affect the later analysis of its parts. This hypothesis is closest in spirit to the Gestalt view. The other is the local-to-global hypothesis which claims that elements are perceived first and are used to construct larger wholes. Of course, if the perception of parts were completely determined locally, such theories could not account for configural effects at all. However, if the parts are locally ambiguous, then the relationship between parts might lead to interactions that "feed back" to local levels, thus causing different perceptions that depend on aspects of the configuration. This view is consistent with many current views (e.g., Selfridge & Neisser, 1960; Rumelhart & Siple, 1974). These two hypotheses are not mutually exclusive in that both local-to-global and global-to-local effects might occur

simultaneously.

The "ambiguous triangles" phenomenon was discovered by Attneave(1968). Equilateral triangles are "multistable" with respect to perceived orientation. There are three possible orientations, but only one of them is perceived at a time (Figure 4A). When many such triangles are placed in a randomly constructed group, people tend to see them as a homogeneous field of identical triangles all pointing in the same direction ("consistency effect," Figure 4B). When several triangles are arranged so that their axes of symmetry are colinear, the component triangles seem to point in the direction that coincides with their aligned axes, and when several triangles are arranged so that their sides are colinear, they seem to point in the direction perpendicular to their aligned sides ("bias effects," Figure 4C & Figure 4D).

Three experiments were performed, which examined the perceived pointing of triangles under various conditions that manipulated the local and global characteristics of stimulus configurations

In *Experiment 1* the axis- and base-aligned configurations are contrasted with single ambiguous triangles. Directional biases are investigated by combining the configural conditions orthogonally with 12, equally spaced directions (Figure 5, columns). To contrast the local-to-global and global-to-local hypotheses a third configural condition, the "combined" condition, where both axis-aligned and base-aligned triangles flank the central triangle (Figure 5, row 4), was added. In the "combined" condition, configurations have a more circular form, instead of a strongly oriented global line. Thus, the global-to-local hypothesis predicts a substantially reduced bias effect for the combined condition relative to the axis-aligned and base-aligned condition alone. The local-to-global hypothesis makes the opposite prediction. The combined effect should provide more configural facilitation for the biased direction than either axis or base alignment alone, since there are more local elements for biasing in the combined condition than in the axis- and base-aligned conditions

Results were presented in the form of the overall probabilities of choosing the biased directions (Figure 6). Clearly there were systematic nonconfigurational biases due to directional preferences(upward, rightward, downward, leftward directions). Vertical directions showed stronger biases than horizontal directions. Upward directions were chosen more often than downward directions. Configural biases are reflected in Figure 6 by the fact that all three configural curves lie above that for the single triangle condition. Note that the combined configuration curve lie consistently below both the axis- and base-aligned curves, the latter two being at essentially the same level, providing support for the global-to-local hypothesis in that the "combined"configuration produces a

smaller bias than either of axis- or base-aligned configuration.

Experiment 2 provides a different test of the global-to-local and local-to-global hypotheses. If the configurational effects found in Experiment 1 are purely the result of global orientation characteristics, then it should not matter what the elements of that configuration are. However, if the configural effects are due, at least in part, to local orientational characteristics of local parts, then changing the shape of the contextual elements should influence perceived direction of pointing. contextual elements used were triangles, circles, and squares (Figure 7). Circles are inherently orientationless: from the local-to-global viewpoint, they should not exert much biases. Triangles and squares have definite intrinsic orientational characteristics, and should affect more strongly. Squares should have the strongest influence because their intrinsic reference frames (when seen as squares) are compatible with only one of the three possible orientations of the triangle.

Results: Probabilities of making the biased responses are shown in Figure 8 for the three types of global configurations and the three shapes of contextual elements. The directional biases are consistent with those found in Experiment1. The fact that element shape produce significant differences in the magnitude of bias supports the local-to-global prediction. The ordering of element conditions is as expected , circles being least effective and squares being most effective.

Global orientational characteristics are also important; The superiority of axis alignment and base alignment over their combination was replicated. The fact that significant biases were found for axis and base alignment using circles as contextual elements is particularly convincing. If circles are properly considered locally orientationless such effects are more easily reconciled with global than local mechanisms.

There are indications that local factors may be more important in the "combined" condition than in the axis- and base-aligned conditions. First, the only condition that did not produce a significant bias effect was the circle-combined configuration. Second, the square elements produced a significantly larger bias than the triangular elements only in the combined condition.

In *Experiment 3* stimuli were constructed such that their global orientational characteristics are independent of their local orientational characteristics (Figure 9). For the conditions in which the local and global biases were consistent (the diagonal stimuli in Figure 9), responses were scored as either consistent with the expected bias or inconsistent with it. For the conditions in which local and global biases conflicted (the off-diagonal stimuli in Figure 9), responses were classified as consistent with the global bias, consistent with the local bias, or neither (the unbiased response).

Results: Generally a much stronger bias was observed when global and local biases are consistent than when they conflict. It is also true that only globally or locally biased responses (to off- diagonal stimuli) are generally more probable than the unbiased response. The results indicate both local and global biases operate in the linear arrays of the axis- and base-aligned conditions. In the "combined" condition there is a very strong local bias but no global bias relative to the alternative, unbiased condition (Figure 10).

General discussion and conclusion. All the results of the three experiments are consistent with the hypothesis that perceived pointing depends on perceptual reference frame at a number of different levels of globality: the entire perceptual field, the whole configuration, and the elements of the configuration.

Palmer's conclusion was two-fold. First, global levels affect more local levels. This accounts for the effects of orientation per se and configural conditions. Second, different processes within a given level interact with each other locally. This accounts for the effects of elements. Whether local levels are capable of affecting more global levels is an open question at this point.

Configural effects

Palmer, S, E. & Bucher, N, M. (1981). Configural effects in perceived pointing of ambiguous triangles. *Journal of Experimental Psychology: Human Perception and Performance, 7*, 88-114.

Palmer & Bucher (1981) replicates and extends the earlier results on the perceived pointing of ambiguous triangles (Attneave,1968; Palmer, 1980) using a different methodology. The previous studies used a self-report procedure in a free response paradigm to measure biases in perceived pointing. Such data are open to the objection that they do not necessarily reflect obligatory perceptual processing. That is, subjects see the figures for long enough that certain mechanisms that might not otherwise come into play could influence the final response. It can be argued that the biasing effects found in such a situation might disappear if processing were terminated as soon as the minimum amount of information required for the response were available and if configural (global-to-local) processing were optional rather than obligatory.

In this article Palmer & Bucher report results from a different paradigm based on perceptual interference. The underlying idea is that if configural effects result from obligatory mechanisms, then biasing directions that conflict with a required directional response will interfere with that response, thereby slowing down *response latencies*, and biasing

directions that are consistent with it will facilitate the response, relative to a neutral control condition. However, if configural effects arise from optional processes, responses will not be affected by such configural biasing conditions.

In *Experiment 1* each triangle was "correctly" seen as pointing up, down, right, or left. Both axis- and base-aligned conditions were used (Figure 11). Both conditions included stimuli in which the relative bias was 0° (configural bias being consistent with the response), -120° (configural bias being 120° counterclockwise from the required response) and 120° (configural bias being 120° clockwise from the required response).

Results: There are systematic variations in response time as a function of direction of the required response: Up and down produce substantially faster responses than right and left averaged over all configural conditions (Figure 12).

When the configural bias conflicts with the required response (the -120 and +120 conditions), latencies are much slower than in the single triangle control condition. This is true for both axis alignment and base alignment. Thus, the present results are qualitatively consistent with the results of previous experiments using the free response procedure. From this Palmer & Bucher (1981) conclude that the configural effects found previously by Palmer(1980), as well as those in the present experiment are not the result of optional processing strategies. They reflect an obligatory mode of perceptual processing that cannot be bypassed, even if such global, configural information is known to be irrelevant to the task at hand.

Experiment 2 examined the effects of varying the number of colinear triangles in the configuration:1, 2, 3, 5, and 7 triangles were aligned so that their axes or bases were colinear (Figure 13).

Results: For the inconsistent conditions, each successive increase in the number of triangles produced a significant increase in reaction time except the increase from 5 to 7 triangles. In contrast, there were no corresponding effects (either interfering or facilitating) for the consistent relative bias conditions(Figure 14).

In *Experiment 3* spacing effects were studied by varying the distance between homologous points of the triangles while keeping the number of triangles constant at three(Figure 15).

Results: As the distance between the triangles increases, the amount of interference in inconsistent conditions decreases dramatically. Still, there is good evidence of interference effects until the triangles are displaced by more than three times the length of their sides(Figure 16). This is about the same point at which additional triangles had negligible effects in Experiment 2. Thus, it provides converging evidence that configural interactions take place within fairly restricted spatial regions.

Experiment 4 examines whether absolute or relative spatial extent is

the important variable by simultaneously varying the size of and spacing between triangles in a configural line (Figure 17). Intertriangle displacement was varied from 0.5 to 2.0 times the length of a triangle side in increments of 0.5 (i.e., the spacing variable was defined relative to the size of the triangle). The two sizes of triangles were chosen so that the larger ones were twice the scalar size of the smaller ones. This ensures that the absolute displacements of large triangles in the 0.5 and 1.0 spacing conditions are the same as those of small triangles in the 1.0 and 2.0 spacing conditions.

The major question of interest concerns whether the results are more simply explained by relative or absolute spacing. The answer should be found in the interaction between spacing and size. If the function that relates reaction time to spacing is well described in terms of relative distance, then the curves for large and small triangles should be parallel when plotted as a function of relative spacing. They should not be parallel as function of absolute spacing, however, because the scale of the curve for the larger triangles will be twice that for the small triangles. The reverse should be true if the function is based on absolute distances: The curves will be parallel as a function of absolute spacing, but not as a function of relative spacing. Since a significant interaction indicates the presence of reliable nonparallelism, the interaction between spacing and size is the most appropriate test for deciding between the relative and absolute spacing hypotheses.

Results: The predictions of the relative spacing hypothesis are confirmed except for the existence of one anomalous data point(Figure 18).

Experiment 5 was undertaken to examine both spacing and number of aligned triangles simultaneously. The main issues are whether these two factors are independent or not and whether they interact with the same other factors. Spacing and number of triangles were combined orthogonally by placing three or five triangles in a linear configuration at a displacement of either 1 or 2 times the length of a side.

In addition to axis and base alignment, the present experiment investigates the "combined" configuration: the pattern formed by superimposing the axis- and base-aligned patterns at their central triangles (Figure 19). As more triangles are added to the combined condition, it becomes distinctly "pluslike" with strong orientational properties. We were interested in the possibility that this extended version of the combined pattern would show greater bias effects than either axis or base alignment, even though the smaller version does not.

Results (Figure 20): Response time shows reliable increases due to more triangles and less space between them. Both of these factors interacted with bias. Despite the fact that number and spacing each interacted with bias, they did not interact with each other. Thus, the

additional interference accrued by five triangles rather than three was about the same regardless of the spacing of those triangles (and vice versa).

The interference effect with three triangles was greater for axis and base alignment than for the combined condition. This result replicates Palmer's(1980) previous findings using the current experimental methods. With five triangles, however, there was substantially more interference for the combined condition than for axis and base alignment. This latter finding confirms the intuitive hypothesis that additional triangles strengthen the orientational properties of the combined configuration far more than they do the orientational properties of a linear configuration.

General discussion: Palmer & Bucher(1981) present a speculative theory accounting for the results following the tradition of Hebb's (1949) work in attempting to explain perceptual organization in terms of neural networks (cell assemblies). The theory is rather similar conceptually to the recent PDP approach to perception.

Textural effects

Palmer, S, E. & Bucher, N, M. (1982). Textural effects in perceived pointing of ambiguous triangles. *Journal of Experimental Psychology: Human Perception and Performance, 8*, 693-708.

A useful strategy for studying the Gestalt effects of perceived pointing of ambiguous triangles is to examine factors other than configural alignment that produce the same sort of bias effects; for example, the orientation of contextual figures surrounding a triangle (see Figures 21D and 21E)

Palmer & Bucher (1982) reports the biasing effects of another factor: textural striping which is quite different from other factors known to induce biases in that it is a more local factor, at least in the sense that it is spatially restricted to the inside of a single triangle. "Textural striping" refers to a regularly spaced, alternating pattern of black and white bars of equal width within a well-defined region of the visual field.

In all of these experiments, we employ the interference method (Palmer & Bucher,1981). Subjects are asked to perceive just one of the three possible pointings for each triangle. For example, they would be required to see the triangles in Figure 21 point directly left(9 o'clock) rather than obliquely (1 or 5 o'clock). We measure the time they take to achieve this designated percept by requiring subjects to make a directional response as soon as they can determine whether the triangle is a "left-pointing" or "right-pointing" one. The rationale for this measure is that if the biasing factor (in this case, textural stripes) affects perceived

pointing, then subjects should take more time to see the triangles point in the designated direction when they are biased away from that direction than when they are biased toward it.

Experiment 1: There were four orientations of triangles for which the correct responses were "up," "down," "left," and "right." This factor was orthogonally combined with the type of bias (stripes parallel to a symmetry axis or stripes parallel to a base) and the interference condition (consistent or inconsistent with the required response). Also present in the stimulus set were neutral, plain triangles in each orientation.

Each triangle subtended about 0.9° of visual angle. The frequency of the stripes was 5.0 cycles per triangle side (Figure 22).

The *results* (Figure 23) showed significant effects due to bias condition, direction and the interaction of these two factors. Responses were much slower to inconsistent trials than to either consistent or plain trials. No difference was found between the consistent and plain trials. Thus, the effect of the textural stripes was almost exclusively to interfere with responses when they biased pointing away from the correct direction; there was no corresponding facilitation when the stripes biased pointing toward the correct direction. Responses to vertical directions are faster than those to horizontal directions. The fact that longer RTs are associated with higher error rates rules out the possibility that speed-accuracy trade-offs are responsible for the obtained RT results.

Experiment 2: It seems likely that bias strength will increases as stripe width increases (i.e., as the fundamental spatial frequency of the square-wave texture decreases). Palmer & Bucher suggest this on the grounds that the perceptual system responds more quickly to lower than higher spatial frequencies (Breitmeyer, 1975).

Four frequencies in octave steps(f, 2f, 4f, and 8f)were used. This results in 2.5, 5.0, 10.0, and20.0 cycles of stripe per triangle (Figure 24).

The only other major change in the design from that in Experiment1 was that the up and down response alternatives were eliminated, leaving just the left- and right-pointing triangles.

Results: (Figure 25) Reliable effects in RTs due to frequency, bias, and the interaction of these two factors: Inconsistent biases produced longer RTs than consistent biases for the two lower spatial frequencies, but not for the two higher frequencies. Reaction times to the inconsistent conditions decreased significantly from 2.5 to 5.0 cycles per side, and again from 5.0 to 10.0, but not from 10.0 to 20.0 cycles per side. The fact that lower frequencies tend to be processed before higher ones (Breitmeyer, 1975) may explain why the textural bias effect diminishes with frequency.

There were significantly more errors in the lowest frequency condition compared to the next higher frequency, whereas the higher frequencies did

not differ from each other

Experiment 3: The results of the previous experiment show that interference decreases as textural frequency increases. Is this effect due to the absolute spatial frequency of the stripes (in cycles per degree of visual angle) or to the frequency of the stripes relative to the size of the stimulus pattern?

If relative frequency is the critical variable, there should be a main effect of the size and a main effect of relative frequency, but no interaction between them. If absolute frequency is the critical variable, then triangle size and relative frequency should interact.

The smaller triangle subtended about 0.5°, whereas the larger triangle subtended about 0.9°. The stripe frequencies used in the smaller triangle were 5.0, 10.1, and 20.2 cycles per degree (2.5, 5.0, and 10.0 cycles per side, respectively), whereas in the larger triangle they were 2.7, 5.5, and10.9 cycles per degree (also 2.5, 5.0, and 10.0 cycles per side, respectively).

Results: Reaction times are slightly, but reliably slower to the small triangles than to the larger ones. However, the size effect does not interact with frequency, bias, or their interaction. Size simply reduces overall RTs by about 10 ms (Figure 26). Therefore, Palmer and Bucher conclude that the frequency effect is a relative one, depending on how the textural frequency relates to the size of the pattern containing it.

Experiment 4: (figure versus ground) What would happen if the stripes were outside the triangle on the perceptual ground? This question is theoretically interesting because it concerns the temporal relationship between figure/ground segregation processes and the textural biasing process. If figure/ground segregation is complete before the bias effect occurs, then one would expect the orientation of the ground texture not to produce any bias. However, if figure/ground segregation is not yet begun or is only partially complete when the textural bias process operates, one would expect the orientation of the ground texture to influence figural interpretation and to produce the same pattern of results found for figural texture.

An example of the ground texture condition is shown in the upper left portion of Figure 27.

Results: The only main effect is due to bias. Texture within a figure seems to be slightly more potent in affecting perceived pointing than the same texture outside it. This suggests that figure/ground segregation is either not complete by the time that the textural effect occurs or not totally effective in filtering out the ground. If it were both complete and effective, there should have been no textural effect for the ground condition at all.

Experiment 5: Do the stripes in the ground in close proximity to the

triangle have a disproportionately large influence on perceived pointing of the figural triangle? If so, the textural effect in the ground should largely or completely disappear when a relatively small region around the triangle is cleared of stripes. Therefore, Palmer & Bucher replaced the ground stripes with a homogeneous gray background within circular regions of different radii to see whether and at what point the effect would disappear (Figure 27).

Results: (Figure 28) When the texture touches the edge of the triangle, there is a large interference effect. When the textural stripes are cleared to a distance just beyond its vertices, significant interference is still present. However, beyond this point there is only weak evidence of textural interference. Clearly the magnitude of the effect diminishes as the distance increases from the edge of the figure to the edge of the textural stripes. These results are consistent with the hypothesis that the biasing processes are fairly local and centered on the region containing the attended figure.

General discussion: Many aspects of the biasing effects due to stripes are nearly identical to those found previously with linear configurations of triangles (Palmer, 1980; Palmer & Bucher, 1981). First and foremost, in both cases the directions of bias are parallel and perpendicular to the orientation of the inducing factor. Second, in both cases the parallel and perpendicular effects are about equal in magnitude. Third, both biases seem to appear almost exclusively as interference effects. There is only weak evidence for facilitation from consistent configural conditions (Palmer & Bucher,1981, Experiment 1) and no evidence for facilitation from consistent textural stripes in the present series. Fourth, both stripes and configural lines produce the same interaction with direction: Interference is greater for horizontal(left and right) than vertical (up and down) directions. Finally, interference is greatest when the biasing elements are closest to the triangle and decreases rapidly with increasing distance.

These parallels in the results suggest that the same mechanisms underlie configural and textural effects.

The *symmetry* properties of both textural and configural displays can explain the direction of bias without appealing to any mediating structure or process. If perceived pointing of ambiguous triangles is somehow biases toward directions that coincide with a global axis of symmetry, then symmetry can account equally well for both axis- and base-aligned textural biases(the parallel and perpendicular biases). Moreover, one would expect them to be about equal in magnitude.

Another reason to prefer the symmetry hypothesis is that it suggests an explanation for why facilitation effects are conspicuously absent: Consistent stimuli are no more symmetrical about the required direction than control stimuli. That is, the unbiased control stimulus, a single

unstriped triangle, has an axis of global bilateral symmetry aligned with the required direction of pointing just as the "consistent" stimuli do. Only the "inconsistent" stimuli lack global symmetry along the relevant directions.

The pattern structure that influences perceived pointing of ambiguous triangles is most effective for low resolution features of spatial structure relative to the individual triangle. This suggests a general bias toward global processing, at least for the sizes of patterns used in these experiments. This result is generally consistent with several recent suggestions that low resolution information is processed before higher resolution information(e.g., Broadbent, 1977; Navon,1977), at least up to a limiting size of more than 6° of visual angle.

The possibility that global axes of symmetry for a whole pattern are affecting the perception of a triangle embedded within it suggests that the law of *Pragnanz* is operating: The percept is as "good" as the prevailing conditions allow (Wertheimer, 1923/1958). In the present case, this means that the perceptual system is biased toward choosing a local axis of symmetry for the triangle that is consistent with the global axis of symmetry.

Reference frame selection: The role of symmetry

Palmer, S. E. (1985). The role of symmetry in shape perception. *Acta Psychologica, 59*, 67-90.

Palmer (1985) studied the role of symmetry in reference frame selection.

The stimulus shown in Figure 29A can be seen as either an upright diamond or a tilted square (Mach,1914/1959; Rock, 1973). Similarly, the stimulus shown in Figure 29B can be seen as either an upright square or a tilted diamond. Upright diamonds tend to be perceived as tilted squares when several of them are configured into a diagonal line, as shown Figure 29C (Mach, 1914/1959), or when one is surrounded by a tilted rectangular frame, as shown in Figure 29D (Kopferman, 1930).

The hypothesis most frequently advanced to account for these shape ambiguity phenomena is that perceived shape depends on a description of the stimulus within a perceptual reference frame (Attneave, 1968; Hinton, 1981; Leyton, 1982; Marr, 1982; Palmer, 1975, 1982, 1983; Rock, 1973).

But why is the perceptual reference frame established at certain orientations rather than others? The theory to be explored by Palmer (1985) is that the visual system tends to orient perceptual frames along axes of local and global symmetries (Palmer, 1982,1983).

Palmer (1985) proposed four assumptions of the symmetry theory: (1)

People perceive at least some aspects of a figure's shape within a perceptual reference frame and its orientation in terms of that frame's orientation relative to some larger environmental frame(see also, Palmer, 1975; Rock, 1973). (2) The human visual system includes a unitary attentional mechanism which establishes a single reference frame at any one time by selecting one frame from among many competing alternatives. (3) There is a strong bias toward selecting a frame oriented along an axis of reflectional symmetry, if one exists, and global symmetries bias frame selection more strongly than merely local one. (See Palmer 1982, for a discussion of local symmetry). (4) There is also a general bias toward selecting environmentally vertical and horizontal frames rather than oblique ones.

The principle justification of the symmetry theory is parsimony. It provides a unified theoretical framework for several qualitatively different phenomena: the ambiguity in perceived pointing of equilateral triangles, the ambiguity in perceived shape of the square/diamond, and the ways in which context biases both of these ambiguities.

Experiment 1 used the interference paradigm. Subjects are required to discriminate squares (defined by gravitationally vertical and horizontal sides) from diamonds (defined by gravitationally diagonal sides) as quickly and accurately as possible under various contextual conditions. When the display contains a gravitationally horizontal or vertical line of squares or diamonds (see Figure 30), the symmetry theory predicts that the configuration will be consistent with the required shape discrimination. When it contains a left or right diagonal line of figures (see Figure 30), however, the theory predicts that the configuration will be inconsistent, because its diagonal symmetries bias the system toward adopting a perceptual frame that competes with the required gravitational frame. The theory predicts substantially slower response times (RTs) in the inconsistent conditions than in the control condition and faster RTs in the consistent conditions than in the control condition.

Two complex configurations were also included in the present experiment: a '+' condition formed by superimposing the vertical and horizontal lines and as 'x' condition formed by superimposing the two diagonal configurations (see Figure 30). The theory predicts that the two diagonal lines in the x configuration will produce less bias than either diagonal line alone. In fact, if central global symmetry is the only factor at work, the + and x configurations should be equivalent to each other and to the control condition because the global symmetries are identical (four-fold) in all three of these cases.

Configural lines of one, three, or five figures were used.

Results : (Figure 31) As predicted by the symmetry theory, subjects took much longer to discriminate squares from diamonds in the

inconsistent conditions (left and right diagonal configurations) than in either the consistent conditions (vertical and horizontal configurations) or the control conditions. No difference was found between the consistent and control conditions. These results are consistent with previous findings using the interference paradigm in that Palmer and Bucher (1981, 1982) have always found large and systematic interference effects in the inconsistent conditions, yet have seldom found any facilitation in the consistent conditions.

The results for the more complex + and x (combined) configurations only partly confirmed the predictions of the symmetry theory. Combining the left and right diagonal lines into the x configuration did indeed result in less interference than for the left and right diagonal conditions alone. However, the x configuration was also significantly slower than either the control or the + configuration.

Increasing the number of figures in each configural line increased RTs in the inconsistent conditions (left and right) and the x condition, but not in the consistent condition (vertical and horizontal) or the + condition as has been found previously in the perception of ambiguous triangles (Palmer and Bucher, 1981).

Experiment 2 : *(spacing between configural elements)*

Palmer and Bucher(1981) found that the amount of configural bias diminished rapidly as the distance between adjacent triangles increased. They suggested that this reflected the local nature of whatever mechanisms were responsible for the configural bias. If the same local mechanisms produce the present biases in perceiving the shape of the square/diamond, as the symmetry theory suggests, the amount of bias should also decrease with increased spacing.

Results : Mean RTs for squares and diamonds are plotted in Figure 32 as a function of spacing between adjacent elements, with the single element stimuli shown as a limiting case of very wide spacing.

Increasing the spacing between elements reduced RTs in the inconsistent conditions for squares, but did not reliably reduce them for diamonds. Thus, the effect of spacing for the present shape discrimination task is partly similar to that found previously with perceived pointing of ambiguous triangles.

Experiment 3 : *(ambiguity and bias in perceiving the* '+/x')

The stimuli were analogous to those in experiment 1 except that '+'s and 'x's were used in place of squares of diamonds (Figure 33).

Results : Mean RTs for discriminating '+'s and 'x's in different configural conditions are plotted in Figure 34. The same general pattern of results was obtained for the +/x as for the square/diamond.

Experiment 4 : *(other contextual effects)*

The present experiment uses contexts consisting of either a

rectangular frame around a square/diamond, several parallel stripes inside it, or a single line bisecting it (Figure 35).

Results : Rectangular frames produced large differences between the consistent and inconsistent conditions for both squares and diamonds (Figure 36). The same was true of the bisecting-line context for squares and diamonds. The textural striping inside of the target figures, however, produced no measurable bias effect for either shape in both cases.

Experiment 5 : *(effects of stripe width)*

It is quite possible that the present 'rectangular-wave' textures were simply not wide enough to produce the effect. Thus, the present experiment includes wide (low frequency) square-wave textures in an attempt to produce significant bias effects, which should become weaker as stripe width decreases (as the spatial frequencies of the stripes increase). The fundamental spatial frequencies of the 'square-wave' textures were either 3.5, 6.5, or 12.5 cycles per side of the target figure (Figure 37).

Results : (Figure 38) The unstriped control condition is plotted as a limiting case of extremely narrow stripes. The RT differences between consistent and inconsistent stripe orientations are quite small (less than 30 ms), but they are reliable for the two widest striping conditions. However, the same difference is not reliable for the narrowest stripes.

General discussion : The results of the foregoing experiments generally support the symmetry theory of reference frames. It is important to realize, however, that these predictions were not made to discriminate between the specific formulation of the theory presented here and explicit alternative theories.

There are two deficiencies of the symmetry theory as presently formulated. First, it is a purely *qualitative* theory that, by itself, is only capable of predicting the presence vs. absence of contextual effects, not their magnitude. Second, it does not explicitly mention boundary conditions for these contextual effects other than lack of strict reflectional symmetry. For instance, if a rectangular frame were presented at sufficiently lower contrast than the target figure, it would almost certainly fail to produce a measurable context effect, even when it was still visible. The same is apparently true of the width of stripes in textures. Thus, the symmetry theory does not take into account a number of factors that will, in reality, determine how strongly the symmetry structure of the context will affect the shape processing of the target figure. To do so, a more *quantitative* formulation is needed, one that includes such factors as the relative contrast and spatial frequencies in the target figure and context.

Theories of reference frame selection

Palmer, S. E. (To be published). Reference frames in the perception of shape and orientation. Chapter to appear in Shepp, B., & Ballesteros, S (Eds.) *Object perception: Structure and Process.* Erlbaum: Hillsdale, N.J.

In this article Palmer examines the role of reference frames in perceiving the shape and orientation of object.

Palmer asks, How do people know that two different objects have the same shape? He says that there are two classes of theories about how shape equivalence might be detected. The following is the Palmer's accounts of the two classes of theories.

The *invariant feature hypothesis* assumes that shape perception is mediated by detecting those geometrical properties of figures that do not change (are invariant) when the figure is transformed in particular ways (The transformations of the Euclidean similarity group which consists of translations, rotations, dilations, reflections and their composites). Any given set of transformation partitions the total set of figural properties into two subsets: those that change when the figure is transformed in these ways and those that do not. Historically, the hypothesis has dominated psychological theories of shape perception for a long time. Explicitly or implicitly, its assumptions underlie the Gestalt theory of shape perception, J.J. Gibson's theory of shape constancy, and the classical "feature set theories" of pattern recognition proposed by Selfridge and Neisser (1963). The hypothesis is attractive for its structural simplicity: Shape is represented as a simple set (or list) of attributes.

Evidence that invariant features hypothesis is *wrong* comes from the observation that when a square is rotated 45° it is generally perceived as an upright diamond rather than a tilted square (Mach,1897).

The second hypothesis, the *reference frame hypothesis*, makes use of the same underlying transformations -- the Euclidean similarity group -- in a some what different way. Rather than ignoring properties that vary over the transformations of the similarity group, it assumes that the effects of transformations are removed by imposing an "intrinsic frame of reference" that effectively eliminates the transformation, thereby achieving shape equivalence; here, "intrinsic" simply means that the frame is chosen to correspond to the figure's structure rather than being imposed arbitrarily by the environment's structure (e.g., gravity) or the observer's structure (e.g., head orientation).

If the same intrinsic frame is always used, shape equivalence will be perfect. But the visual system does not always choose the same frame each time. Palmer proposes three assumptions that account for anomalies in perceived shape equivalence. (1) Shape is perceived relative to a

reference-frame-like structure in which the orientation of the axes is taken as the descriptive standard (e.g., Rock, 1973). (2) The perceptual system has some *heuristics* for assigning an intrinsic reference frame to an object such that the orientation of the frame relative to the object will be constant over different orientations. (Because heuristics are imperfect rules of thumb, the first two assumptions together imply that there will be certain circumstances in which the wrong orientational assignment will be made causing anomalies in perceived shape equivalence.) (3) There are biases toward picking other salient orientations as the reference orientation, especially gravitational vertical or the top-bottom axis of retina. (The shape of a figure is perceived relative to its own intrinsic frame of reference when it has the type of structure that clearly defines one, and relative to an extrinsic frame when it does not.)

Palmer conducted experiments on frame selection to examine how intrinsic reference frames are selected. The "interference paradigm" (Palmer & Bucher, 1981, 1982) was used in the following experiments.

The first theory Palmer examined was the *elongation theory* of frame selection which says that the elongation of the stimuli as the spatial structure produces the Gestalt-like biases in frame selection.

Experiment 1 tested the elongation theory using rectangular frames: It examines the bias effects by changing the aspect ratio (length-to-width ratio) of rectangular frames (Figure 39). The theory's predictions are (1)that there will be no bias effects for square frames, and (2) that the magnitude of the bias effect should increase monotonically as the aspect ratio increases. The subjects' task was to discriminate triangles pointing either directly left or directly right. RTs were measured.

Results : (Figure 40) Contrary to the prediction of no bias effect for square frames, these non-elongated frames produced a highly reliable bias effect. There seem to be a slight trend toward higher RTs for the longer frames, but even the difference between the most extreme aspect-ratio conditions fails to reach statistical significance. Global elongation is unlikely to be a viable theory of these kinds of contextual effects.

A second theory Palmer examined was the *symmetry theory* of frame selection, which says that the visual system uses symmetry rather than elongation as the principal type of spatial structure for selecting the orientation of its reference frame; the reference orientation established for the whole display will coincide with its global axis of symmetry, if one exists.

Experiment 2 (testing the symmetry theory) examines the bias effect on perceived pointing of ambiguous triangles as the orientation of a surrounding rectangular frame that is changed in 15° steps (Figure 41).

The theory's prediction is that RTs would be short for the "consistent" conditions (the axis of global symmetry coincides with the correct

response), long for the "inconsistent" conditions (the axis of global symmetry coincides with one of the other two symmetry axes of the triangle), and intermediate when global symmetry is broken.

Results showed a large and systematic effect of orientation, quite similar to the predictions of the symmetry theory (Figure 41).

Experiment 3 (testing the symmetry theory) investigated the effects of bending a rectangular frame along its axis, which causes the effect of breaking the axis-aligned symmetry (the one along the long axis) while preserving the base-aligned symmetry (the one along the short axis) (Figure 42).

The symmetry theory predicts that "straight" frames should have approximately equal biasing effects on an interior triangle in their axis-aligned and base-aligned orientations, but "curved" base-aligned frames should have a much bigger biasing effect than "curved" axis-aligned frame. The reason is that the base-aligned symmetry axis is intact after bending the frame, whereas the axis-aligned symmetry axis is broken.

Results confirmed the predictions (Figure 43).

Experiment 4 (testing the symmetry theory): A single line is used as the contextual element. When the line is axis-aligned, displacing it sideways (perpendicular to its length) breaks the global symmetry of the configuration, whereas when the line is base-aligned, displacing it sideways preserves global symmetry (Figure 44).

The theory predicts that the bias effect for axis-aligned lines will be close to zero for all positions except the central one (in which global symmetry is observed) -- which will be large -- whereas that for base-aligned lines will be uniformly strong across a broad range of positions.

The main *results* conform rather well to the predictions of the symmetry hypothesis (Figure 45).

Experiment 5 (testing the symmetry theory) examined the compositionality of the frame effect by measuring the bias effects produced by square's individual sides and all possible combinations of them: pairs, triples, and the complete square frame. The stimuli included configurations with consistent and inconsistent orientations for both left- and right-pointing triangles (Figure 46).

The symmetry hypothesis predicts that the symmetrical cases will produce reliable bias effects whereas the asymmetrical cases will not.

Results : (Figure 46) Six of the seven symmetrical stimuli produced the six highest bias scores. This result is consistent with the hypothesis. However, there were results that were inconsistent with the hypothesis: All except one of the asymmetrical configurations produced statistically reliable amounts of bias, and most problematic, the configuration that produced the least bias of all was a symmetrical one.

Hereafter Palmer examines the *low spatial frequency theory* of frame selection as an alternative to the symmetry theory.

Gestalt phenomena such as the contextual effect can be explained in terms of the content of images at low spatial frequencies (Ginsberg, 1971,1986). Janez(1983) developed a precise mathematical formulation of Ginsberg's low spatial frequency hypothesis. He hypothesized that the Gestalt effects arose through differential activation in orientation channels at low spatial frequencies, and proposed that reference frames are selected by a process that depends on the dominance of low frequency power at certain orientations relative to others. He formalizes this concept in terms of a dominance ratio, D, whose denominator represents the activity in low spatial frequency channels at orientations parallel or perpendicular to the required response, and whose numerator represents the activity in corresponding channels at orientations parallel or perpendicular to other possible directions of pointing. Thus, the higher the value of the ratio, the more activity there is in the irrelevant orientational channels, and the higher RT is expected to be.

Janez applied his model to results of several of the early published experiments on perceived pointing of ambiguous triangles (Palmer & Bucher, 1981, 1982) and perceived shape of the ambiguous square/diamond (Palmer, 1985), and he had notable success. However, further explorations revealed some puzzling discrepancies between data and Janez's theory: Dominance ratio predicts the results of some experiments well only in the low spatial frequency channels, others well only in the high frequency channels, and still others well only with a combination of channels(Figure 47).

Experiment 6 : (testing the *low spatial frequency model* using ambiguous triangles with various contexts) (Figure 48)

Results :The bias effect data were fitted to the dominance ratio predictions (in Figure 47 as the curve labeled "multiple"). The fit of the model is quite poor in all channels. The maximal linear combination produces a correlation of only 0.49, which is barely above the value needed to achieve significance at the 0.05 level.

Experiment 7 : (Symmetry versus spectral power)

One way in which spatial frequency theories can be tested experimentally against the symmetry hypothesis is by examining the contextual effects of single versus double sine wave gratings. Both theories agree that if a single triangle is placed on a single sinusoidal grating oriented as in Figure 49 A, its perceived pointing will be biased perpendicular to the orientation of the stripes, as shown by the arrow. Given that the observers' task is to see the triangle point directly right (versus directly left), this stimulus is inconsistent with the required response, and should lead to long reaction times and/or relatively many

errors. However, when the two inconsistent gratings are superimposed to form a double grating (Figure 49 C) the predictions of the two theories diverge. Spatial frequency theories predict that the double grating will lead to performance at least as poor as for either inconsistent single grating alone, because the double grating's power is still concentrated at orientations inconsistent with the required percept. The symmetry theory predicts that the double grating will lead to much better performance than either single grating alone, because the combination produces an emergent axis of symmetry which is consistent with the required response.

Results : As predicted by both theories, response to the single C (consistent) gratings were much faster than those to the two single I (inconsistent) gratings which did not differ from each other. The results for double gratings conform well to the predictions of symmetry theory and are incompatible with the spatial frequency account: the I1 + I2 combination produced faster responses than C + I1 and C+I2 combinations (Figure 50)

Experiment 8 : low pass filtered stimuli.

If the low spatial frequency channels are indeed responsible for Gestalt effects, then it should be possible to eliminate or greatly reduce the configural orientation effect simply by high-pass filtering the stimuli to take out the power in specified low frequency bands. Palmer is planning to use a series of different cut-offs for the high-pass filtering operation: 0 (no filtering), 1/4, 1/2, 1, 2, and 4 cycles per side (Figure 51). It seems intuitively clear that some configural bias effect is still present in those stimuli even with 4 cycles/side as the cut-off frequency. Experimental test is needed to confirm this prediction. However, it is not yet conducted.

If the bias effects are not measurably affected by filtering, it would constitute strong evidence that dominance in the low spatial frequency channels is not necessary for this Gestalt effect to occur, although it still might be sufficient.

Future theoretical directions

Spatial frequency models are not strong candidates for explaining the kind of Gestalt contextual effects that have been examined. While symmetry theory seems to do better than spatial frequency models on several scores, it alone does not seem to be adequate to the job either.

The most promising direction for new theoretical developments is "connectionism" or "PDP" models. The dynamic properties of networks during the process of settling into a state of minimum energy are very suggestive of some crucial phenomena -- e.g., the fact that ambiguous triangles are multistable to begin with, and the ways in which contextual structure seems to influence this multistability. The properties of the densely connected parallel neural networks are hauntingly similar to the ideas advanced many years ago by Gestalt theorists in their "field theories"

of perceptual phenomena, and they are of considerable interest on these grounds alone.

Reference frame effects in depth

Palmer, S., Simone, E., & Kube, P. (In press). Reference frame effects on shape perception in two versus three dimensions.

The question addressed in this article is whether reference frames used in shape processing operate in a two-dimensional (2-D) or three-dimensional (3-D) representation of space. Nearly all modern theories of perception assume that visual processing makes use of at least two fundamentally different kinds of spatial representations. The first is a logically prior representation of 2-D properties of the proximal stimulus. The second is a representation of the 3-D properties of the distal stimulus.

The principle question we wish to answer is whether the processes that select a perceptual reference frame are based on information about the structure of the 2-D image, the 3-D environment, or some combination of the two.

When the sides of the figure are perceived as parallel and perpendicular to the axes of the 2-D frame, the description of the figure corresponds to a "square" shape. When they are perceived as diagonal to the axes of the frame, the description of the figure corresponds to a "diamond" shape. (Figures 52C and 52D) However, they can also be seen three dimensionally as lying in several parallel depth planes, as indicated in Figures 52E and 52F. The interesting phenomenological impression is that when the diagonal configurations are perceived in depth, the tendency to see their shapes relative to the tilted 2-D reference frame of the retinal configuration seems to disappear.

The task in the following experiments forced observers to see a particular one of the two alternative shape descriptions for each stimulus: namely, the one aligned with the *gravitational* reference frame rather than the one aligned with the configural reference frame.

How much is the size of the configural orientation effect reduced when the figures in the configuration are perceived to lie in different depth planes? The 2-D hypothesis implies that it will not be reduced at all, and the 3-D hypothesis implies that it will be completely eliminated.

Experiment 1 : The stimuli include the depth cues of relative size by making the upper figures smaller, interposition by occluding a ground plane behind the figures, height in the picture plane by placing farther figures higher in the image, and linear perspective by converging the parallel lines of the bowling-allay-like ground plane toward a vanishing point at the horizon (Figure 53).

The subjects were instructed to discriminate between gravitationally defined squares and diamonds as quickly and accurately as possible. RTs were measured.

Results :(Figure 54) The amount of interference in the 3-D conditions is only about 1/5 as large as that in the corresponding 2-D conditions. Even so, there is still a difference in 3-D conditions between the single-figure control condition and the inconsistent diagonal conditions of about 25 ms and one of 35 ms between the consistent vertical and inconsistent diagonal conditions. These latter two effects clearly show that some interference is still present in the 3-D stimuli, despite the large decrease in the size of the effect. The pattern of results is consistent with the hypothesis that the interference effect occurs *primarily* at a 3-D level of perceptual organization.

Experiment 2 is designed to rule out at least some of the most obvious factors that might compromise the depth interpretation. The comparison is made between the configural orientation effect for the standard 2-D stimuli and that for control stimuli which included some factors (not all of them) that produced the 3-D effect in Experiment 1, yet would result in 2-D perception (Figure 55). The control stimuli included the depth cues of relative size, height in the picture plane, and occlusion of a background.

Results : The pattern of results for the 2-D stimuli replicates that of the first experiment. The same pattern of results were found for the control stimuli. (Figure 56) Thus, the data are clearly incompatible with the "superficial features" hypothesis that mere differences in size or presence of an occluded background surface are sufficient to produce the decrease in interference observed in Experiment 1.

Experiment 3 : Experiment 2 did not control for the presence of linear perspective, and this might be the critical factor. Furthermore, it might be argued that simply seeing depth per se in the stimulus somehow produces the observed drop in interference, rather than seeing the target figures in different depth planes.

Conditions were created in which the diagonal figures could appear to lie either in the same depth plane or in different depth planes just by changing the orientation of the ground plane relative to the configural line (see Figure 57). To do this, the depth information from relative size had to be eliminated.

The *results* are consistent with those in Experiment 1. There are large interference effects due to configural orientation for the 2-D condition. There are smaller, but still reliable, interference effects for the 3-D condition. Still, the amount of interference was clearly less in the 3-D conditions than in the 2-D conditions for both squares and diamonds.(Figure 58)

The pattern of results across all three experiments is quite clear: when

people perceive the target figures in different depth planes, the configural interference effect is much smaller than when they perceive them in the same depth plane.

Kruschke and Palmer (in press) found that the configural orientation effect is sensitive to depth information in the form of binocular disparity, provided that stereopsis is required for the task. The results require modification of the theory of reference frame selection to include stereoscopic depth information. The results of Palmer, Simone, & Kube (in press) suggest that pictorial depth information should also be taken into account. Together, these results strongly suggest that theoretical accounts of reference frame effects should be based in 3-D processing.

II. Coding theory

Coding theory developed by Leeuwenberg and his associates provides a set of rules for describing visual patterns (line drawings) as a string of symbols. A visual pattern such as a square is initially transformed into a "primitive code," which consists of a string of symbols corresponding to lines and angles. The primitive code is then shortened into an end code by using syntactic rules which make use of redundancies in the primitive code. The number of elementary components in the end code is called information load, and is considered as an index of pattern complexity (or simplicity). For example, a primitive code of Figure 59 is

$$\lambda\alpha\nu\alpha\lambda\alpha\nu$$

and of Figure 60 is

$$\mu\beta\nu\alpha\nu\beta\mu\beta\nu\alpha\nu.$$

The same figure can receive a different primitive code if one starts differently. For instance, if one started at the lower right-hand corner of Figure 59, again with a starting direction to the right, the first element of the code would be an angle, and the primitive code would be

$$\alpha\nu\alpha\lambda\alpha\nu\alpha\lambda.$$

A primitive code is reduced to a shorter, end code by syntactic rules. Syntactic rules are concerned with redundancies in primitive codes, which involves iteration, continuation, reversal, symmetry, distribution, symbolization, and subcodes (or "chunks").

Iteration is repetitions of a subsequence. If a code contains a subsequence that is repeated n times without interruption, then the block of repetitions can be replaced by n*[ ], where the code of the subsequence is placed between the brackets as in the two following examples:

abbbc=a 3*[b] c

aaabbb=3*[a] 3*[b].

Continuation is a special case of iteration, in which the same subsequence is repeated to a natural ending. For example, if a right angle and side, $\alpha\lambda$, are repeated four times, the result is a square, and the figure returns to its starting point. This type of repetition to a natural ending is symbolized by << >> (van Tuijl, 1980) (or by @*( )), so the square would be coded <<$\alpha\lambda$>> (or @*($\alpha\lambda$)).

Continuation may also be used when a uniform curve continues until it intersects a line that has already been drawn. In such a case the uniform curve is represented as <<β>> (or @*(β)). Or, even when a straight line is continued to an intersection or an end point of an already existing line, the straight line is represented by <<0>> (or by @*(&) where & means a grain of length).

Reversal and *symmetry* are coded in the following way. Any string of

elementary symbols in a primitive code can be rewritten in backward order by the reversal (r) operation,

$$r[\alpha\beta\gamma] = \gamma\beta\alpha.$$

When the original figure displays spatial symmetry, this is often reflected in symmetry in the code, that is, a string of symbols followed immediately by the same string of symbols in reverse order. Two varieties are possible:

$$\alpha\beta\gamma\gamma\beta\alpha = \alpha\beta\gamma\, r[\alpha\beta\gamma] = \Sigma[\alpha\beta\gamma] \; (= \mathrm{SYM}[\alpha\beta\gamma])$$

$$\alpha\beta\gamma\beta\alpha = \alpha\beta\gamma\, r[\alpha\beta] = \Sigma'[\alpha\beta(\gamma)] \; (= \mathrm{SYMM}[\alpha\beta(\gamma)]).$$

Distribution is used when two alternating strings (factors) are separately written in angle brackets as follows (consider that A, B, C, etc are any substrings):

<A><BCD> = ABACAD
<ABA><LMN> = ALBMAN
<ABA><MN> = AMBNAMANBMAN
<AB><LMNM> = ALBMANBM.

The substrings in the factors (e.g., ABA and MN) are used over and over until the entire distributed sequence starts over.

Symbolization allows to replace a substring with a new symbol when the substring appears more than once in a string. The first appearance of the original substring should be kept intact. However, its subsequent appearances can be replaced by the new symbol. For example, in the string

$$\alpha\beta\gamma\nu\alpha\beta\gamma\mu\nu\mu\alpha\beta\gamma,$$

one may define $y = \alpha\beta\gamma$ and get a string

$$\alpha\beta\gamma\nu y\mu\nu\mu y$$

with a side notation that $y = \alpha\beta\gamma$.

Subcodes or "chunks." Parentheses around a segment of a code signify a subcode or "chunk" that is to be treated as a unit. For example, in iteration

3*[(AB)] = ABABAB
3*[(A)(B)] = AAABBB.

The *information load* of a code is the number of parameters in the code--the number of angles, line lengths, numbers, and symbol appearances. One apparent exception is <<0>>, which has no information load. This is because <<0>> provides no extra information about a given visual pattern. The symmetry symbol carries a unit of information load.

Depending on the initial primitive code, the same pattern may receive two or more final codes. In such cases it is assumed that the visual system selects the code with the least information load in accordance with the minimum principle.

Visual Pattern completion

Buffart, H., Leeuwenberg, E., & Restle, F. (1981). Coding theory of visual pattern completion. *Journal of Experimental Psychology: Human Perception and Performance, 7*, 241-274.

Buffart et al.(1981) applied the coding theory to visual pattern completion. An example of visual pattern completion is given in Figure 61. When people look at this figure, most of them perceive a circle partly occluded by a square. Visual pattern configurations that may lead to a pattern completion are abundant. However, pattern completion is not always the most preferred interpretation of such a configuration; in some cases mosaic interpretations (two figures side by side) are preferred to completions (Figure 62C). Furthermore, even when pattern completion occurs, the way it occurs is not determined in a singular way (Figures 62A and 62B). Buffart at al. assert that whether or not visual pattern completion occurs, and if it occurs, what interpretation is preferred, can be predicted by applying coding model to a given pattern. More specifically, they predict that the interpretation with the least information load will be most preferred. That is, when the information load of the final code of a pattern completion is smaller than that of a mosaic interpretation, the completion will be preferred, and vice versa; if the information loads for the completion and the mosaic interpretation are the same, people's response will be ambiguous. For example, in Figure 63 two possible interpretations of a simple display with coding paths are shown. Most people select interpretation A (completion), and as Buffart et al. predict, the information load for A is smaller than that for B.

Experiments 1 & 2 tested their predictions. Subjects (psychologists and graduate students in Experiment 1 and secondary school children in Experiment 2) were presented with 25 visual patterns (Figure 64), and were asked to trace for each pattern the contour of the subpattern which they thought to be the best interpretation of the whole configuration.

Results confirmed the predictions (Figure 65). Of the 25 patterns, 16 had completions with lower information loads than the mosaic interpretation, 7 had equal information loads, and the other 2 had more economical mosaic interpretations. When completions had lower information loads than mosaics, 96% of the subjects produced completions. When the two types of interpretations were equally economical, 45% chose completions. When the mosaic interpretations had lower information loads, only 10% chose completions.

Interpretation of complex line patterns

van Tuijl, H. F. J. M. (1980). Perceptual interpretation of complex line patterns. *Journal of Experimental Psychology: Human Perception and Performance. 6*, 197-221.

van Tuijl (1980) applied the coding theory to the perceptual interpretation of complex line patterns which included intersections. A complex pattern can be interpreted as consisting of subpatterns, but the way such a pattern is decomposed (or subdivised) into subpatterns can not be determined singularly. van Tuijl predicts that the subpatterns that is described by the least information load will be the preferred interpretation.

Experiment 1 tested this prediction. The subjects were presented with 20 complex patterns (Figures 66, 67, 68, and 69). After presentation of each pattern, two possible subdivisions are shown, and each subject selected the subdivision which he or she thought that they would make for themselves.

Results (Table 1) were consistent with the prediction in most cases. However, there were several unpredicted responses, too; the result for pattern 14 was the reverse of the prediction; those for patterns 17-20 showed the clear-cut preference of one interpretation to the other, despite the fact that the coding theory predicted ambiguities.

To account for these anomalies in the results, van Tuijl proposed two supplemental principles, namely, the object principle and the efficiency principle. The object principle says that each subpattern must be seen as an object rather than simply a line drawing. For example, a part in the subdivision b of pattern 18 (Figure 69) should be seen as a hook so that the width of the line would be incorporated into its code (Figure 70). As a result of this modification, subdivision a of pattern 18 becomes more preferable than subdivision b. The object principle also applies to patterns 14 and 17. In both of these patterns, the subdivisions into triangles are rejected by the principle, since if these triangles are seen as objects with *surface*, it is unnatural that all the contours of these triangles are seen in the original complex patterns. This analysis explains the results for patterns 14 and 17.

The efficiency principle is based on the quantification of the Gestalt law of good continuation. If the information load of the *primitive* code of subpatterns is lower, there are more continuation and more efficiency in the subpatterns. More specifically the relative efficiency of subdivision a compared with subdivision b is defined by the equation,

$$e_p(a/b)=\{I_p(b)-I_p(a)\}/\{\max[I_p(a),I_p(b)]\}$$

where $I_p(a)$, for example, represents the information load of subpattern a at

the level of primitive code. Similarly, the relative efficiency of subdivision a compared with subdivision b at the level of *final* code is defined by the equation,

$$e_f(a/b)=\{I_f(b)-I_f(a)\}/\{\max[I_f(a),I_f(b)]\}$$

where $I_f(a)$, for example, represents the information load of subpattern a at the level of final code. And, the ultimate efficiency (E) of subdivision a compared with subdivision b is defined as the sum of $e_p(a/b)$ and $e_f(a/b)$:

$$E(a/b)= e_p(a/b) + e_f(a/b).$$

This efficiency analysis is consistent not only with the results for patterns 19 and 20, but also with all the rest of the results of Experiment 1 (Table 2).

Experiment 2 tested the validity of the efficiency principle using a different experimental paradigm. Patterns were presented tachistoscopically. First, a subpattern was presented. Then, a complete pattern was presented. The subject pressed the right button if the subpattern was part of the complete pattern, and pressed the left button if the subpattern was not detected in the complete pattern. RTs were measured. The subpatterns that were true parts of the complete patterns were divided into two classes: more efficient subpatterns (easy) and less efficient subpatterns (difficult). It was predicted that the RTs for the easy subpatterns would be shorter than those for the difficult ones.

Results were consistent with the prediction (Table 3). The results for patterns 5 and 6 did not reach significance. However, inspection of these two patterns revealed that in these patterns the more efficient subpatterns were classified in an erroneous way.

Coding theory of motion

Restle, F. (1979). Coding theory of the perception of motion configurations. *Psychological Review, 86*, 1-24.

Restle (1979) analyzed the Johansson's (1950) experiments on motion perception by using a coding model. Johansson in his experiments displayed a small number of dots in relatively slow, oscillating real motions, with a cycle time of 1-4 sec. Each motion either was in a circular path at uniform velocity or was a parallel projection of such motion. That is, straight-line motions were sinusoidal in velocity, and motions in an elliptical path moved fastest at the minor axis and slowest at the major axis, in both cases being a projection of uniform circular motion.

Restle invented a coding model for representing such motions. A basic circular motion is specified by three parameters: amplitude (α), phase (ϕ), and wavelength (λ) (Wavelength is expressed in cycles per second). An

elliptical motion is taken to be a projection of a circular motion and therefore requires two more items of information, namely, the axis of rotation of the plane on which the circular motion occurs relative to the picture plane on which the motion is displayed to the observer (β) and the angle of tilt or rotation (τ). An elliptical motion of a system S is therefore symbolized as $M_{\alpha\phi\lambda\beta\tau}(S)$. Oscillation on a straight line is treated merely as a very thin ellipse in which the plane of the circle is orthogonal to the picture plane ($\tau=90°$). Uniform motion in a circle is taken to be an ellipse with $\tau=0°$. These two parameters are illustrated in Figure 71.

If $\tau=0°$ and the motion is circular, then it is not possible to specify the axis of the tilt (β). However, a normal circular motion starts at 0°, the right-hand edge of the circle. Suppose that such a circular motion is rotated 90° to the left, that is, $\beta=90°$. Then the motion will start at the top of the circle. This change is exactly the same as would be produced by a phase shift of 90° in the motion, with $\beta=0°$. In this way, orientation and phase are interchangeable in the case of circular motions.

Motions are coded in the following way. If the motions of two dots a and b are seen as independent from each other, they are coded as

$$M\alpha_1\phi_1\lambda_1\beta_1\tau_1(a)+M\alpha_2\phi_2\lambda_2\beta_2\tau_2(b)$$

with ten parameters. Sometimes motions are perceived in a hierarchical way. Suppose that the whole system (S) of points a and b has a motion M_1 and the point b on that system moves, with respect to S, with a motion M_2. The code is

$$M\alpha_1\phi_1\lambda_1\beta_1\tau_1(S)[M\alpha_2\phi_2\lambda_2\beta_2\tau_2(b)].$$

It may happen that some of the parameters are the same in the system motion, M_1, and in the motion, M_2, of the subpart. If the two motions have the same wavelength, phase, and tilt, the code can be written

$$M\alpha_1\phi_1\lambda_1\beta_1\tau_1(S)[M\alpha_2\phi_1\lambda_1\beta_2\tau_1(b)].$$

To simplify notation, replace a repeated parameter by a dot and suppress subscripts of parameters. Using these notational simplifications, the above expression is written

$$M_{\alpha\phi\lambda\beta\tau}(S)[M_{\alpha\ \cdot\cdot\beta\ \cdot}(b)]$$

which has seven parameters in all. The number of independent parameters in the description of motions contributes to the information load in the present coding model.

Application of the Coding Model to Johansson's Early Experiments. In Johansson's (1950) experiments, dark spots were seen to move on a lighted screen. Experienced observers reported the motion configurations they saw, and in many instances large groups of subjects concurred. Restle

repeated most of Johansson's experimental conditions, along with some variations. The display consisted of bright dots on a dark screen, observed in dim light at approximately the same visual angle as used by Johansson.

Grouping by common or related motions: Experiments 1, 2, and 3.

In *the first condition of Experiment 1*, Johansson presented a subject with four unmoving points (Figure 72A) and asked if they appeared to be organized. Four independent points have I(information load)=4, since each point has a location(L), and each location must be coded by a parameter. Four points seen as an organized set of points which lie equally spaced on a straight line have I=3, because it requires three parameters to describe them, namely, a starting location(L) for one point, a distance to the next point(d), and the number of times that distance must be repeated. According to the coding theory, subjects should have said that the points were organized. However, the prominence was P=*f*(4/3)=*f*(1.33), which is not very high. (The function, *f*, is not defined by Restle.)

The result: Reports of some perceptual organization were elicited.

A second condition of Experiment 1 presented the points moving up and down in unison (Figure 72B). If the points are interpreted as independent, each has a location L and a motion, the motion having all five parameters. Four such points, each consuming six parameters, have an information load of 24. On the other hand, if the points are organized together, there is only one motion of the system (I=5), and the location of the points on that moving system requires only 3 parameters, L, d, and 3, to yield a total I=8. The interpretation of unrelated motions is much more expensive than organized motion (24 vs. 8), and the prominence of the organizations is P=*f*(24/8)=*f*(3.0), which is much higher than in the case of stationary points.

The result: As the model predicts, observers report that the points are much more strongly grouped when they move together than when they are still.

In Experiment 2 (Figure 72C), the points move with unequal amplitudes. If grouping depends on common motion, they should not be perceived as grouped. If the observer were to consider the four points as unrelated, the locations would have I=4, and three of the points would move in an unrelated way, yielding a total I=19. Alternatively, the observer could see four points on a rotating rod, spaced by a code with I=3 and with a single motion I=5, for a total information load of 8. Thus, the prominence of the unified grouping is *f*(19/8)=*f*(2.375).

The result: Obsevers report that there is a rod which oscillates about a fixed axle. Thus, Wertheimer's (1923) common fate hypothesis must be modified to admit that the visual system may extract not only a common motion but also motions with some properties in common but that vary in amplitude.

Experiment 3: (Figure 72D) As six unrelated points, the configuration has six locations and four motions (I=6+20=26). Seen as a swinging jump rope, the configuration requires one motion (I=5) and the location of six equally spaced points, Ld^5 (I=3). The total information load of the jumping-rope interpretation is therefore I=5+3=8, and the prominence is P=*f*(26/8)=*f*(3.25).

The result was completely in accord with the prediction based on the coding model.

Formation of subgroups: Experiments 5, 6, 7.

In his *Experiment 5* (Figure 73), Johansson (1950) asked whether subgroups of dots become grouped together when they have a common motion and separated if they have contrasting motions. The points a and b move together along the vertical paths, and points c and d move together but in the opposite direction. The code of four independent motions is very inefficient (I=20). The code of two independent motions of pairs of points is much better (I=10). The third coding, that the two pairs of points follow related motions, has an information load of only 7.

Results: 13 of 14 observers definitely saw the figure in two subgroups, and 11 of the 13 subjects saw the subgroups as related.

Experiments 6 and 7: The motions of points are described in Figure 74.

Results: No observer sees the four points as all unrelated, all see the points grouped so that dots in common phase form subsets irrespective of positions, and most observers see all four points as related. Since all four points are seen as interrelated, the simple common fate theory is incomplete. Furthermore, the result does not depend on proximity of the dots. The phenomena arise from the motions themselves.

Vector analysis of motions:Experiments 17, 18, 19, 20, and a Gogel's (1974) Experiment.

Experiments 17 and 18: In Experiment 17, two points were in vertical motion, and two other points followed a path 15° from the vertical (Figure 75). In Experiment 18, one pair of points moved vertically, the other pair in a circle (Figure 76).

Results: In both experiments, observers saw two *related* subgroups; in Experiment 17 the sloping motion was perceptually analyzed into horizontal and vertical components, so that the observer saw the four points on a line that was moving up and down and saw two points sliding back and forth on that line; in Experiment 18 the circular motion was analyzed into horizontal and vertical components, equal in magnitude and 90° out of phase.

The results are predicted by coding analysis. In both experiments three interpretations are possible: four unrelated motions, two unrelated motions each carrying two points, and two motions in a hierarchical structure. The second interpretation has a lower information load than the first, and the

third the lowest of all in each cases. In Experiment 17 two types of hierarchical structures are possible as shown in Figure 75C; both types were seen by observers.

Experiments 17 and 18 go far beyond Wertheimer's common fate: Not only are points grouped by common motion but a motion itself can be divided into two component motions by what Johansson called a perceptual vector analysis.

In *Experiment 19* Johansson used only two points. The motion pattern and the three main interpretations, B, C1, and C2, are shown in Figure 77. These three interpretations are the cases of vector analysis again. The coding model says that these interpretations are equally stable.

Results: The prediction of the coding model was confirmed. The three interpretations are ambiguous, and all can be seen by an observer.

Gogel's (1974) experiment (Figure 78) used three points, one test dot in horizontal motion and two inducing dots in vertical motion that were out of phase with one another and at opposite ends of the test dot's path, so that the test dot joined first one inducing dot and then the other alternately. Several interpretations are possible. One is of three unrelated motions (Figure 78A) with I=15. A second interpretation (Figure 78B) is to have the system follow one of the inducing points and then to split up the residual motion of the other two points (I=9). In the third interpretation (Figure 78C) the system follows the motion of the test point, and the residual motions are $M_{\alpha..\beta.}(b)$ and $M_{\alpha..\beta.}(c)$; with five information units for the system motion, the total is I=9. The fourth interpretation is that the system describes a rocking motion like a seesaw, with the two inducing points b and c lying on this system (Figure 78D). It is difficult to code this interpretation since it involves a curved path and a rocking motion. However, Restle (1979) suggests that I of 9 would be appropriate for this interpretation (pp. 11-12). This analysis suggests that the second, third, and fourth interpretations (Figures 78A, 78B, and 78C) would be ambiguous.

Results: Restle reports that Interpretations B and C were vividly apparent, and Interpretation D could also be seen.

Experiment 20: The paths of two motions crossed (Figure 79). Interpretations A, B, C, and D are all more efficient than are separate motions, which would yield I=10. The coding model gives I=8 to Interpretation A, I=7 or 8 to Interpretation B (I is not definite since B involves collision), and I=7 to Interpretations C and D.

Results: All the four interpretations can be observed.

In the above series of experiments, it is shown that the coding model can give a detailed account of motion analysis, in which a single physical motion of a dot is analyzed into two or more components. Furthermore, the model can predict ambiguities in interpretation.

Motion synthesis: Experiments 21, 24, and a Restle's experiment.

In *Experiment 21* Johansson used the same crossing motion paths as in Experiment 20, but he changed the phase relations so that point b lagged 90° behind point a. Recall that in Experiment 18 (Figure 76) the circular motion of points a and d was vector analyzed into two rectilinear motions, 90° out of phase. In Experiment 21, the reverse occurs, that is, two linear motions out of phase are synthesized into a circular apparent motion.

The motion pattern is shown in Figure 80. Interpretation A, as two independent motions, has I of 10 and is uneconomical. Interpretations B and C have the system follow one point; relative to the system, the other point then describes a circular motion, and I=8. In Interpretation D, the two points appear to rotate around a common center in one direction, and then the center itself seems to rotate in the other direction: Its information load is also 8.

Results: The model predicts Interpretations B, C, and D. All three are in fact seen.

Experiment 24 is similar to Experiment 21 except that a third point is introduced that follows a path at 45° in orientation between the other points and with a 45° phase lag between the other two points. Figure 81 shows the motion unfolding in eight successive positions. Interpretation A, of three unrelated motions, is very uneconomical (I=15) and cannot be seen. Interpretation B is that either point a (0°) or point c (90°) is seen to move in a straight line, with the other two points rotating around it in two different orbits; the code (I=11) is uneconomical. In Interpretation C, point b is seen to move in a straight line diagonally, and points a and c are seen to rotate around it in a single orbit (I=8). Interpretation D is of the three points rotating around in a single orbit, this orbit itself rotating in the opposite directions (I=8).

Results: Both Interpretations C and D are easily seen. In addition, Restle was able to fixate point a, see it moving up and down, and see points b and c rotating around it: In such a display, a, b, and c become the points of a rigid right-angle triangle that rotates around one of its acute angles, and as a rigid body, this interpretation also has an information load of 8.

Restle's experiment: Restle added to the display in Experiment 21 a fourth point at 135°. Figure 82 shows that the circle-within-a-ring interpretation (B) still has I=8. Interpretation A is that one point moves in a straight line, and the other three points occupy at least two orbits; this interpretation is less economical than Interpretation B.

Results: The circular motion of Interpretation B clearly dominates. However, if one fixates a single point, it can be seen moving in a straight line with a rigid square rotating around it.

The three experiments described above show that the coding model of motion can predict not only vector analysis but also vector synthesis in visual motion perception.

Residuals of motion analysis: Experiments 27, 28, 28A(or a second experiment by Restle), and 29.

Experiment 27 repeats Experiment 18 but uses only two points instead of four. One point follows a vertical path, the other point, off to the right, follows a circular path, and both start at the top.

Results: Most subjects see the system moving up and down, with the point on the right also making a horizontal linear motion. This is a typical motion analysis of a circle into two straight-line motions.

In *Experiment 28*, Johansson asked what would happen if the motion analysis did not work out so simply because the two dots had unequal vertical components of motion. To answer this question, Johansson used the same long vertical path of point a, but he changed the motion of b into an ellipse only half as high as it was wide, as shown in Figure 83. Three interpretations are possible; to consider the motions of the two dots as unrelated (Interpretation A, I=10); to analyze the common vertical component of motion, the height of the ellipse, which then leaves both of the dots in motion with respect to the system and therefore requires the subject to see three motions when there are physically only two (Interpretation B, I=9); or to take the full vertical motion of point a as the system motion, which requires that point b be seen to follow an elliptical path with a rotation *opposite to* its physical rotation (Interpretation C, I=9).

Note that the code for Interpretation B with three motions has less information load than the code for Interpretation A with two motions. This is because when the motion of a is divided into two parallel vectors, the vectors share the same phase, wavelength, orientation, and tilt.

Result: Observers see Interpretation B. The coding model has trouble with this result. The model predicts that Interpretation C can be seen also, but that is not the case. The next experiment is planed to test if observers can see Interpretation C in a slightly different context.

Experiment 28A (Restle's second experiment): This experiment is a modification of Experiment 28 with a third point, c, moving vertically in unison with point a (Figure 84).

Results: Restle could perceive two interpretations that correspond to Interpretations B and C in Figure 83.

There seem to be two possible interpretations of the preference for Interpretation B over C in Johansson's Experiment 28. One, proposed by Johansson(1950), is that the system prefers to use the shortest common component, that is, to make the motion of the system as small in amplitude as possible. A second possibility is that the visual system prefers straight lines and circles over ellipses.

These two interpretations are pitted against one another in Johansson's *Experiment 29*, in which the straight path of point a is shortened and b

retains its large circular path, as shown in Figure 85. Interpretation A (two unrelated motions) has I=10. Interpretation B analyzes all the motions into horizontal and vertical straight lines, but produces motions in three different directions and has I=10. Interpretation C analyzes out the short vertical component of point a, and what is left is an elliptical motion of point b. Since the elliptical motion has the same wavelength (λ) as the system, the information load of Interpretation C is 9. The analysis of the coding model agrees with Johansson's idea that the shortest common component will be factored out in motion analysis.

Result: Observers see the motion in Interpretation C. In this situation the perceptual system seems to have no prejudice against ellipses.

Discussion: The application of the coding model to motion perception is quite successful in predicting the hierarchical structure of the interpretations of motions; common motions are coded and interpreted as the reference frames. And in relation to these reference frames, residual motions are analyses or synthesized.

Coding theory of human walking motion

Cutting, J. E. (1981). Coding theory adapted to gait perception. *Journal of Experimental Psychology: Human Perception and Performance, 7*, 71-87.

Johansson (1973) demonstrated that the actions of human beings could be identified from the movements of lights mounted on the major joints of the body. That is, with the surround darkened, the flow pattern of these lights is sufficient to determine the presence of an individual painting a wall, bicycling, walking, running, or doing push-ups.

Cutting (1981) adapted Restle's (1979) coding theory for motion perception to the perception of human walking motion (or gait). The adaptation required some modifications of Restle's model, since Restle's coding model is designed for projections of simple circular motions of a few points and not for complex motion patterns like human locomotion. Before describing the modification of coding model (which requires two steps), Cutting first presents a demonstration that shows how well people can identify a human walker from a moving configuration of lights that simulate a human walker.

Demonstration 1: Previous studies (Johansson, 1973; Cutting,1978a; Cutting & Kozlowski,1977; Cutting, Proffitt, & Kozlowski, 1978) have shown that the lights mounted on the joints of human body were sufficient for perceiving walking. This demonstration explores the perception of human walking from the lights mounted *off* the joints of a human body. A computer program was used to display lights as if they were mounted

halfway between the major joints (Figure 86). The total number of lights were seven representing only the right side of the body. (One of the lights was mounted on the head to make the display look natural.)

Results: All 10 viewers reported seeing a person walking although they were not quite sure of the locations of the light on the body.

Experiment 1: Cutting suggests that although lights off joints are sufficient for the perception of walking, lights on joints might be better stimuli than lights off joints for the task. This experiment is designed to compare these two types of stimuli. However, Cutting says that he was afraid that demand characteristics and other extraneous variables might intercede, if he were to ask viewers simply to compare on- and off- joint displays. Thus he chose a indirect method: He asked viewers to discriminate male walkers from female walkers with on- and off-joint stimuli.

Results: The judgments of gender were generally more accurate for on-joint stimuli than for off-joint stimuli.

A first coding model: This model was proposed to account for the result of Experiment 1. The notational system takes the following form: L=M(x), where L stands for the particular light under consideration and M(x) represents the motion of a particular point. M(x) can be any complex vector and is used as a primitive within this system. With this system on-joints stimuli are coded in the following way if they are considered as independent. (See the upper left panel of Table 4). First, the center of the motion of the body is described as $M(C_m)$. The motion of the light on the head with respect to the center of motion can be considered null. So, the coding of the motion of head is $1= M(C_m)+M(He) = M(C_m)$. The light on the shoulder is coded as $2=M(C_m)+M(S)$ and the light on the wrist as $3= M(C_m)+ M(S)+M(E)+M(W)$, where M(E) stands for the elbow. The movements of the lights mounted on the hip and ankle are determined in a similar manner.

The coding of the lights mounted off joints is as follows (See the upper right panel of Table 4). In this coding the lights are considered as independent. As for the head the code is the same as in the on-joint version. The movement of the light on the upper arm, mounted exactly halfway between the shoulder and the elbow, is described as $2'= M(C_m)+ M(S)+M(E)/2$, where M(E)/2 means that the length of the pendulum is halved but that the angular excursion as measured at the pivot remains the same. The movement of the light on the lower arm is composed of four complex vectors: those of the highest order center of moment, shoulder, elbow, and half of the wrist. Thus, $3'=M(C_m)+M(S)+M(E)+M(W)/2$. In an analogous manner, the composite vectors are determined for the movements of the lights mounted on the upper leg (4') and lower leg (5').

In the coding representations described above (for both the on- and

off-joint stimuli) the vectors are considered as independent, and the information load for each stimulus is the total number of vectors. When the stimuli are considered as coherent systems, the codes for the lights are reduced by substitution of common vectors and the information loads become less. (See the lower panel of Table 4.) It is apparent from the table that the reduction of codes is more efficient for the on-joint walker than for the off-joint walker. This result is reflected in the prominence value (P). Thus the coding analysis suggests that the on-joint representation is better than the off-joint representation. The same point can be seen in the tree structure representations of the codings shown in Figure 87: The on-joint walker is represented by a two branch system while the off-joint walker requires a four branch system.

Demonstration 2: Insufficiency of the first coding model is demonstrated. An anomalous walker was displayed to viewers, which was created by displacing various parts of body *but holding their absolute motion constant.* For example, the head was placed below the ankle on the screen. Likewise, the right shoulder was placed below the ankle but considerably behind the location of the head. The right elbow was placed marginally above the ankle, and so forth. Thus a bizarre arrangements were generated (Figure 88).

Results: None reported seeing the presence of a human walker. All reported coherence. But, to some viewers the canonical stimuli (normal walking patterns) are far better as coherent and impressive stimulus events than is the anomalous display.

A second coding model: The problem of the first coding model is that it can not distinguish a normal, canonical walker from the abnormal motion pattern in Demonstration 2. Thus Cutting proposes a new notational form: L=M(x,y), where L is movement of the particular light under consideration as a function of the movement M of point x with respect to point y. The comparative analysis of the canonical walker and the spatially anomalous walker is described in Table 5. It shows that the prominence of the canonical walker is larger than the prominence of the anomalous walker.

III. Treismam and her associates

Feature integration theory

Treisman, A. (1985). Preattentive processing in vision. *Computer Vision, Graphics, and Image Processing*, *31*, 156-177.

Treisman and Gelade (1980; Treisman and Schmidt, 1982) proposed a feature integration theory of attention. Their hypothesis was that at a preattentive stage, sensory inputs from the visual field are decomposed into features on separable perceptual dimensions, and under an unpredictable context the features of an object are integrated into the coherent percept of the object only by focusing attention to the location of that object. This hypothesis was supported by converging evidence reported in the two articles mentioned above. Treisman (1985) reviews some of the main findings of these earlier studies, and along with these, presents some new lines of evidence.

Feature integration theory predicts that texture segregation is easy when areas differ in simple properties like shape and color and difficult when a boundary is defined solely by a conjunction of properties (e.g., green triangles and red circles on the left and red triangles and green circles on the right). The former case is demonstrated in Figures 89a and 89b (Treisman and Gelade, 1980) and the latter in Figure 89c. Similarly segregation is easy when the boundary divides *P*s and *O*s from *R*s and *Q*s (Figure 89d); the letters on one side have a diagonal slash whereas those on the other side do not. If the areas mix *P*s with *Q*s and *R*s with *O*s (Figure 89e), there is no single distinguishing element, and texture segregation becomes much harder.

Feature integration theory is also supported by experiments using the visual search paradigm. If a single blue letter is embedded in a display of brown and green letter of other colors, it "pops out." Detection appears to be spatially parallel. There is no need to check each of the brown and green letters before the blue one can be found. Similarly, if a single curved letter (e.g., "S") is presented in a display of straight or angular letters (e.g.,"X" and "T"), it is also immediately salient. But if the task is to find a target which conjoins two properties (e.g., green and T), each of which is present in other distractors (e.g., green "X"s and brown "T"s), the search is much more difficult. Latencies increase linearly with the number of distractors, as if attention had to be focused on each item in turn (Treisman and Gelade, 1980). The slope relating search time to display size (number of distractors) is twice as steep on trials where the target is absent as on trials where it is present, which suggests a serial self-terminating search.

The role of attention can be tested more directly by giving subjects a

cue in advance, which tells them where the target will occur if it is present at all. If attention is needed to detect conjunction targets, the precue should eliminate the serial checking phase. On the other hand, with targets defined by a single feature, the cue should have very little effect; separate features are registered in parallel anyway. Displays like those in Figure 90a were used; shapes varied in shape, size, color, and whether they were outlined or filled. The target was defined either by a conjunction of properties, for example, a large brown outline triangle, or by a single property like red or large or outline. The location of the target was precued by flashing a pointer. The precue was valid on 75% of the trials on which the target occured. It was invalid on 25% of trials; in these cases the target occurred somewhere other than cued location. On invalid trials attention would be directed to the wrong location rather than distributed across the whole display. An invalid cue should therefore give rise to costs rather than benefits relative to the condition with no cue. The accuracy of performance for feature targets and that for conjunction targets were matched by presenting the display for a longer duration for the conjunction targets. The question was whether the effect of the cue would be greater for conjunction than for feature targets. Figure 90b shows the results; for conjunction targets, there was a substantial benefit from a valid cue, while for feature targets the cue had very little effect.

If attention is necessary for conjoining features, errors of conjunction can be predicted when attention is overloaded. Displays were briefly presented which contained a row of three colored letters in the middle and two black digits at each end of the array (Figure 91a; Treisman & Schmidt, 1982). In order to ensure that attention would not be focused on any single letter, subjects were asked to report first the digits, and then any colored letters that they were reasonably sure they had seen. Subjects reported almost as many "illusory conjunctions" in which the color of one letter was recombined with the shape of another as they did correct conjunctions. Some of these conjunction errors were made with high confidence and appeared to be genuine perceptual illusions. Does the occurrence of illusory conjunctions of shape and color depend on how similar the stimuli are on other dimensions? It seems that it does not (see Figure 91b). Subjects are as likely to attribute the color of the large filled triangle to the small outline circle as to attribute to it the color of the small outline triangle.

Interdependencies between the accuracy of target identification and the accuracy of target localization provide another evidence for feature integration theory. If we do conjoin only by attending to an object, we should be forced to locate a conjunction target in order to identify it correctly, whereas this would not be necessary for a feature target. Subjects were shown displays like those in Figure 92 and were asked both to identify the target and to say where it was (Treisman and Gelade 1980).

In the feature task, they had to decide on each trial whether there was an orange letter or an *H*. In the conjunction task they had to decide whether there was a blue *O* or a red *X*. Treisman and Gelade analyzed the conditional probability that the identity was correct given that the location was wrong. They expected this probability to be above chance for feature targets, and it was. Thus subjects could sometimes tell correctly that there was an orange letter in the display while mislocating it by two or more squares. For conjunction targets, on the other hand, correct identification was completely dependent on correct localization, as it should be if attention must be focused on a location in order correctly to combine the features it contains.

It seems, then, that information about features can be "free-floating" or indeterminate in location, but information about conjunctions is available only through accurate localization. If attention is over-loaded, free-floating features may recombine at random when their associations were originally arbitrary. In a natural scene, however, many conjunctions are ruled out by our prior knowledge.

Search asymmetry

Treisman, A., & Souther, J. (1985). Search asymmetry: A diagnostic for preattentive processing of separable features. *Journal of Experimental Psychology: General,114*, 285-310.

When a target in a visual search task is detected with little change in latency as the number of distractor items is varied, it is inferred that its critical property (or properties) is processed spatially in parallel. The increase in latency (or reaction time) in such a result is less than 5- or 6-ms per item. This pattern of result is called the pop-out effect.

Parallel search and pop-out are contrasted with the pattern of latencies characterizing serial processing. The main diagnostic for serial search is a linear increase in search latency as distractors are added to the display. When the slope on negative (target absent) trials is twice as steep as the slope on positive (target present) trials, it is inferred that the serial search is also self-terminating (Sternberg, 1966). In other words, subjects respond on positive trials as soon as they find the target, but check the complete display before deciding that it is absent. These inferences from search times have been questioned (e.g., Townsend, 1972), and it is certainly true that some parallel models can mimic the linear increasing functions generated by serial processing. However, in choosing to interpret linear increasing functions with a 2:1 slope ratio as evidence for serial self-terminating search, Treisman and her associates rely on additional evidence, such as the relation between the variances of search

latencies and display size, and the dependence of correct identification on accurate localization for targets that appear to be detected serially (Treisman & Gelade, 1980).

When search is serial, it is inferred that the search requires focused attention. A further prediction from feature-integration theory is that if serial attention is needed to conjoin features, it should also be needed to localize the absence of a feature from a particular item, whenever the same feature is present in other items. Thus a target characterized by a unique feature should be detectable by parallel processing. On the other hand, if the feature is present in all items except the target, each will have to be checked serially in order to localize the one item which is not conjoined with the relevant feature. Experiment 1 tested the presence of the predicted asymmetry between search latencies for the target with a unique feature and for the target without it.

Experiment 1: A pair of items were used as stimuli: a circle either with or without a vertical line which intersected the base (see Figure 93). In one condition (*presence*), the target had the line and the distractors did not, so subjects could look for the presence of the line; in the other condition (*absence*), each distractor had the line but the target did not, so subjects were to look for the absence of the line.

Results: The mean search times are shown in Figure 94. For the target with the line (*feature present*), positive responses gave a slope of 4.0 ms per item; negatives gave a slope of 2.9 ms. On the other hand, for the target without a line (*feature absent*), positives gave a slope of 19.7 ms per item and negatives a slope of 38.9 ms per item. The prediction of asymmetry was confirmed.

The results suggest that the circle with an intersecting line possesses one or more features which are absent from an intact circle. But the results does not specify what those features are; possible candidates are straightness, vertical orientation, intersection, angles, and line ends (terminators). Further experiments would be needed to determine which are critical.

Experiment 2: This experiment had two aims. The first was to replicate the line search task (in Experiment 1) comparing homogeneous and heterogeneous shapes as distractors, to see whether the flat pop-out function for the presence of the line target depended on the distractors all being identical circles. This aim was set up because several earlier studies have shown a large distractor heterogeneity effect in search and suggested that identical stimuli may be processed in a special way. In order to see if distractor heterogeneity interacts with search for feature presence or absence, Treisman and Souther used displays consisting of randomly mixed circles and isosceles triangles, again with or without vertical lines intersecting the base.

The second aim was to compare search for presence and for absence with another simple feature, the color green. The color green differs from the line feature in a critical respect: it is a substitutive feature in that its absence implies the presence of another color, which may be equally salient and preattentively detectable. Subjects were told either to look for the presence of a green target among red and black distractors, or to look for a target that was not green (and was therefore red or black) among distractors that were all green. Search asymmetry was not expected in this color experiment.

Results: The calculated best-fitting slopes and intercepts for the functions relating search times to display size are given for each condition in Table 6. The mean search times for the heterogeneous condition are shown in Figure 95. As in Experiment 1, there is a striking asymmetry between the search latencies for the line target and for the absence-of-line target.

A new finding is that heterogeneity has a different effect on search for feature presence and search for feature absence. There is no effect of distractor heterogeneity on search for the presence of a line. Thus feature pop-out, when it occurs, does not depend on all the distractors being identical.

In search for a shape which lacked an intersecting line, heterogeneity of the carrier shapes significantly slowed performance. Heterogeneity seems to have made subjects more cautious in deciding that each shape did have an intersecting line and was therefore not the target.

The color conditions differ strikingly from the line conditions: No asymmetry is present here. Both the green target and the nongreen target seem to be detected fast and with minimal effects of the number of distractors and no effect of irrelevant variations in shape.

Experiment 3: This experiment tested a more hypothetical pair of features-*closure* and *free ends* (or *terminators*)-in the same search paradigm. More specifically, search for a triangle among angles and lines was compared with search for an angle among triangles. The angles and diagonal lines were identical to those which formed the triangle (see Figure 96). The question was whether the pattern of performance would closely resemble the shape and line condition or the color condition (in Experiment 2). If closure functions as a perceptual feature which characterizes triangles but not their component angles and lines, the task with the triangle target could become a search for the presence of the closure feature (analogous to search for the presence of an extra line intersecting a shape). Conversely, search for an angle in triangles could either be mediated by search for the absence of closure (analogous to search for the single shape with no intersecting line, or, if terminators also function as preattentive features, by search for the presence of

terminators. In the latter case, there might be no asymmetry; the pattern of performance should resemble that obtained with the colors.

Results: (Figure 97) When the target was a triangle in angle and line distractors, it was detected almost as fast as the shape with line, and with little effect of display size. The result implies that the triangle has a primitive feature which is preattentively detected and which is not present in the angles and lines.

The results with the nontriangle target (right angle) were less clear. Display size had a significant effect. However, the slope was much less than the feature-absent slope with the shape and line displays of Experiments 1 and 2, averaging only 6.1 and 9.5 ms per item for positive and negative displays, respectively. It seems that the removal of a triangle line, at least for some subjects, leaves a stimulus with a positive feature which can be detected preattentively. The implication may be that both a triangle and an angle have different and complementary primitive features, perhaps closure for the triangle and free ends or terminators for the right angle.

Experiment 4: This time the displays contained circles with and without gaps. In one condition, the target was a circle with free ends (a gap) in a display of circles without gaps: in the other condition, the target was a complete circle with no gap in a display of circles with gaps (Figure 98). The tasks could be defined in two ways: as search for the presence or for the absence of line ends, or as search for the presence or absence of closure (a closed circle). In this experiment, the effect of feature discriminability on search for presence and absence was also tested by varying the size of the gap. Line ends are, in a sense, a categorical or discrete feature; if the size of the gap is above threshold, they are either present or not. If the presence of a gap is coded by the detection of line ends their spatial separation should have little effect on search. Closure, on the other hand, can be defined perceptually in two different ways. By one definition, it is synonymous with connectedness, which is the inverse of free ends and categorical in the same way. By another definition, however, it should be a graded feature, depending on the degree to which an area is enclosed by a convex contour.

Results: (Figure 99, Table 7) The results show a striking asymmetry in the difficulty and the strategy of search. When the target was a circle with a gap, search was fast, independent of gap size and little affected by display size. The data suggest that the presence of the gap is detected categorically, perhaps because the line end or terminator feature pops out of the display.

On the other hand, when the target was a closed or connected circle, search appeared to be serial, its rate strongly affected by the size of the gap in the distractors. The implication is that the closed circle lacks any

unique distinctive feature which can be preattentively detected by the perceptual system.

How can these findings be related with the finding in Experiment 3 that triangle targets pop out of displays containing angles and lines? First, the new results confirm that the triangle was not detected by the absence of free ends, because the complete circle target also differed from the circles with gaps in having zero instead of two line ends or terminators. Second, they show that the relevant target feature in the triangle displays was not the connectedness of the outer contour. In this categorical sense of the word, closure does not seem to be preattentively available.

Another distinctive characteristic of the triangles in the displays of Experiment 3 was their acute angles.

Experiment 5 investigates search for acute angle targets among right angles and lines, to see whether this produces the same flat functions that was obtained with triangle targets in Experiment 3.

Results: (Figure 100) With the acute angle targets, there is clearly a substantial and significant effect of display size, whereas with the triangle targets there was almost none. The data give no evidence that acute angles are coded preattentively and in parallel, and appear to rule out the possibility that the parallel preattentive detection of triangle targets is mediated by feature detectors for acute angles.

Treisman and Souther return to closure as the most likely property mediating early parallel detection of triangles. However, in order to retain this hypothesis, they redefine the term , clearly distinguishing it from connectedness. It is suggested that the relevant sense of closure may be the second sense that was defined earlier (in the section of Experiment 4). In this sense the feature is a graded one, which should mediate categorical pop-out only if the distractors totally lack it, and not if they possess it to some degree but quantitatively less than the target. In Experiment 4, the complete circle begins to emerge preattentively when the gap size is large enough to reduce the distractors to semicircles. The right angle distractors in triangle target displays, may be below the threshold to activate closure detectors at all, so that the triangle differs categorically from the angle and line distractors.

General Discussion: The hypothesis that Treisman and Souther suggest to account for parallel search and presence-absence asymmetries is that perceptual features are separately registered in different maps. Figure 101 shows a crude representation of two separate modules which analyze colors and orientations, respectively, into ordered stacks of *feature maps*. A possible implementation of spatial attention could be through connections to a *master map* of locations, in which the positions of any discontinuities in stimulation are coded without specific information on the nature of the discontinuity. Because attention can also be guided by

preattentively detected features, it must be assumed that any given feature map can also selectively index locations containing the relevant feature in the master (location) map. Any feature concurrently accessed by the attentional spotlight would be conjoined. Serial search for feature absence is explained by the same assumptions previously used in feature-integration theory to account for serial search in conjunction tasks (Treisman & Gelade, 1980).

Two different strategies are available: (a) to inspect a feature map and to detect categorically the presence or absence of activity anywhere in that map, or perhaps to discriminate between two clearly different overall levels of pooled activity. This strategy can be used when the target has a distinctive, preattentively detected feature which the distractors do not share, or which the distractors possess to a lesser degree. The search in this case is parallel or global, over the display as a whole, and the target will pop out. (b) When target features must be localized (i.e., when the target is defined by the absence of a feature or when the target and the distractors differ only quantitatively on the relevant dimension), focused attention and serial scanning would be required. Latencies show a linear relation to display size, with a 2:1 ratio of slopes on negative and positive displays.

There was another finding that needs an explanation. Treisman & Souther found large differences in slopes across different conditions (or experiments), in all of which search appeared to be serial and self-terminating. For example in Experiment 4, the rate of scanning for closed circle targets varied dramatically with the gap size of the distractors. Treisman & Souther suggest two possible explanations. So far they have attributed the differences in slope to the idea that the more discriminable each distractor is from the target, the quicker it can be rejected in the course of serial scanning. However, the scanning rate in some conditions would be very high if these were assumed to be the only variable (as little as 13 ms per item for closed circles among distractors with the largest gap size).

An alternative account can be proposed if one considers the effects of target-distractor discriminability on the level of *pooled* activity among feature detectors. Suppose that the relevant feature distinguishing the target from the distractors is shared by both, but they possess it to differing degrees. For example, the target might be more "closed" than the distractors. The pooled response to displays containing one target will differ from the pooled response to displays containing only distractors by the same fixed increment or decrement, regardless of the number of distractors. According to Weber's Law, however, this fixed difference should have a larger impact at low levels of background activity (few distractors) than at high levels (many distractors). Thus, with large

displays (many distractors), subjects may serially scan small *groups* of items rather than individual items.

By the same reasoning, search for absence using the pooled activity measure should suffer bigger decrements in discriminability with increases in the number of items than should search for presence. Thus the pooled response hypothesis and Weber's law provide an account of search asymmetry.

Treisman, A., & Gormican, S. (1988). Feature analysis in early vision: Evidence from search asymmetries. *Psychological Review, 95,* 15-48.

Two kinds of decomposition into more primitive elements are possible: analysis into properties and analysis into parts. These two forms of analysis are orthogonal, because each local part must have at least a minimal set of properties. In this article the authors are concerned with dimensional analysis, with properties rather than parts. They define a *dimension* as a set of mutually exclusive values for any single stimulus (Garner, 1974; Treisman, 1986). In this article the authors are concerned primarily with evidence for separability of features *within* a dimension rather than with separability of one dimension from another. Separability is a relation between features rather than an absolute property of an individual feature.

The pop-up effect in search may offer one of the most direct tests for separable features, detected through early, spatially parallel and automatic coding. The target is identified preattentively, and its presence tends to "call" attention.

Treisman suggested elsewhere that subjects check a pooled response from the relevant feature map for the presence of activity anywhere in that map (Treisman, 1985; Treisman & Souther,1985). The idea of a pooled response to a particular feature, independent of spatial locations, has also been proposed in computational vision by Ballard (1984) as a tool for segmenting the visual field.

The pooled response model makes an interesting prediction: A target should be preattentively invisible if and when it is defined only by the absence of a feature that is present in all the distractors. If we measure only a pooled response to the relevant feature, we expect the difference between displays containing n-1 instances of the relevant feature and displays containing n instances to decrease rapidly as n is increased. Once the difference becomes unreliable relative to "noise" in the system, subjects should be forced to search serially.

For discriminations on one shared dimension, subjects should be able to pool the relevant feature activity over groups of items when the difference between target and distractors is large without running the risk of

increased misses or false alarms. In fact, Weber's law should determine the discriminability of groups of a given size when they do and do not include a target. This law states that the size of the just noticeable difference is a constant ratio of the background level. According to Weber's law, in deciding whether a target is present within an attended group, subjects will compare the activity in the pooled response of a group containing a target and a group of the same size containing only distractors. When the distractors produce a low level of activity, subjects must discriminate a group with more activity (because the target replaces one distractor) from groups with a uniformly low level. On the other hand, when the distractors produce a high level of activity in the relevant detectors, subjects must discriminate a group with less activity from groups with a level that is uniformly high. The application of Weber's law to different levels of pooled distractor activity predicts an asymmetry of search for targets with more of the relevant property against a low background level and for targets with less of the relevant feature against a high background level.

In the following section the authors report a series of findings regarding the determinants of pop-out and search asymmetry in a number of apparently simple discriminations. The experiments using simple stimuli can be divided into five groups: those testing quantitative dimensions-line length, darkness of grey, and number of lines; those testing spatial properties of a single line-orientation and curvature; those exploring the coding of prototypical values and deviations; those exploring possible emergent features created by the arrangement of two straight lines-intersection, juncture, and convergence; and those testing examples of relational or topological properties-connectedness and containment (inside vs. outside).

Quantitative Dimensions

In the search paradigm (Treisman & Souther, 1985) the presence-absence difference (e.g., between circles with and without an added line) may represent only the ends of a continuum of neural response. Between *some* and *none* there could be *more* and *less* activity. To test the claim that pop-out is mediated by a positive signal from the target rather than by faster detection of homogeneity for the simpler distractors, the authors predict that there should also be a search asymmetry favoring the target that has more of a shared property when target and distractors differ only in degree on a quantitative dimension.

In *Experiment 1* Treisman & Gormican varied the line length of target and distractors; in *Experiment 2*, their contrast (darkness vs. lightness of grey on a white background); and in *Experiment 3*, the number of lines (pairs vs. single lines). According to the pooled response model, the longer line, the darker grey dot, and the pair of lines among singles are expected to be

the positively signaled targets against the background of less distractor activity; and the shorter line, the lighter grey dot, and the single line to be signaled only by a reduction of activity from a higher background level produced by the more extreme distractors.

Experiment 1 and 2 included two levels of discriminability to test whether search would become parallel when discriminability was high, and if so, whether an asymmetry would remain.

Experiment 1: (Line Length) In both the easy and difficult condition, the longer line was 8 mm (subtending 1.1° at a distance of 42 cm). In the difficult condition the shorter line was 6.5 mm and in the easy condition it was 5 mm. (Figure 102a)

The results, shown in Figure 102b and Table 8, confirmed the hypothesis that a search asymmetry would be present and that it would favor the more extreme value as target.

Experiment 1a. (Line Length: Search With Matched Distractors) The account of Experiment 1, in terms of Weber's law and a pooled response, attributes the search asymmetry to the different distractor backgrounds rather than to the direction in which the target contrasts with the distractors. The smaller target is harder to find, not because it is smaller, but because the distractors are larger in this condition than in the other. The same absolute difference in length is judged as less prominent when distractors are larger than when they are smaller. To test this claim Treisman and Gormican conducted Experiment 1a, which used both a larger and a smaller target with the same medium-length distractors so that the ratios of the lengths in two conditions would be equal to each other. They predicted no asymmetry of search latencies in this experiment because the Weber fraction was the same in the two conditions. (The distractors were 7.5 mm long. The targets were either 10 mm long or 5 mm long.)

Results: The asymmetry found in Experiment 1 was no longer present.

Experiment 2: (Contrast) Two sets of displays were used to test two different levels of discriminability.

Experiment 3: (Number or Proximity of Lines) (See Figure 103a)

Results of Experiments 2 & 3 are shown in Figure 103b and 104, and in Table 8. Again, all showed a search asymmetry favoring the more extreme value as target. This time, however, with the easier discriminations the search functions were almost flat.

Line Curvature and Line Orientation

In the next experiments two attributes of a single line were tested- the contrast between straight and curved and between vertical and tilted. Treisman and Gormican's aim was to see whether any asymmetry would be present between performance with a curved (or tilted) target among straight (or vertical) distractors and with a straight (or vertical) target among curved (or tilted) distractors. With both curvature and orientation,

one value (straight or vertical) can be taken as standard and unique for that dimension. Other stimuli can take a range of values that depart to various degrees from the standard value. Treisman and Gormican were interested in the possibility that a unique coding exists for the standard value, with deviations represented as reduced activity relative to the standard value. Alternatively, it may be the case that deviations from the standard are positively coded, leaving the standard to be detected only by default.

Experiment 4: (Curvature) Treisman and Gormican tested the three levels of discriminability. Figure 105a shows the displays used to test straight and curved targets.

Results: (Figure 105b) Search asymmetry was found. When subjects were looking for a single straight line in a background of curves, they appear to have checked items or groups of items serially. The slope of response latencies against display size increased sharply as the discrimination became more difficult. Curvature appears to be sensed directly.

Experiment 5: (Orientation) See Figure 106a.

Results: (Figure 106a and Table 8) A striking asymmetry was found, and again it favored the non-standard value. A tilted target was detected equally fast for all display sizes tested, whereas a vertical target among tilted lines was found more slowly the more distractors were present.

The results do not distinguish two possible ways of coding straight and vertical: They could be represented simply by the absence of activity in the detectors for curved and for tilted (i.e., as the null or default values on those two dimensions). Another possibility is that straight and vertical are coded as the presence of activity in a population of detectors for these standard or reference values and that the same detectors are also activated (almost as much) by the curved or tilted lines. Following the analogy to the standard circles and circles plus lines in the Treisman and Souther (1985) experiment, the curved or tilted lines could have been coded as straight or vertical lines with an additional feature marking the nature of the deviation, just as the circle with the added line is coded as the standard circle with an additional feature (the intersecting line). This interpretation may be preferable in light of results from other experimental paradigms showing more accurate coding and easier labeling of standard values when the stimuli are presented one at a time (e.g., Attneave & Olson, 1967; Rosch-Heider, 1972).

To control for the possibility that the asymmetry of search performance in Experiments 4 and 5 are generated by the visual frame effects of a rectangular aperture of the tachistoscope, *Experiments 4a, 5a, and 5b* are conducted.

Experiment 4a: (Curved and straight line displays/Control with circle aperture). (See Table 8).

Experiment 5a: (Line orientation/Control with circle aperture). (See Table 8).

Experiment 5b: (Line orientation/Control with tilted frame & with vertical frame) (See Table 8).

Results of Experiments 4a, 5a, and 5b: (See Table 8) From the results of these experiments Treisman and Gormican conclude the following: (a) the effect of display size in search for straight and for vertical targets was not due *solely* to competing activity produced by the frame (because it was still present, at least to some degree, with circular frames; and (b) the null, or standard, value for line orientation is at least partly defined by alignment with the edge of a visible or inferred framework rather than simply the one that is vertical on the retina or with respect to gravity.

Experiment (not numbered/Control with both target and distractor tilted): (See Table 8).The aim of this experiment is to rule out the possibility that search asymmetries reflect, not so much a more difficult task when the target has the standard value (vertical, in Experiment 5), but an easier task when the distractors have the standard value.

Results: (Table 8)The search latencies were unaffected by the number of distractors.

The only condition in which search latencies were affected by the number of distractors, suggesting serial search with focused attention, was the condition with a vertical (or frame-aligned) target among tilted distractors. It seems, then, that there is a special difficulty in detecting a standard target rather than a special case in coding standard distractors.

Treisman and Gormican's original conclusion, that standard values of orientation and straightness are represented only as the absence of a distinctive feature (because they share the reference value with the tilted or curved lines), seems to fit the data from this enlarged set of experiments.

Prototypes and Deviations of Shape and Color

Experiment 6: (Circles and Ellipses; Search for a circle among ellipses as distractors and for an ellipse among circles as distractors). One might expect the visual code for circles (prototype) to be simpler or more economical, which might make them easier to detect in a search task. However, the results with curved versus straight lines and tilted versus vertical lines suggest that the reverse might be true. If a general property of perceptual coding is that it gives least response to standard values and represents stimuli as departures from a standard or norm, the asymmetry might be in the opposite direction.

There were two conditions: In one condition the orientation was fixed (the ellipses were always vertical); in the other condition, the ellipses were haphazardly oriented. (Figure 107a).

Results: (Figure 107b) Neither target popped out, but there was a large

asymmetry favoring search for the target ellipse rather than the target circle. Search for the ellipse was fast, suggesting that groups of circles could be checked in parallel for the presence of a target ellipse, whereas this was impossible for a target circle among distractor ellipses. There was no effect of fixed versus varied orientation on search for ellipse targets, but varied distractor orientations did slow search for the target circle.

Experiment 7 (Color) explored the possibility that a search asymmetry would favor detection of a deviating color among distractors that are prototypes, relative to detection of prototypical color targets among distractor colors that deviate from them.

Results: (Figure 108, Table 8) Response latencies were significantly longer when the prototypical values definded the targets, and there was a significant interaction with display size. The effects were in the predicted direction. That is to say, the prototypical colors were found more slowly and with more effect of distractors than the deviating colors. However, the effects were much smaller than with other dimensions. It seems unlikely that the effects were so small simply because the discriminations were very easy. The intercepts were no lower than average, and the error rates were higher than for any other experiment giving equally fast and flat search functions. There is a hint in these results that parallel processing is more natural for color than for properties of lines or shapes, even when the discriminations are difficult and accuracy is not guaranteed.

Implications for Pooled response model. It may be worth trying to link the prototype-deviation asymmetry to neural channels for color and to use the analogy to throw light on other dimensions, like curvature and tilt, that also give search asymmetries. Coarse coding is certainly used on the color dimension: Each stimulus value activates more than one channel, and each channel is activated by many different values. However, the prototypical red, green, and blue dots that were used in Experiment 7 probably have produced more activity within their own primary channel and less on either neighboring channel than the magenta, lime, and turquoise. A magenta dot would primarily affect the red channel, but it would also produce some activity in the blue channel. Again, Treisman and Gormican draw an analogy with the circle-plus-line experiment. Detection of a magenta target might be mediated by the added presence of activity on the blue channel as well as by the shared activity on the red channel. A red target, on the other hand, would produce more activity than magenta on the shared red channel, but against a background level that was already high through the effects of the multiple magenta distractor dots. Figure 109a shows the model.

This interpretation of the color asymmetry matches the hypothesis proposed for the curvature and orientation dimensions. It retains the idea that standard values are coded as the absence of activity on the deviating

dimensions; but it assumes that they are positively coded on their own channels, with the proviso that the deviating stimuli also produce substantial activity in the prototype channel. When the target is a prototype, it activates its own channel more than any individual distractor does, but the increase must be detected against a high background level produced by pooled distractors. When the target is the deviating stimulus, it activates the prototype channel less than the prototype, but in addition it produces activity on another channel on which the prototype distractors produce little or no effect. The asymmetry then follows from Weber's law: Detecting *some* against a background of *none* should be easier than detecting *more* against a background of *some*.

There are alternative models, shown in Figure 109b and 109c, that would also give rise to the asymmetry in cases where the detectors are not grouped into widely spaced channels and where the deviating stimuli maximally activate their own separate detectors. In each case the hypothesis is that detectors that are maximally sensitive to standard or reference values are more strongly activated by off-standard values than detectors for nonstandard values are by standard values. (Note that the functional detectors are not necessarily assumed to be single neural units.)

Line Arrangements

The next three experiments tested some possible emergent features created by the spatial arrangement of two straight lines. The features were intersection, juncture, and convergence (vs. parallelism).

Experiment 8: (Intersection; Search for an intersection target among line and angle distractors and for a line target among intersection distractors) See the left panel of Figure 110a.

Experiment 9: (Juncture; search for a right angle among right angles with a gap and for a right angle with a gap among right angles without a gap) See the central panel of Figure 110a.

Experiment 10: (Convergence/ Parallelism; Search for a pair of parallel lines among distractor pairs of converging lines and for a pair of converging lines among distractor pairs of parallel lines) See the right-hand panel of Figure 110a.

Results of Experiments 8, 9, and 10: The search latencies are shown in Figure 110b, each below its relevant display type. None of the tasks appears to allow parallel search. Each showed a significant increase in latency as the number of distractors increased. The rate of serial search was very slow both for the joined lines and for the parallel lines. Search for the separate lines and for the converging lines was considerably faster than search for the joined or parallel lines. Neither, however, appears to be detected in parallel by the pop-out criterion. The results for intersection conflict with those of Julesz and Bergen (1983), who found easy texture segregation between pluses and *L*s and parallel search for plus among *L*s:

Their displays may have allowed the use of other, primitive features besides the presence of intersection. The results of Experiments 8, 9, and 10 provide no evidence that any of these three pairs of line arrangements generates an emergent feature that is preattentively coded (Pomerantz, Sager, & Stoever, 1977; Treisman & Paterson, 1984).

Topological Properties: Connectedness and Containment

The last two experiments tested two topological properties-line connectedness and containment (dot inside a boundary)-together with their opposites-line ends (terminators) and exclusion (dot outside a boundary).

Experiment 11: (Connectedness and Terminators) This experiment was reported by Treisman and Souther (1985). The stimuli were closed circles (subtending 1.5°) and circles with radomly located gaps. They tested three different gap sizes (one eighth, one fourth, and one half the circumference).

Results: (Figure 111 and Table 8) The circles with gaps popped out of displays of closed circles, but the closed circles were found only through apparently serial, self-terminating search, the rate of which varied with the size of the gap. The results suggest that the different search rates for closed circles reflect search through groups of different sizes, with items within groups checked in parallel to see if their pooled response on the dimension of closure exceeds the criterion for target presence.

Experiment 12: (Containment-Inside vs. outside) The stimuli were mixed displays of two different convex container shapes with a 2.5-mm black dot either inside or outside each shape and mixed displays of two different concave container shapes, again with 2.5-mm dots either inside or outside. (Figure 112a)

Results: (Figure 112b and Table 8) Serial search appeared to be necessary in both cases. Concave shapes gave slower search rates than did convex shapes. In both experiments, there was a significant search asymmetry giving steeper slopes for the inside dot target than for the outside dot. This is consistent with the idea that the relevant feature is the noncontained dot.

Evidence for Serial Search

In the series of experiments described above, Treisman and Gormican have interpreted any search function that increased substantially with display size as implying a serial scan, either of single items or of groups of items. They say that this assumption needs to be checked. Although one can devise parallel models that mimic serial processing (Townsend, 1972), they take reaction time functions that increase linearly with display size as prima facie evidence of serial search. They consider that ratios of positive to negative slopes that approximate 0.5 suggest that the search is self-terminating. They accept, however, that converging evidence from a number of other tasks is necessary to support these inferences (Treisman &

Gelade, 1980).

The grand means for the 37 conditions with slopes greater than 10 ms per item are shown in Figure 113a; the remaining 17 conditions (which gave apparently parallel search) are shown in Figure 113b. The proportion of the variance with display size that was due to linearity was .987 for the positives and .9998 for the negatives. The ratio of positive to negative slopes averaged 0.53 across the 37 experiments. This is very close to the ratio of 1:2 predicted by serial self-terminating models.

Role of Eye Movements

A final possibility to consider is that the apparently serial scan reflects successive eye movements and fixations rather than serial focusing of attention. A critical test is to compare search rates when eye movements are ruled out by brief presentations. Treisman and Gormican compared search for a shorter line among longer lines in displays of one to six items when exposure durations were limited to 180 ms and when they continued until the response was selected (as in all their previous experiments).

Figure 114a shows the results. There was a highly significant effect of display size on search latencies with the brief exposure. However, the slopes were significantly lower than with the unlimited exposure. A number of explanations for the difference are possible: The latencies with unlimited exposure might include some eye-movement time or some rechecking time, or the search times with limited exposure might have been curtailed because the display disappeared before all items could be checked. To test this last possibility, Treisman and Gormican made the assumption that subjects who missed 23% of targets with displays of six items were able to check on average only 77% of the display-that is, 4.62 items. Similarly, the fact that 17% of the targets were missed with displays of four items suggests that on average only 83% of the items were checked-3.32 items. Figure 114b shows the graphs replotted against display sizes corrected in this way for the mean proportions of targets missed in each condition. The difference in slopes has almost disappeared with this correction, suggesting that curtailed processing contributes more to the reduced slopes than the elimination of eye movements.

General Discussion

A basic assumption, with which Treisman and Gormican's data are consistent, is that early vision is analytic; it decomposes stimuli along a number of dimensions and into a number of separable components. In visual search task, we suggest that pop-out occurs when the target has a unique feature, which is coded early in visual processing and which is not shared by the distractors. The features may either be discrete and categorical elements (e.g., terminators) that can be only present or absent, or they may be values on a continuous dimension that activate nonoverlapping

populations of functional detectors and that therefore also mediate categorical discriminations.

Treisman and Gormican reported a series of search experiments whose results may help to diagnose some of the functional features coded early in visual processing. They emphasize, however, that no search task allows direct inference to the complete code for a particular stimulus in any absolute sense.

References

Attneave, F. (1968). Triangles as ambiguous figures. *American Journal of Psychology, 81*, 447-453.

Attneave, F. & Olson, R. K. (1967). Discriminability of stimuli varying in physical and retinal orientation. *Journal of Experimental Psychology, 74*,149-157.

Ballard, D. H. (1984). Parameter nets. *Artificial Intelligence, 22*, 235-267.

Breitmeyer, B. G. (1975). Simple reaction time as a measure of the temporal response properties of transient and sustained channels. *Vision Research, 15,* 1411-1412.

Broadbent, D. E. (1977). The hidden preattentive processes. *American Psychologist, 32*, 109-118.

Buffart, H., Leeuwenberg, E., & Restle, F. (1981). Coding theory of visual pattern completion. *Journal of Experimental Psychology: Human Perception and Performance, 7*, 241-274.

Cutting, J. E. (1978a). Generation of synthetic male and female walkers through manipulation of a biomechanical invariant. *Perception, 7*, 393-405

Cutting, J. E. (1981). Coding theory adapted to gait perception. *Journal of Experimental Psychology: Human Perception and Performance, 7*, 71-87.

Cutting, J. E. & Kozlowski, L. T. (1977). Recognizing friends by their walk: Gait perception without familiarity cues. *Bulletin of the Psychonomic Society, 9*, 353-356

Cutting, J. E., Proffitt, D. R., & Kozlowski, L. T. (1978). A biomechanical invariant for gait perception. *Journal of Experimental Psychology: Human Perception and Performance, 4*, 356-372.

Garner, W.R. (1974).*The processing of information and structure.* Potomac, Md,:Erlbaum.

Ginsberg, A. (1971). *Psychological correlates of a model of the human visual system.* Unpublished master's thesis. Air Force Institute of Technology.

Ginsberg, A. (1986). Spatial filtering and visual form perception. In K.R. Boff, L. Kaufman, & J.P. Thomas (Eds.), *Handbook of Perception and Human Performance, Volume II: Cognitive Processes and Performance.* New York: John Wiley & Sons.

Gogel, W. C. (1974). Relative motion and the adjacency principle. *Quartery Journal of Experimental Psychology, 26*, 425-437.

Hinton, G.E. (1981). A parallel computation that assigns canonical object-based frames of reference. *Proceedings of the 7th International Joint Conference on Artificial Intelligence.* 683-685.

Janez, L. (1983). Stimulus control of the visual reference frame: Quantitative theory. *Informes de Psychologia*, 133-147.

Johansson, G. (1950). *Configurations in event perception.* Stockholm, Sweden: Almqvist & Wiksell.

Johansson, G. (1973). Visual perception of biological motion and a model for its analysis. *Perception & Psychophysics, 14*, 201-211.

Julesz, B., & Bergen, J. R. (1983). Textons, the fundamental elements in preattentive vision and perception of textures. *Bell System Technical Journal, 62*, 1619-1645.

Koffka, K. (1935). *Principles of Gestalt psychology.* New York: Harcourt Brace Jovanovich.

Kopfermann, H. (1930). Psychologische Untersuchungen uber die Wirkung zweidimensionaler korperlicher Gebilde. *Psychologische Forschung. 13*, 293-364.

Kruschke, J. K. and Palmer, S. E. (In press). Depth in reference frames for shape perception.

Leeuwenberg, E. L. J. (1967). *Structural information of visual patterns: An efficient coding system in perception.* The Hague, The Netherlands: Mouton.

Leyton, M. (1982). A unified theory of cognitive reference frame. *Proceedings of the 4 th Cognitive Science Conference.*, Ann Arbor, MI.

Mach, E. (1914). *The analysis of sensations.* Open Court. (Republished in 1959, New York: Dover.)

Marr, D. (1982) *Vision.* San Francisco, CA: W.H.Freeman.

Navon, D. (1977). Forest before trees: The precedence of global features in visual perception. *Cognitive Psychology, 9*, 353-383.

Palmer, S.E. (1975). Visual perception and world knowledge: notes on a model of sensory-cognitive interaction. In: D.A. Norman and D.E. Rumelhart (eds.), *Explorations in cognition.* Hillsdale, NJ: Erlbaum.

Palmer, S, E. (1980). What makes triangles point: Local and global effects in configurations of ambiguous triangles. *Cognitive Psychology, 12*, 285-305.

Palmer, S.E. (1982). Symmetry, transformation, and the structure of perceptual system. In: J. Beck and F. Metelli (Eds.), *Organization and representation in perception.* Hillsdale, NJ: Erlbaum.

Palmer, S. E. (1983). On goodness, Gestalt, groups, and Garner. Paper presented at annual meeting of Psychonomic Society, Sandiego, California.

Palmer, S.E. (1983). The psychology of perceptual organization: a transformational approach. In: J. Beck, B. Hope and A. Rosenfeld (Eds.), *Human and machine vision.* New York: Academic Press.

Palmer, S. E. (1985). The role of symmetry in shape perception. *Acta Psychologica, 59*, 67-90.

Palmer, S. E. (To be published). Reference frames in the perception of shape and orientation. Chapter to appear in Shepp, B., & Ballesteros, S (Eds.) *Object perception: Structure and Process.* Erlbaum: Hillsdale, N.J.

Palmer, S, E. & Bucher, N, M. (1981). Configural effects in perceived pointing of ambiguous triangles. *Journal of Experimental Psychology: Human Perception and Performance, 7*, 88-114.

Palmer, S, E. & Bucher, N, M. (1982). Textural effects in perceived pointing of ambiguous triangles. *Journal of Experimental Psychology: Human Perception and Performance, 8*, 693-708.

Palmer, S., Simone, E., & Kube, P. (In press). Reference frame effects on shape perception in two versus three dimensions.

Pomerantz, J. R., Sager, L. L., & Stoever, R. G. (1977). Perception of wholes and their component parts: Some configural superiority effects. *Journal of Experimental Psychology: Human Perception and Performance, 3*, 422-435.

Restle, F. (1979). Coding theory of the perception of motion configurations. *Psychological Review, 86*, 1-24.

Rock, I. (1973). *Orientation and form.* New York: Academic Press.

Rosch-Heider, E. (1972). Universals in color naming and memory. *Journal of Experimental Psychology*, 93, 10-20.

Rumelhart, D.E., & Siple, P.A. (1974). Process of recognizing tachistoscopically presented words. *Psychological Review. 81*, 99-118.

Selfridge, O., & Neisser, U. Pattern recognition by machine. *Scientific American.* 1960, *203*, 60-68.

Selfridge, O.G., & Neisser, U. (1963). Pattern recognition by machine. In E.A. Feigenbaum and J. Feldman (Eds.), *Computers and thought.* New York: McGraw-Hill.

Sternberg, S. (1966). High-speed scanning in human memory. *Science, 153*, 652-654.

Townsend, J. T. (1972). Some results on the identifiability of parallel and serial processes. *British Journal of Mathematical and Statistical Psychology, 25*, 168-199.

Treisman, A. (1985). Preattentive processing in vision. *Computer Vision, Graphics, and Image Processing, 31*, 156-177.

Treisman, A. (1986). Properties, parts and objects. In K. Boff, L. Kaufman, & J. Thomas (Eds.), *Handbook of perception and human performance, Volume 2: Cognitive processes and performance* (Chapter 35, pp. 1-70). New York: Wiley.

Treisman, A., & Gelade, A. (1980). A feature integration theory of attention. *Cognitive Psychology, 12*, 97-136.

Treisman, A., & Gormican, S. (1988). Feature analysis in early vision: Evidence from search asymmetries. *Psychological Review, 95*, 15-48.

Treisman, A., & Paterson, R. (1984). Emergent features, attention and object perception. *Journal of Experimental Psychology: Human Perception and Performance, 10*, 12-31.

Treisman, A., & Schmidt, H. (1982). Illusory conjunctions in the perception of objects. *Cognitive Psychology, 14*, 107-141.

Treisman, A., & Souther, J. (1985). Search asymmetry: A diagnostic for preattentive processing of separable features. *Journal of Experimental Psychology: General,114*, 285-310.

van Tuijl, H.F.J.M. (1980). Perceptual interpretation of complex line patterns. *Journal of Experimental Psychology: Human Perception and Performance. 6*, 197-221.

Wertheimer, M. (1923/1958). Untersuchungen zur Lehre von der Gestalt II. *Psychologische Forschung, 4*, 301-350. Abridged translation by M. Wertheimer: Principles of perceptual organization. In D. C. Beardslee & M. Wertheimer (Eds.), *Readings in perception.* Princeton, NJ: Van Nostrand,1958.

Weyl, H. (1952). *Symmetry.* Princeton, N.J.: Princeton University Press.

Table 1

Structural Information (I) of Alternative Subdivisions of Patterns Used in Experiment 1 (see Figure 2) and Frequency (f) of Responses to Each Subdivision

	Subdivision							
	a		b			a		b	
Pattern	I	*f*	I	*f*	Pattern	I	*f*	I	*f*
1	2	15	4	1	11	3	15	5	1
2	3	14	4	2	12	2	14	4	2
3	4	10	5	6	13	2	14	4	2
4	3	11	6	5	14	3	2	4	14
5	2	13	6	3	15	3	10	3	6
6	2	12	4	4	16	6	10	6	6
7	2	13	5	3	17	3	16	3	0
8	4	14	6	2	18	3	13	3	3
9	4	14	5	2	19	5	16	5	0
10	2	14	3	2	20	2	16	2	0

Table 2

Structural Information and Relative Efficiency of Revised Codes of Subdivisions Used in Experiment 1 (see Figure 2)

	Subdivision						
	a	b		a	b		
Pattern	$I_p(a)$	$I_p(b)$	$e_p(a/b)$	$I_f(a)$	$I_f(b)$	$e_f(a/b)$	E(a/b)
1	20	32	+.38	3	6	+.50	+.88
2	36	36	.00	4	5	+.20	+.20
3	44	48	+.08	5	7	+.28	+.36
4	20	20	.00	3	7	+.57	+.57
5	15	20	+.25	3	7	+.57	+.82
6	24	32	+.25	4	5	+.20	+.45
7	8	32	+.75	4	6	+.33	+1.08
8	13	20	+.35	5	7	+.29	+.64
9	12	29	+.58	5	7	+.29	+.87
10	16	20	+.20	2	3	+.33	+.53
11	12	45	+.73	6	7	+.14	+.87
12	8	32	+.75	4	5	+.20	+.95
13	8	40	+.80	4	5	+.20	+1.00
14	29	16	−.45	11	8	−.27	−.72
15	28	28	.00	4	4	.00	.00
16	36	44	+.18	8	7	−.13	+.05
17	16	26	+.38	5	10	+.50	+.88
18	20	20	.00	3	4	+.25	+.25
19	36	64	+.43	6	5	−.17	+.26
20	20	48	+.58	3	3	.00	+.58

Note. It should be noticed that the E(a/b) values are only relevant to the alternative subdivisions of the patterns to which they belong. They convey no information about the relative efficiency of the 20 a subdivisions with respect to one another. $I_p(a)$ = structural information of the primitive code of Subdivision a. $I_p(b)$ = structural information of the primitive code of Subdivision b. $e_p(a/b)$ = relative efficiency of Subdivision a compared with b at primitive code level. $I_f(a)$ = structural information of the final code of Subdivision a. $I_f(b)$ = structural information of the final code of Subdivision b. $e_f(a/b)$ = relative efficiency of Subdivision a compared with b at final code level. E(a/b) = ultimate efficiency of Subdivision a compared with b.

Table 3

Means and Standard Deviations of Reaction Times (in sec) to Easy and Difficult Subpatterns (see Figure 12) and Values of t For Dependent Observations

	Subpattern				
	Easy		Difficult		
Pattern	*M* reaction time	*SD*	*M* reaction time	*SD*	t_d
1	1.301	.383	2.099	1.144	−3.22**
2	1.350	.997	2.676	1.048	−3.58**
3	1.023	.516	2.124	1.072	−4.27**
4	1.762	.695	2.817	1.541	−3.60**
5	1.680	.907	2.394	2.240	−1.48
6	2.031	1.931	2.674	1.227	−1.62
7	.964	.451	1.566	.733	−3.19**
8	1.432	.617	2.118	.761	−3.63**
9	1.412	.331	2.161	.744	−5.01**
10	.886	.252	1.998	1.186	−4.38**
11	1.021	.399	2.350	1.347	−4.77**
12	.944	.332	1.909	1.335	−3.05**
13	1.650	.609	3.279	1.869	−2.86**
14	1.893	.922	2.630	1.320	−2.68**
15	1.245	.514	1.522	.567	−2.46*
16	1.260	.625	2.042	1.673	−1.84*
17	1.206	.519	2.534	1.227	−5.27**
18	1.221	.531	1.696	.751	−3.22**
19	1.345	.691	2.288	.970	−3.88**
20	1.221	.536	1.627	.625	−2.66**

Note. Easy and difficult subpatterns correspond to Target a and Target b in Figures 12–14.
d = dependent.
* $p < .05$. ** $p < .01$.

Table 4

Vector Analyses for Computer-Generated Walkers

On-joint walker: $I_i = 13$	Off-joint walker: $I_i = 15$
$1 = M(C_m) + M(He) = M(C_m)$	$1' = M(C_m) + M(He) = M(C_m)$
$2 = M(C_m) + M(S)$	$2' = M(C_m) + M(S) + M(E)/2$
$3 = M(C_m) + M(S) + M(E) + M(W)$	$3' = M(C_m) + M(S) + M(E) + M(W)/2$
$4 = M(C_m) + M(Hi)$	$4' = M(C_m) + M(Hi) + M(K)/2$
$5 = M(C_m) + M(Hi) + M(K) + M(A)$	$5' = M(C_m) + M(Hi) + M(K) + M(A)/2$
Reduced code by vector substitution: $I_r = 7$, $P = f(I_i/I_r) = f(1.86)$	Reduced code by vector substitution: $I_r = 11$, $P = f(I_i/I_r) = f(1.36)$
$1 = M(C_m)$	$1' = M(C_m)$
$2 = 1 + M(S)$	$2' = 1' + M(S) + M(E)/2$
$3 = 2 + M(E) + M(W)$	$3' = 1' + M(S) + M(E) + M(W)/2$
$4 = 1 + M(Hi)$	$4' = 1' + M(Hi) + M(K)/2$
$5 = 4 + M(K) + M(A)$	$5' = 1' + M(Hi) + M(K) + M(A)/2$

Note. M = movement of the point that follows it; C_m = highest order center of moment; *He* = head, *S*= shoulder; *E* = elbow; *W* = wrist; *Hi* = hip; *K* = knee; *A* = ankle. Numbers refer to the movements of lights shown in Figure 2. I_i = total number of vectors needed to specify the lights independently; I_r = total number of vectors needed to specify the lights as a coherent system. P is the prominence of the perceived configuration as a function (f) of I_i divided by I_r. See also Footnote 1.

Table 5

Vector/Center Analyses for Computer-Generated Stimuli

Canonical walker: $I_t = 19$	Spatially anomalous "walker": $I_t = 19$
$1 = M(C_m,g) + M(He,C_m) = M(C_m,g)$	$1' = M(x,g) + M(He,i) = M(x,g)$
$2 = M(C_m,g) + M(S,C_m)$	$2' = M(x,g) + M(S,ii)$
$3 = M(C_m,g) + M(S,C_m) + M(E,S)$	$3' = M(x,g) + M(S',iii) + M(E,S')$
$4 = M(C_m,g) + M(S,C_m) + M(E,S) + M(W,E)$	$4' = M(x,g) + M(S'',iv) + M(E',S'') + M(W,E')$
$5 = M(C_m,g) + M(Hi,C_m)$	$5' = M(x,g) + M(Hi,v)$
$6 = M(C_m,g) + M(Hi,C_m) + M(K,Hi)$	$6' = M(x,g) + M(Hi',vi) + M(K,Hi')$
$7 = M(C_m,g) + M(Hi,C_m) + M(K,Hi) + M(A,K)$	$7' = M(x,g) + M(Hi'', vii) + M(K',Hi'') + M(A,K')$
Reduced code by vector/center substitution: $I_t = 7$, $P = f(I_t/I_r) = f(2.71)$	Reduced code by vector/center substitution: $I_t = 13$, $P = f(I_t/I_r) = f(1.46)$
$1 = M(C_m,g)$	$1' = M(x,g)$
$2 = 1 + M(S,C_m)$	$2' = 1' + M(S,ii)$
$3 = 2 + M(E,S)$	$3' = 1' + M(S',iii) + M(E,S')$
$4 = 3 + M(W,E)$	$4' = 1' + M(S'',iv) + M(E',S'') + M(W,E')$
$5 = 1 + M(Hi,C_m)$	$5' = 1' + M(Hi,v)$
$6 = 5 + M(K,Hi)$	$6' = 1' + M(Hi',vi) + M(K,Hi')$
$7 = 6 + M(A,K)$	$7' = 1' + M(Hi'',vii) + M(K',Hi'') + M(A,K')$

Note. M = movement of point following it; C_m = highest order center of moment; *He* = head; *S* = shoulder; *E* = elbow; *W* = wrist; *Hi* = hip; *K* = knee; *A* = ankle, *g* is an arbitrary ground point. Arabic numbers refer to movements of lights shown in Figure 3; lowercase italicized Roman numerals refer to arbitrary, unrelated points in space, as shown in the upper right panel of Figure 3. Primed values of joints indicate that the locations are different for each occurrence of a particular joint. In the general form of the notation, $M(x,y)$, I am considering the movement of point x with respect to point y, a mechanically determinable point based on the vector structure of x. I_t = total number of vector/center doubles needed to specify the lights independently; I_r = total number of vector/center doubles needed to specify the lights as a coherent system. P is the prominence of the perceived configuration, as a function (f) of I_t divided by I_r.

Table 6

Functions Relating Search Times to Display Size (4, 8, 12 Items) in Each Condition of Experiment 2

Condition	Slope	Slope ratio	Intercept	% Variance due to linearity
Presence: Homogeneous				
Shape and line				
Positive	1.5	2.33	503	69
Negative	3.5		480	100
Color				
Positive	0.1	20.0	488	2
Negative	2.0		454	66
Presence: Heterogeneous				
Shape and line				
Positive	1.8	0.89	510	80
Negative	1.6		481	53
Color				
Positive	2.5	0.96	470	82
Negative	2.4		469	60
Absence: Homogeneous				
Shape and line				
Positive	18.3	1.86	559	98
Negative	34.0		598	100
Color				
Positive	3.0	0.47	529	98
Negative	1.4		526	30
Absence: Heterogeneous				
Shape and line				
Positive	22.6	2.56	616	97
Negative	57.8		586	99
Color				
Positive	1.0	—*	536	37
Negative	−1.8		548	97

Note. In search for presence, the target was a shape with an added intersecting line or a green shape. In search for absence, the target was a shape without an intersecting line or a nongreen shape. The data are those from the two groups of 6 subjects who were run in both the homogeneous and the heterogeneous conditions. *No meaningful slope ratio can be given here because of the negative slope. Essentially both functions are flat against display size.

Table 7

Measures Relating Search Time to Display Size in Experiment 4

Performance measure	Slope	Slope ratio	Intercept	% Variance due to linearity
Target: Gap				
Large gap (1/2)				
Positive	1.6	5.00	503	54
Negative	8.0		504	95
Medium gap (1/4)				
Positive	3.1	2.03	495	100
Negative	6.3		506	93
Small gap (1/8)				
Positive	4.7	1.28	508	96
Negative	6.0		503	89
Target: No Gap				
Large gap (1/2)				
Positive	6.2	2.11	526	89
Negative	13.1		544	91
Medium gap (1/4)				
Positive	14.8	2.26	505	100
Negative	33.5		524	99
Small gap (1/8)				
Positive	33.6	1.82	488	100
Negative	61.3		516	100

Table 8
Summary of Search Experiments

Feature tested	No. of cards × trials per card	Response	Subjects: Female	Subjects: Male	Target	Search Rates: Positive	Search Rates: Negative	Intercept (mean of positive and negative)	% errors (display size): 1	% errors (display size): 6	% errors (display size): 12
Line length											
Easy	12 × 3	Key press	8	0	Short	14.3	28.3	504	1.7	4.4	3.2
					Long	7.6	15.5	499	0.4	3.8	3.6
Difficult	12 × 3	Key press	4	4	Short	40.0	81.1	565	2.3	3.2	5.3
					Long	29.7	64.7	570	2.0	3.8	5.5
Matched distractors	12 × 3	Key press	7	1	Short	20.6	53.3	587	0.8	2.0	4.7
					Long	20.4	53.0	564	0.6	3.3	5.4
Grey											
Easy	8 × 3	Key press	3	5	Light grey	2.9	−2.4	503	2.5	2.2	1.9
					Dark grey	4.8	−1.7	465	0.8	0.9	1.0
Difficult	12 × 3	Key press	3	5	Light grey	13.7	28.6	613	4.4	1.7	4.4
					Dark grey	5.8	19.2	597	2.1	4.9	4.7
Number (1 vs. 2)	8 × 4	Key press	8	0	One	10.5	32.5	498	1.8	2.0	2.3
					Two	1.7	7.3	480	2.0	1.3	0.9
Curved/straight	8 × 2	Vocal	7	1	Straight	4.2	9.8	605	0.4	1.6	0.0
Easy					Curved	3.1	7.0	577	1.5	0.4	0.4
Medium	8 × 2	Vocal	7	1	Straight	12.4	22.2	598	0.4	2.3	1.6
					Curved	3.0	11.6	577	0.0	0.8	1.6
Difficult	8 × 2	Vocal	7	1	Straight	29.0	54.7	598	0.0	6.6	7.4
					Curved	6.1	12.9	598	1.5	0.3	2.4
Control with circle aperture	8 × 3	Key press	5	3	Straight	83.5	124.4	533	0.5	2.5	8.2
					Curved	18.3	31.2	588	0.5	0.3	2.4
Line orientation	8 × 3	Key press	4	4	Vertical	28.3	29.6	537	2.4	5.0	6.8
					Tilted	4.6	2.5	491	1.5	1.0	2.4
Control with circle aperture	8 × 3	Key press	3	5	Vertical	17.1	17.9	564	5.0	3.7	4.2
					Tilted	2.0	4.3	515	3.5	1.7	2.0
Control with tilted frame, head fixed	8 × 3	Key press	6	2	Tilted	9.6	15.7	682	6.3	3.0	1.5
					Vertical	3.1	7.0	552	2.8	0.8	1.5
Control with vertical frame, head fixed	8 × 3	Key press	6	2	Vertical	31.9	44.0	601	2.9	7.0	5.7
					Tilted	5.1	7.0	495	1.5	1.3	1.0
Control with both target and distractor tilted	8 × 3	Key press	4	4	Less Tilted	−2.3	2.4	658	2.6	2.9	1.5
					More Tilted	−6.1	−2.2	609	4.4	1.3	1.6
Color	24 (8 per color) × 2	Key press	2	6	Prototype	4.7	4.9	524	4.2	3.8	4.0
					Deviation	2.5	1.1	523	4.1	3.0	3.2
Circles vs. ellipses											
Fixed orientation	8 × 3	Key press	6	2	Circle	36.4	55.6	559	1.8	6.5	6.0
					Ellipse	10.5	18.7	510	1.5	3.6	2.8
Varied orientation	8 × 3	Key press	6	2	Circle	44.1	80.3	548	0.7	5.3	9.0
					Ellipse	10.9	19.6	482	1.9	0.8	4.1
Intersection	8 × 3	Vocal	8	0	Plus	16.4	23.5	494	3.2	1.0	8.5
					Line	14.1	21.8	524	1.7	1.0	5.4
Juncture	8 × 4	Key press	6	2	Angle	34.4	74.4	501	1.4	6.1	6.7
					Lines	19.4	23.9	509	1.9	2.4	2.9
Convergence	8 × 4	Key press	3	5	Parallel	32.2	61.3	493	1.5	3.5	5.5
					Converging	14.6	29.5	491	2.0	1.0	3.5
Closure and terminators											
Easy	8 × 4	Vocal	5	3	Closed	6.2	13.1	535	0.8	1.2	0.8
					Gap	1.6	8.0	504	1.0	1.4	1.0
Medium	8 × 4	Vocal	5	3	Closed	14.8	33.5	515	1.5	1.6	1.9
					Gap	3.1	6.3	501	0.4	1.0	0.8
Difficult	8 × 4	Vocal	5	3	Closed	35.6	61.3	597	1.7	2.5	6.4
					Gap	4.7	6.0	506	1.7	1.7	1.4
Containment											
Convex	8 × 4	Key press	3	5	Inside	24.0	41.3	457	0.9	2.2	6.7
					Outside	8.9	15.3	492	4.1	2.8	6.2
Concave	8 × 4	Key press	3	5	Inside	30.0	65.9	496	3.1	4.5	9.0
					Outside	12.9	53.1	522	3.0	6.4	4.1
Control convex											
No dot	8 × 4	Key press	6	2	Outside	15.6	39.7	480	1.7	2.3	2.7
Dot	8 × 4	Key press	6	2	Outside	7.1	17.3	518	2.7	0.8	2.9

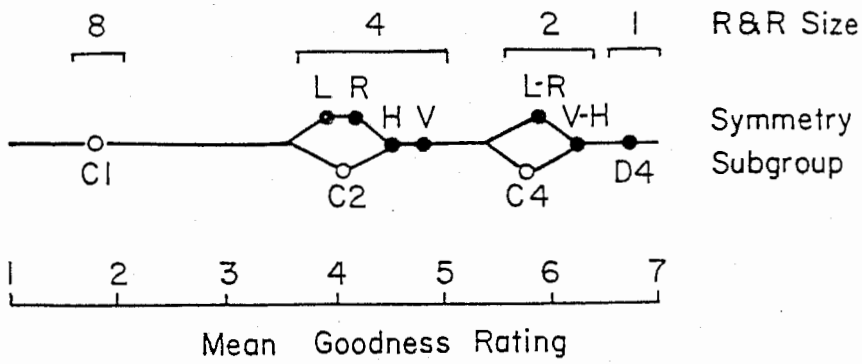

D4 = (I, V, H, L, R, 90, 280, 270)

V-H = (I, V, H, 180)

L-R = (I, L, R, 180)

C4 = (I, 90, 180, 270)

V = (I, V)

H = (I, H)

L = (I, L)

R = (I, R)

C2 = (I, 180)

C1 = (I)

Fig. 1

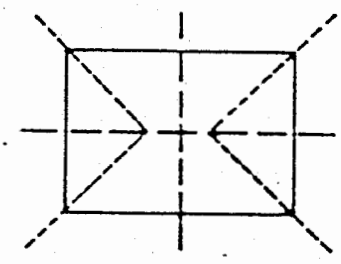

Fig. 2

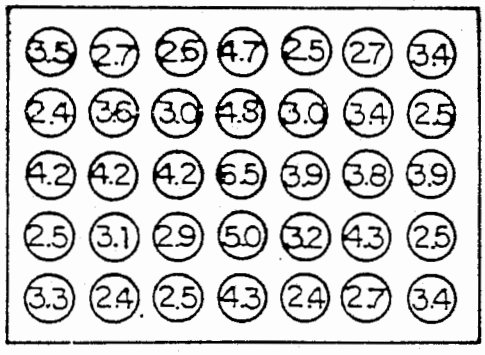

Fig. 3

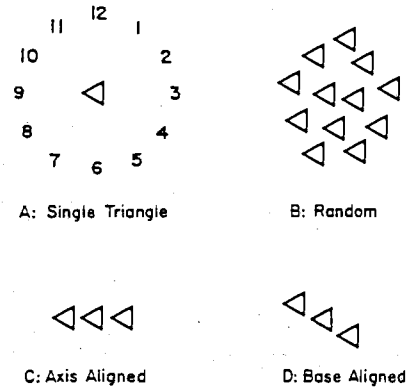

Fig. 4

FIG. 1. Perceived pointing of ambiguous triangles. A single triangle (A) can be seen to point in one of three directions (toward the 1, 5, or 9 in this example). In a random array (B) all triangles are perceived to point in the same direction. The direction of perceived pointing can be biased by axis-aligned configurations (C) and by base-aligned configurations (D).

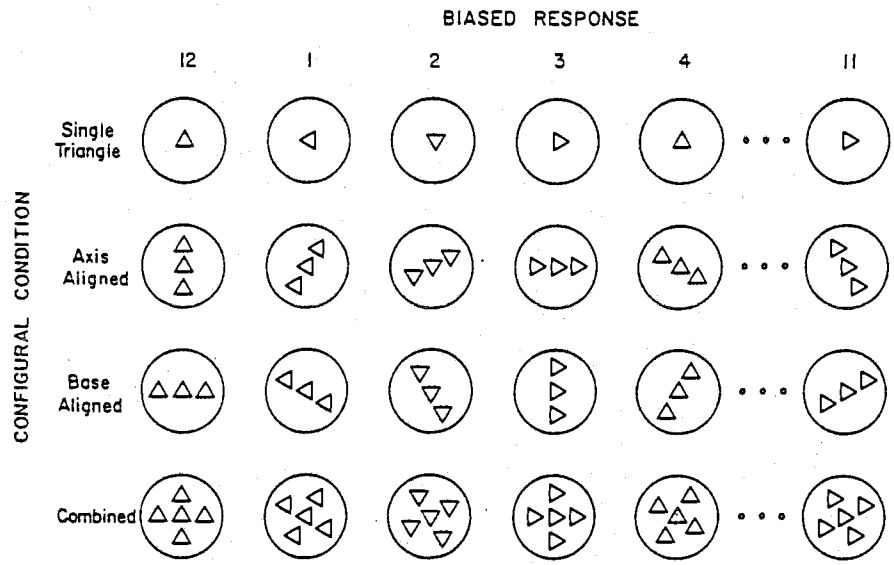

FIG. 2. Stimulus set for Experiment 1. Single triangles, axis-aligned, base-aligned, and combined configurations are combined orthogonally with twelve equally spaced directions.

Fig. 5

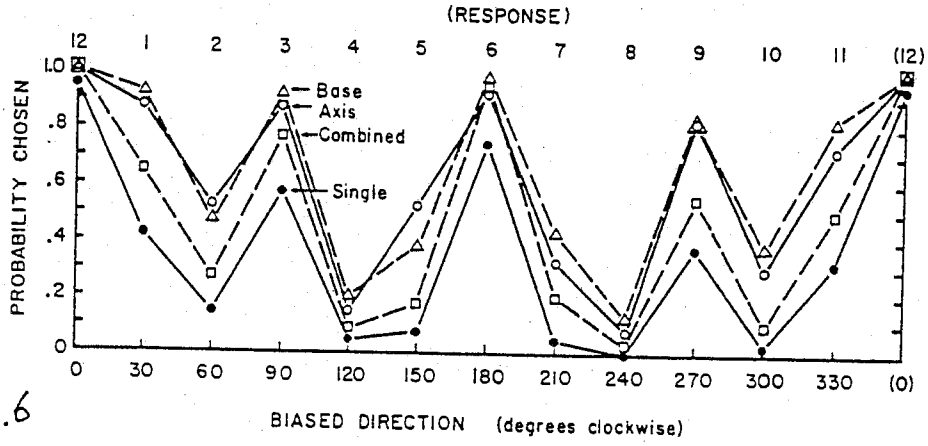

Fig. 6

FIG. 3. Results of Experiment 1. Probability of seeing stimuli point in the biased direction is plotted as a function of direction and configural conditions.

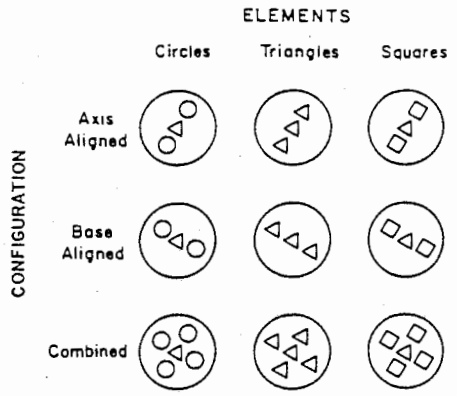

FIG. 4. Examples from the stimulus set of Experiment 2: Configuration conditions are combined orthogonally with the shape of the contextual elements for triangles biased toward pointing 30° clockwise from vertical (1 o'clock).

Fig. 7

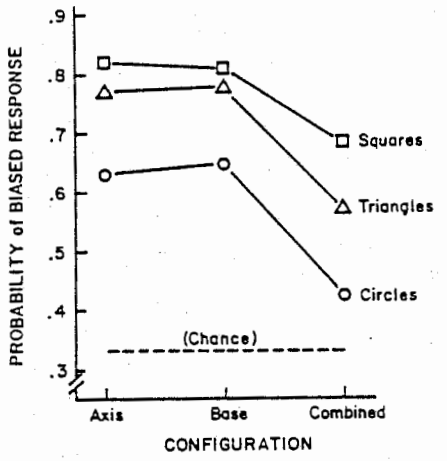

FIG. 5. Results of Experiment 2. Probability of seeing triangles point in the biased direction is plotted as a function of configural conditions and the shape of the contextual elements.

Fig. 8

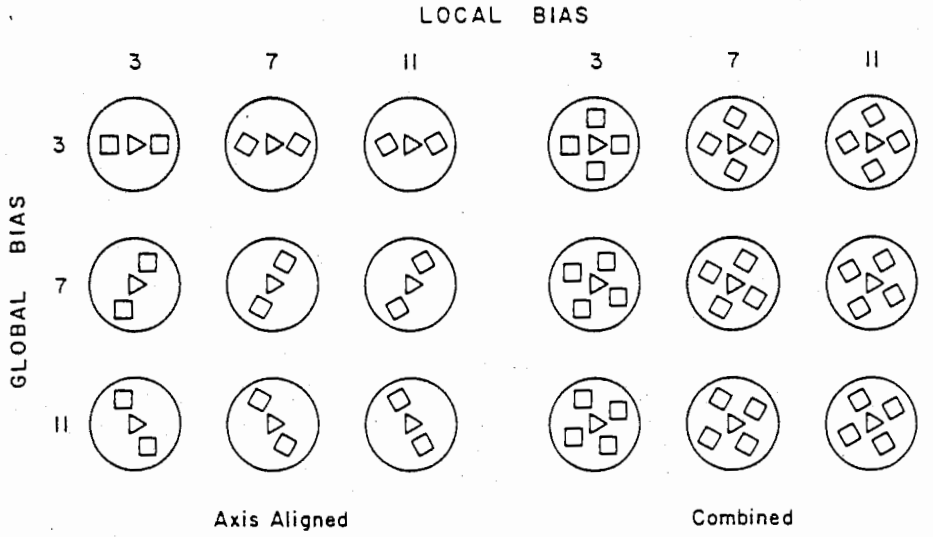

FIG. 6. Examples from the stimulus set of Experiment 3. Global and local biases are combined orthogonally for the axis-aligned and combined configurations including a triangle that can be seen pointing toward 3, 7, or 11 o'clock.

Fig. 9

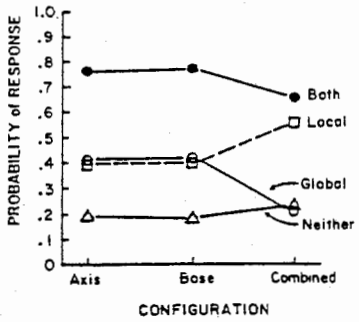

Fig. 10

FIG. 7. Results of Experiment 3: Probability of seeing triangles point in the biased direction is plotted as a function of configural condition and the type of bias: both local and global, local only, global only, or neither global nor local.

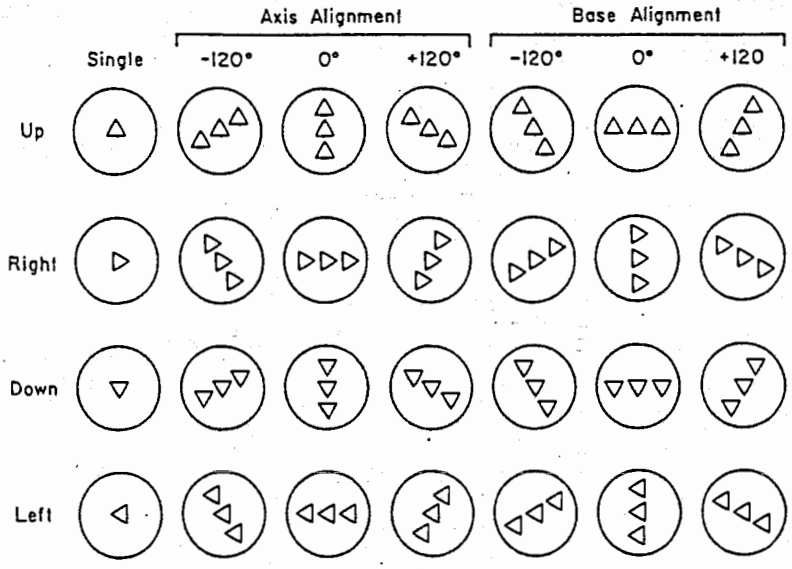

Fig. 11

Figure 1. The complete stimulus set for Experiment 1. (Triangles pointing up, down, right, or left were shown singly or in configurations aligned along their axes or bases. The configural line was oriented so that it was either consistent or inconsistent with the required directional response.)

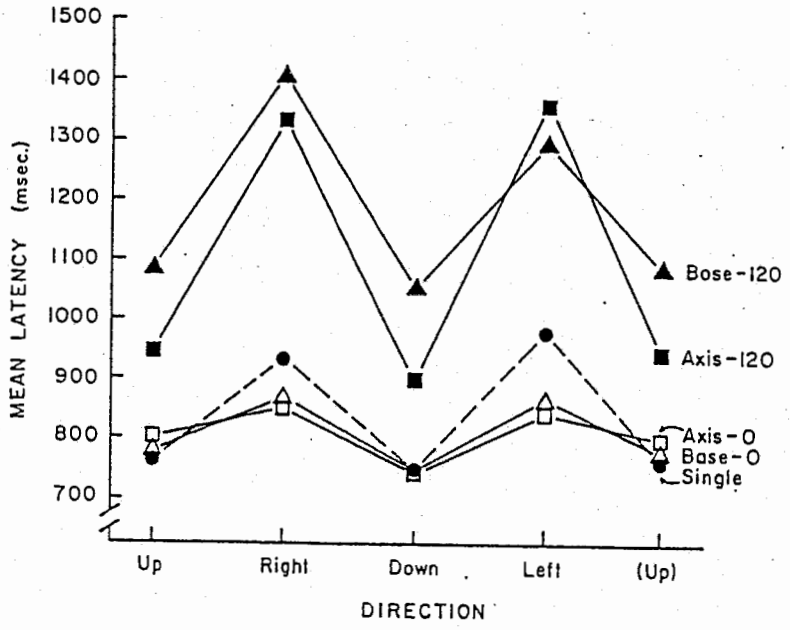

Fig. 12

Figure 2. Results of Experiment 1. (Mean reaction time as a function of direction for single triangles [dashed line], consistent configurations [solid lines, open symbols], and inconsistent configurations [solid lines, filled symbols].)

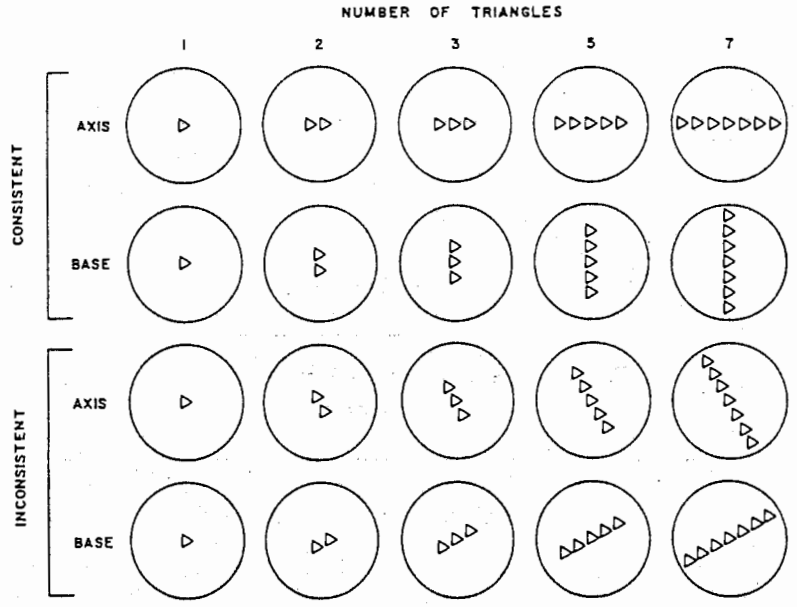

Fig. 13

Figure 3. Examples of the stimulus set of Experiment 2. (Configurations composed of 1, 2, 3, 5, or 7 triangles were aligned along their axes or bases in consistent or inconsistent biases.)

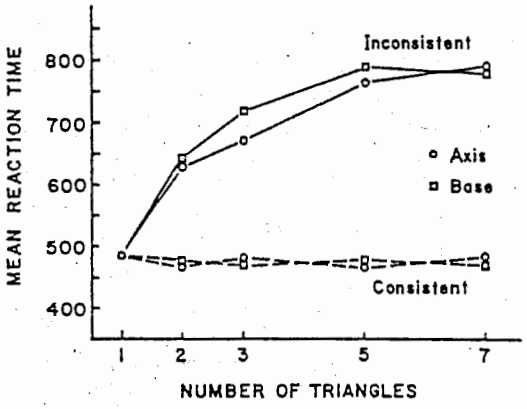

Fig. 14

Figure 4. Results of Experiment 2. (Mean reaction time in milliseconds is plotted as a function of number of aligned triangles for axis and base alignment in consistent and inconsistent biases.)

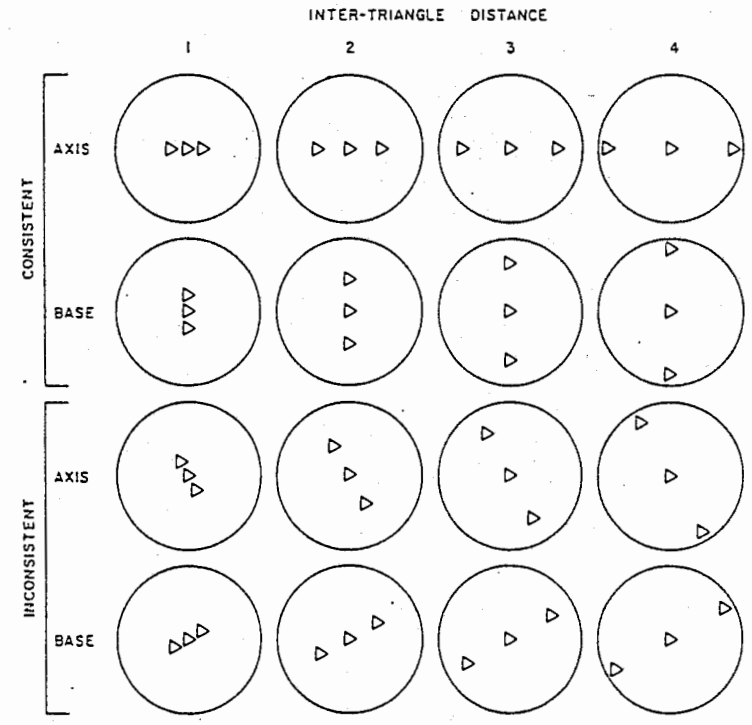

Fig. 15

Figure 6. Examples from the stimulus set of Experiment 3. (Configurations of three triangles at displacements of 1, 2, 3, or 4 times the length of a side were aligned along their axes or bases in consistent or inconsistent biases.)

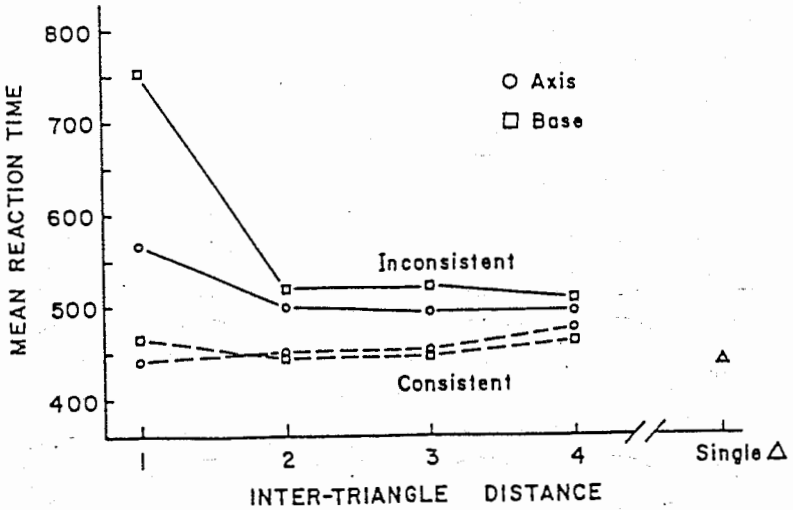

Fig. 16

Figure 7. Results of Experiment 3. (Mean reaction time in milliseconds is plotted as a function of intertriangle distance [in units of side length] for axis and base alignment in consistent and inconsistent biases.)

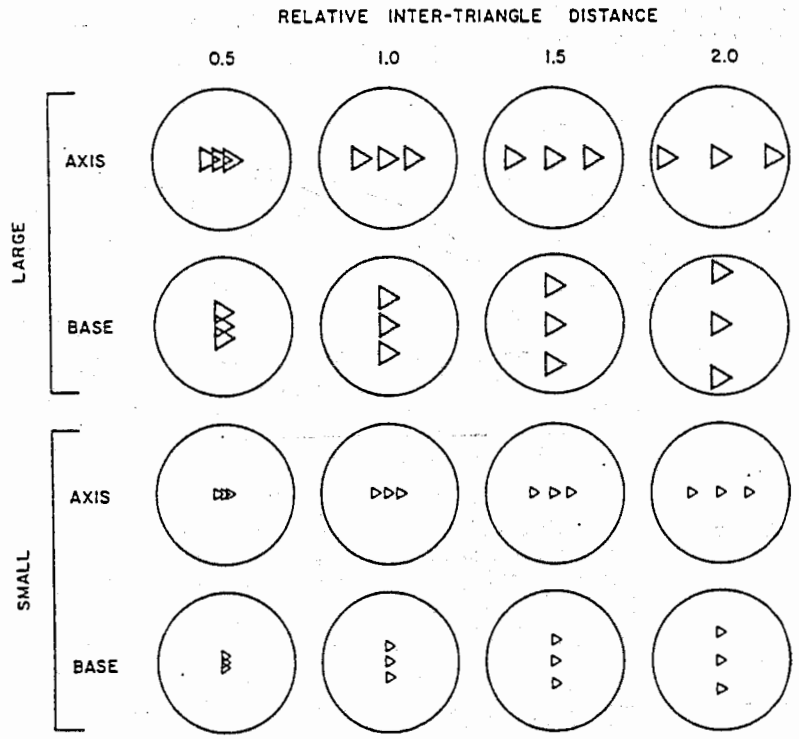

Fig. 17

Figure 9. Examples from the stimulus set of Experiment 4. (Configurations of small or large triangles were aligned along their axes or bases at displacements of .5, 1.0, 1.5, or 2.0 times the length of a side in consistent or inconsistent biases.)

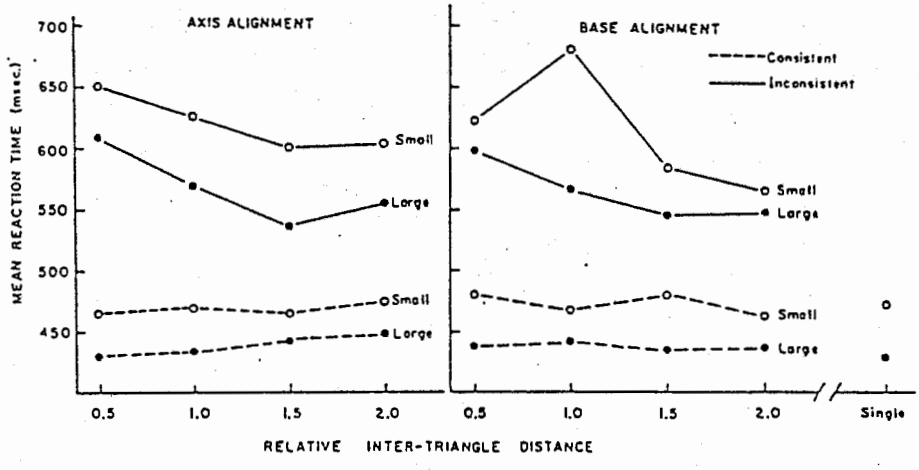

Figure 10. Results of Experiment 4. (Mean reaction time as a function of relative intertriangle distance [in units of side length] for axis and base alignment in consistent and inconsistent biases.)

Fig. 18

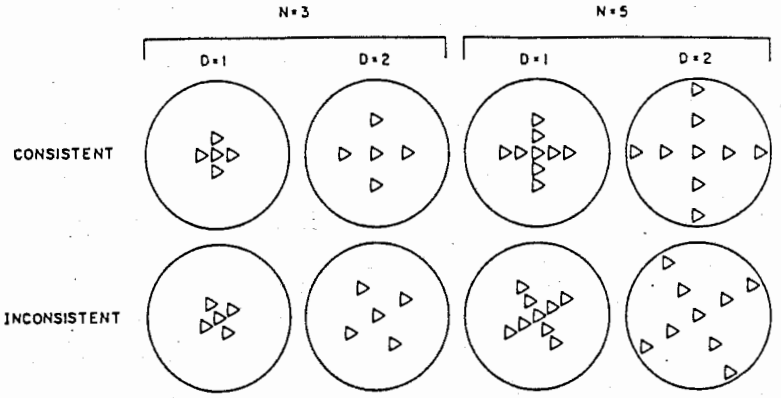

Figure 11. Examples of the stimulus set of Experiment 5. (Combined configurations were constructed with close or wide spacing using three or five triangles per line in consistent and inconsistent biases. Axis- and base-aligned configurations were also used with analogous numbers and spacings of triangles.)

Fig. 19

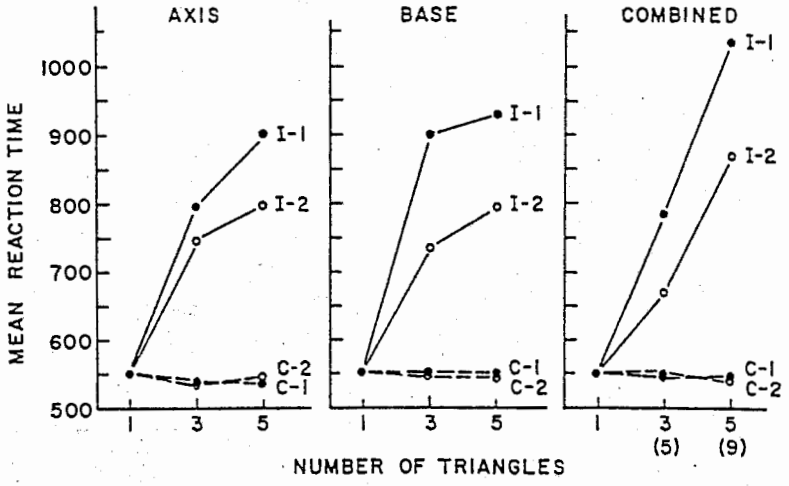

Figure 12. Results of Experiment 5. (Mean reaction time in milliseconds as a function of number and spacing of triangles for axis-aligned, base-aligned, and combined conditions in consistent [C] and inconsistent [I] biases.)

Fig. 20

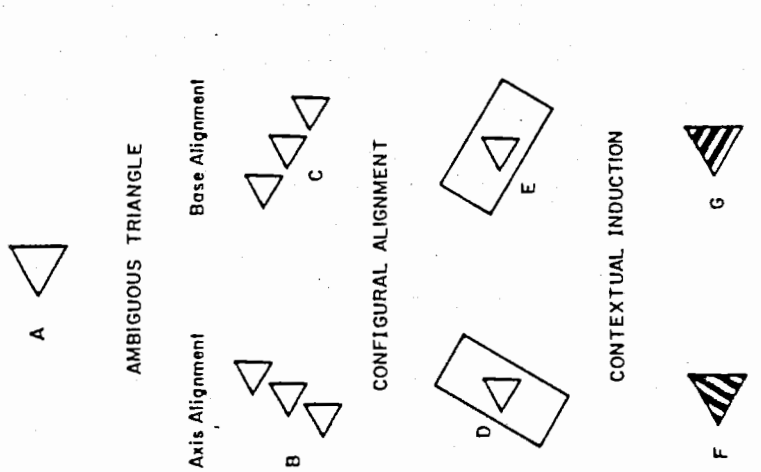

Figure 1. Perceived pointing of ambiguous triangles. (A single triangle [A] can be seen as pointing in any one of three directions. Perceived pointing can be systematically influenced by the introduction of several factors: configural alignment of a number of triangles along one of their axes of symmetry [B] or along one of their bases [C], contextual figures that surround a triangle and are oriented parallel to an axis of symmetry in the triangle [D] or parallel to a base of a triangle [E], and textural striping oriented along one of the triangle's axes of symmetry [F] or parallel to a base [G].)

Fig. 21

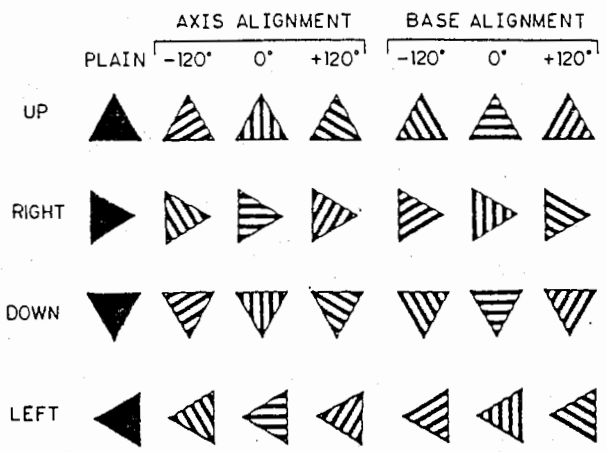

Figure 2. The complete stimulus set for Experiment 1. (Triangles shown pointing up, down, right, or left were either plain or had textural striping aligned along their axes or bases. The stripes were oriented so that they were either consistent or inconsistent with the required directional response.)

Fig. 22

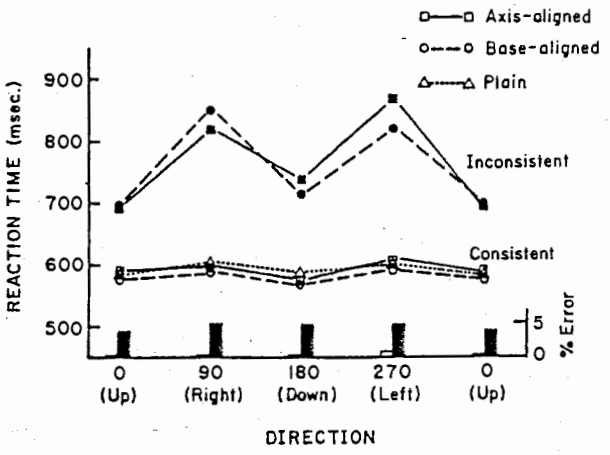

Figure 3. Results of Experiment 1. (Mean reaction time and error rates are presented as a function of direction for plain triangles [open triangles], consistent textural striping [open circles, squares, and bars], and inconsistent textural striping [filled circles, squares, and bars].)

Fig. 23

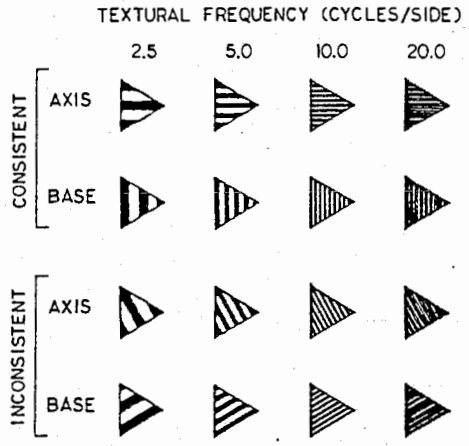

Figure 4. Examples of the stimulus set of Experiment 2. (Triangles contained textural frequencies of 2.5, 5.0, 10.0, and 20.0 cycles per triangle side aligned along their axes or bases in consistent or inconsistent biases.)

Fig. 24

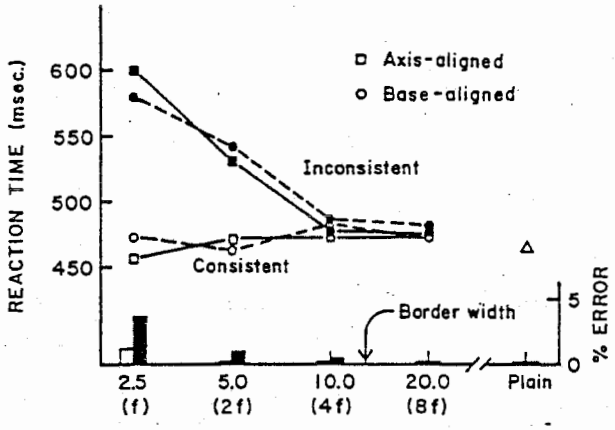

Figure 5. Results of Experiment 2. (Mean reaction time and error rates are presented as a function of textural frequency for axis and base alignment in consistent biases [open circles, squares, and bars], inconsistent biases [filled circles, squares, and bars], and plain triangle control [open triangle]. The width of a triangle's border is shown by the arrow.)

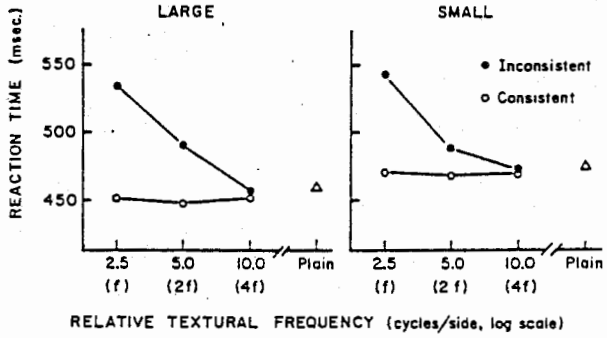

Figure 6. Results of Experiment 3. (Mean reaction time is presented as a function of relative textural frequency in consistent biases [open circles], inconsistent biases [filled circles], and plain controls [open triangle], plotted separately for small and large triangles.)

Fig. 26

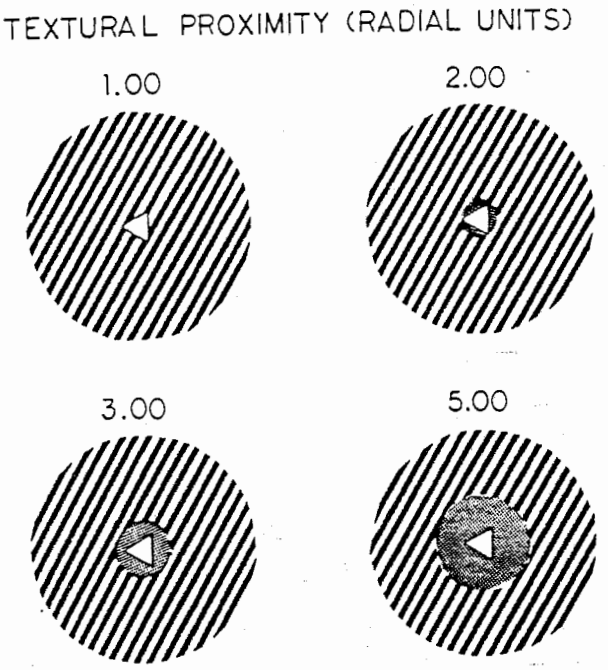

Fig. 27

Figure 7. Examples of the stimulus set of Experiments 4 and 5. (Textural striping at varying distances from the triangle is measured in radial units, using the distance from the center of the triangle to the midpoint of a side as the unit.)

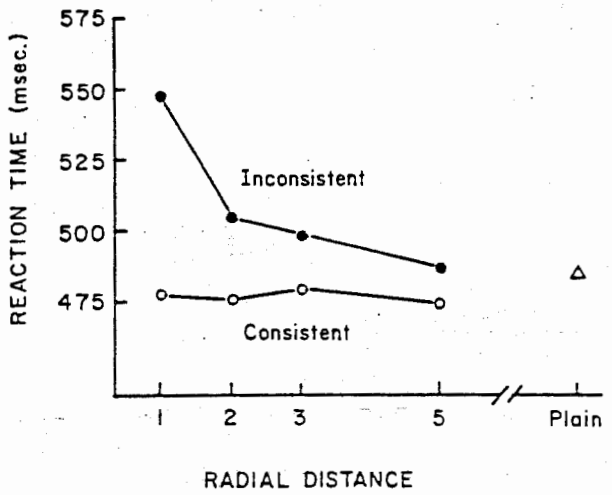

Fig. 28

Figure 8. Results of Experiment 5. (Mean reaction time is measured as a function of radial distance of textural striping from the triangle for consistent and inconsistent biases. Also included is mean reaction time to plain field control.)

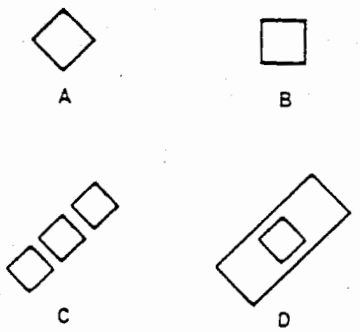

Fig. 29

Fig. 1. The ambiguous square/diamond in different orientations and contexts that change its perceived shape.

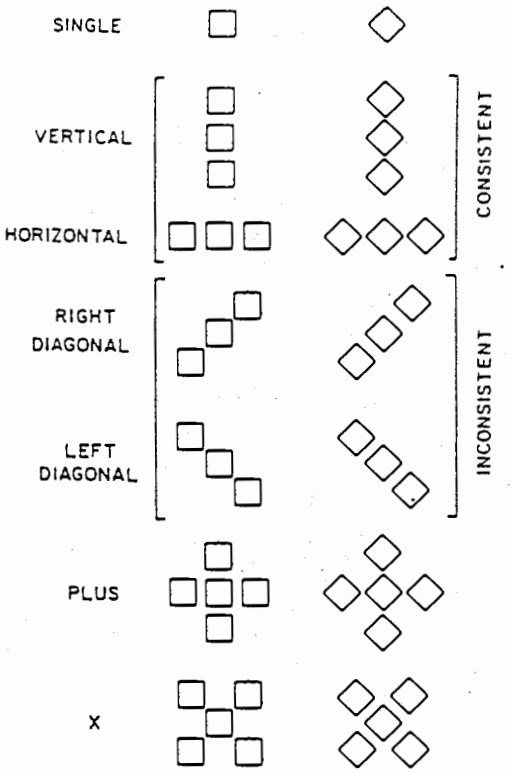

Fig. 30

Fig. 3. Stimuli for experiment 1: Squares (left column) and diamonds (right column) in seven configural conditions.

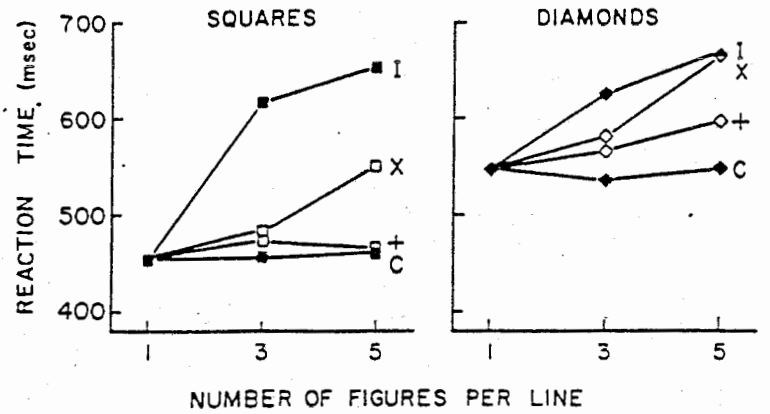

Fig. 4. Results of experiment 1: Mean RT to discriminate squares from diamonds as a function of number of figures in the configural lines for consistent (C), inconsistent (I), plus (+), and × configurations.

Fig. 31

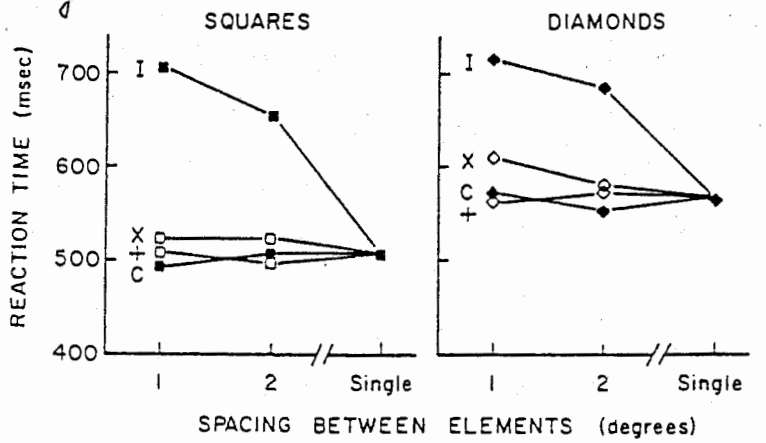

Fig. 5. Results of experiment 2: Mean RT to discriminate squares from diamonds as a function of spacing between adjacent elements for consistent (C), inconsistent (I), plus (+), and × configurations.

Fig. 32

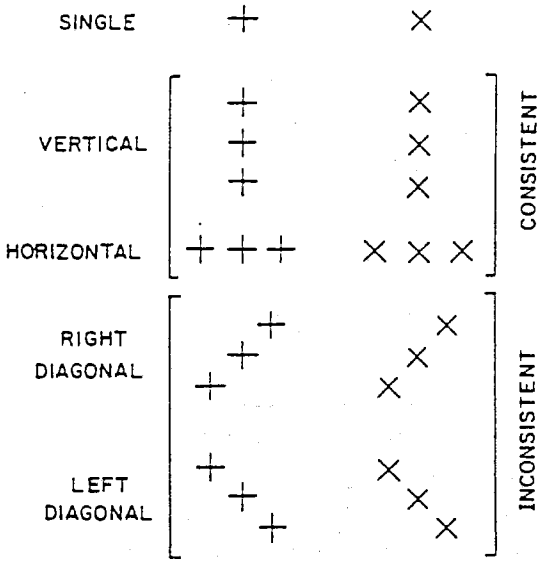

Fig. 6. Stimuli for experiment 3: Pluses (left column) and ×'s (right column) in five configural conditions.

Fig. 33

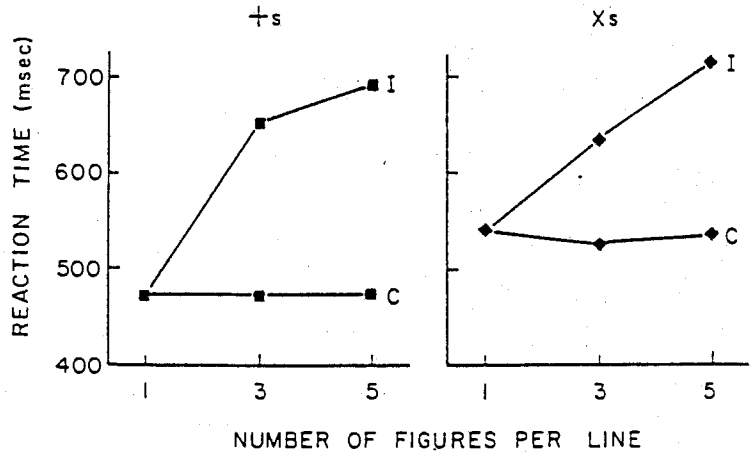

Fig. 7. Results of experiment 3: Mean RT for consistent (C) and inconsistent (I) configural conditions as a function of the number of figures per configural line.

Fig. 34

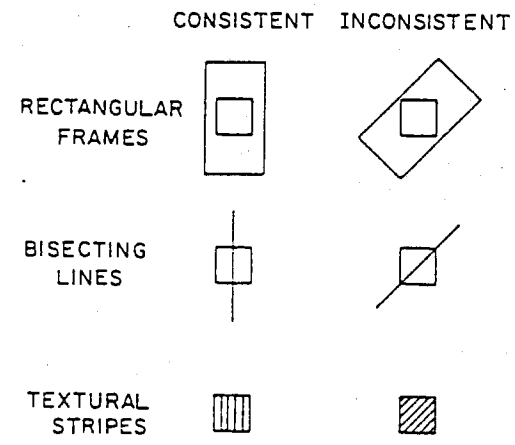

Fig. 8. Stimuli for experiment 4: Squares are shown in consistent and inconsistent contexts consisting of rectangular frames, bisecting lines, and textural stripes.

Fig. 35

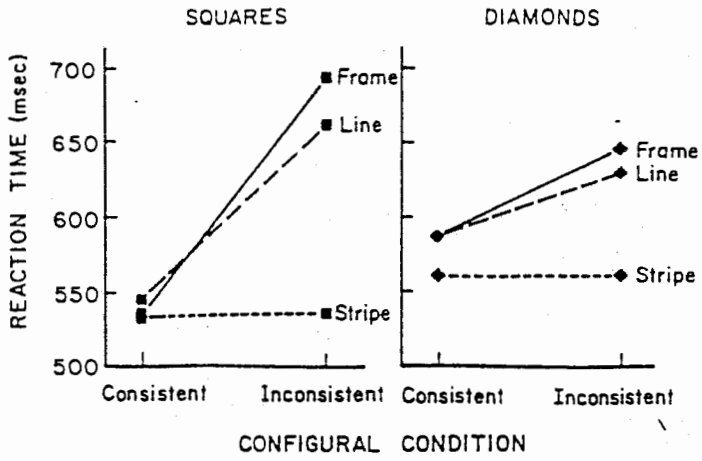

Fig. 9. Results of experiment 4: Mean RT to discriminate squares from diamonds for consistent and inconsistent contexts consisting of rectangular frames, bisecting lines, and textural stripes.

Fig. 36

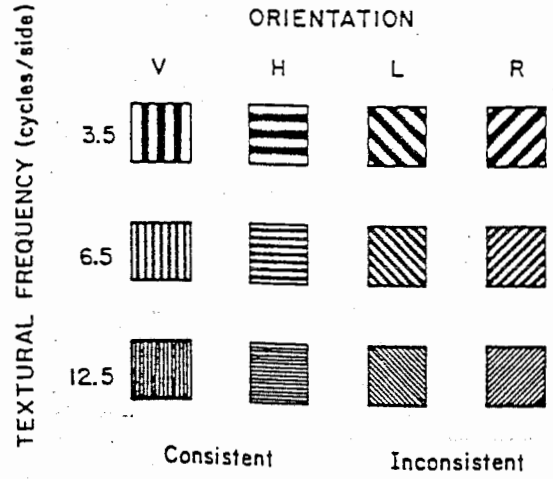

Fig. 10. Stimuli for experiment 5: Squares are shown with textural stripes at vertical (V), horizontal (H), left diagonal (L), and right diagonal (R) orientations for three stripe widths.

Fig. 37

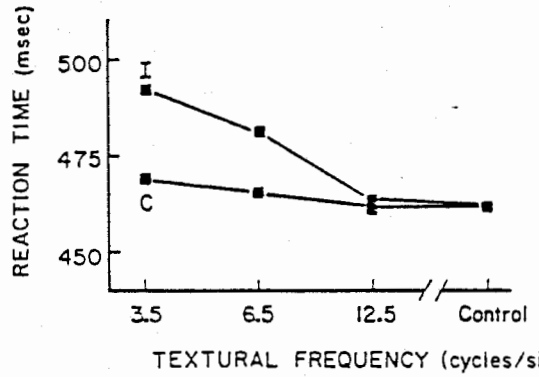

Fig. 11. Results of experiment 5: Mean RT for consistent and inconsistent conditions as a function of textural frequency.

Fig. 38

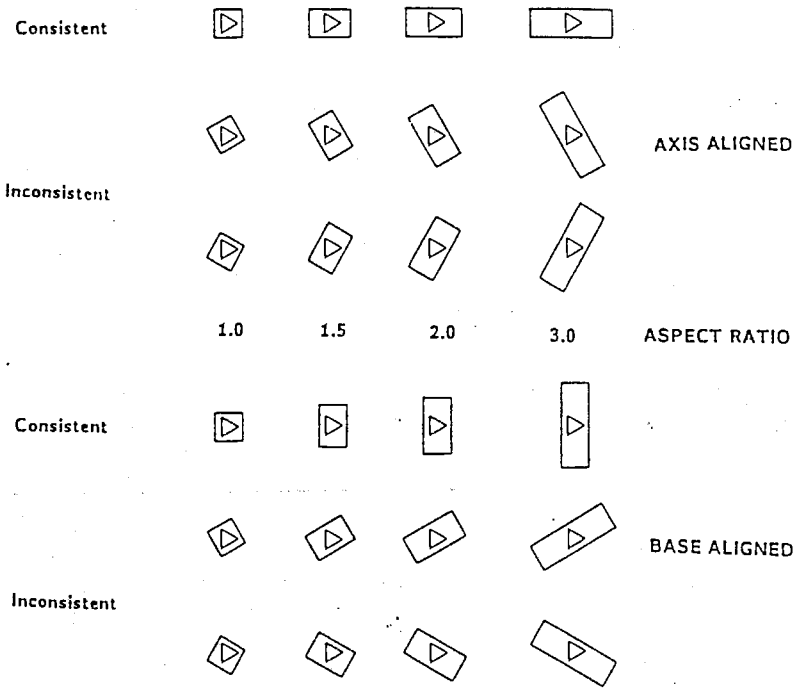

Figure 7. Stimuli in Experiment 1 (Frame Elongation). Axis- and base-aligned rectangular frames

Fig. 39

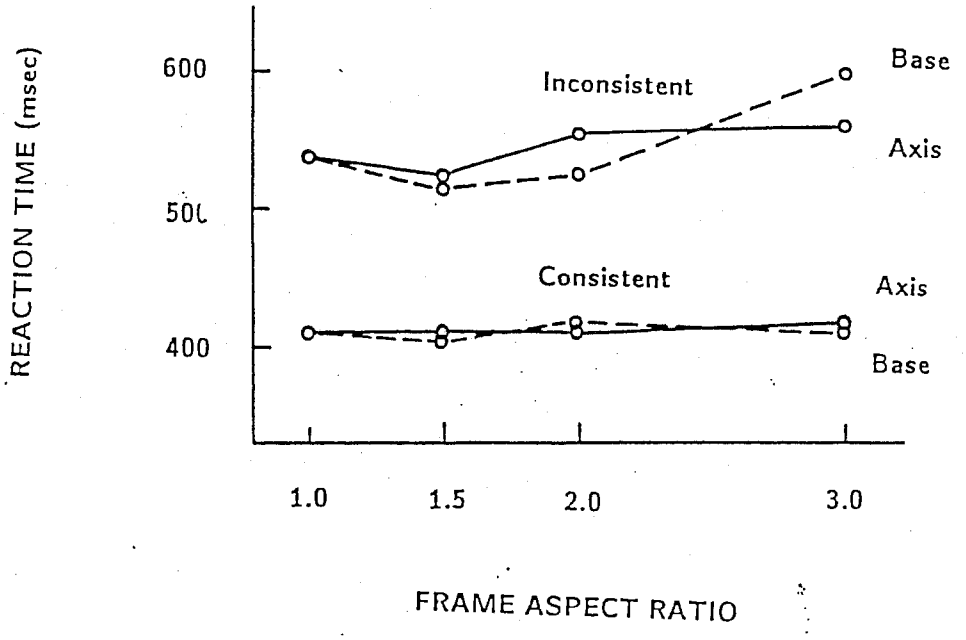

Figure 8. Results of Experiment 1 (Frame Elongation). Mean RTs are plotted

Fig. 40

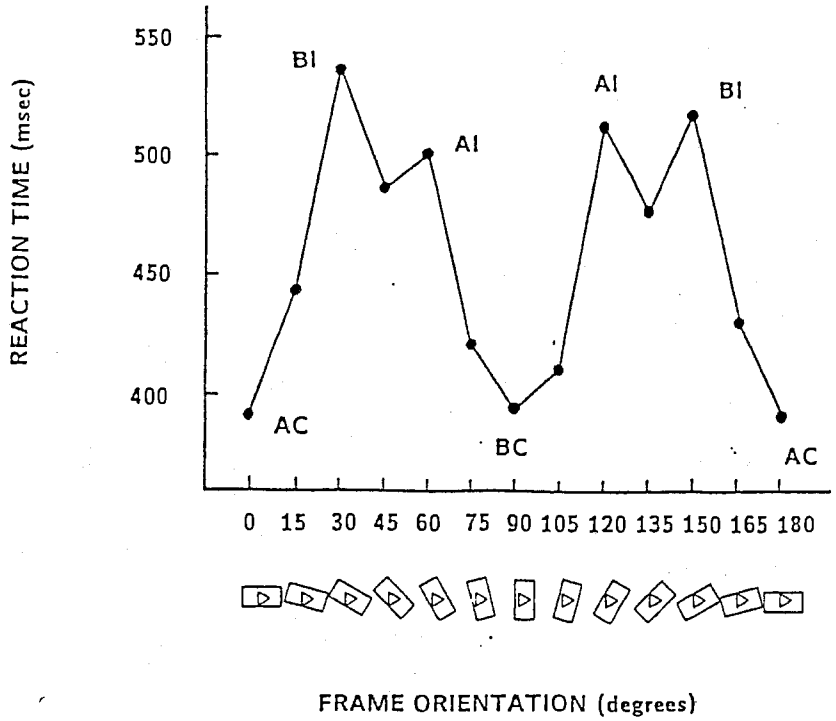

Figure 11. Results of Experiment 2 (Frame Orientation). Mean RT is shown as a function of frame orientation (AC = axis-consistent; BC = base-consistent; AI = axis-inconsistent; BI = base-inconsistent).

Fig. 41

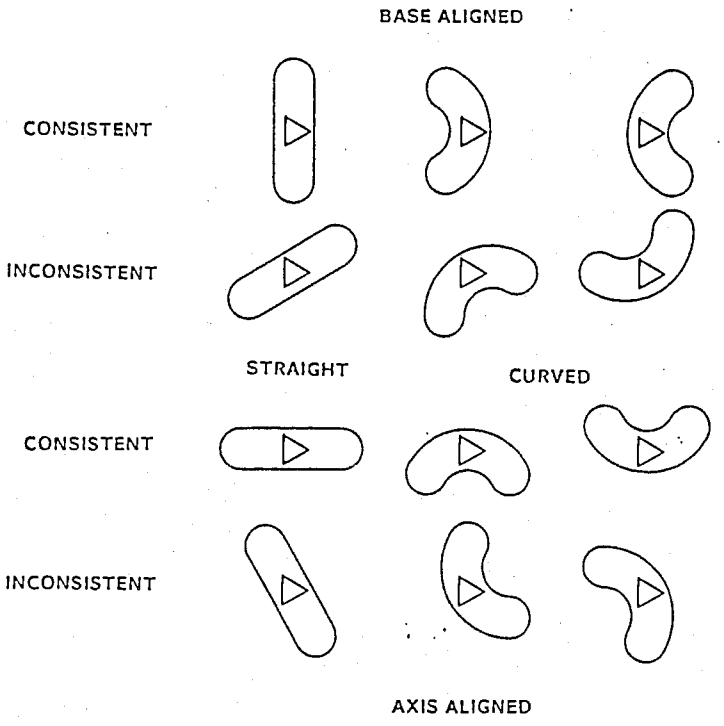

Figure 12. Example stimuli from Experiment 3 (Curved Frames). Bending the frame along its long axis preserves the symmetry of base-aligned conditions but breaks the symmetry of axis-aligned conditions.

Fig. 42

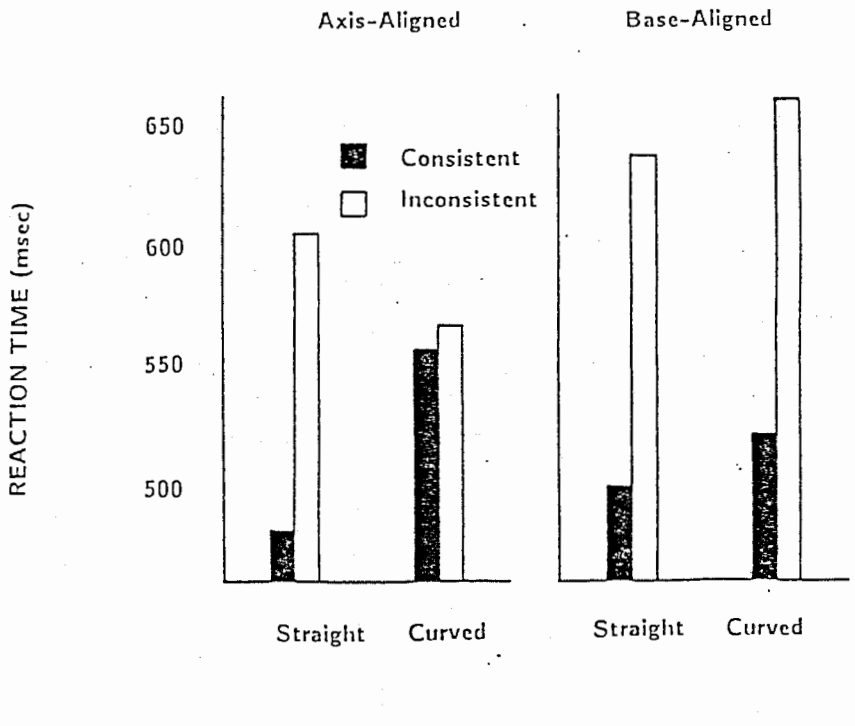

Figure 13. Results of Experiment 3 (Curved Frames). Bending the axis-aligned frames eliminates the bias effect, whereas bending the base-aligned frames does not, as predicted by symmetry theory.

Fig. 43

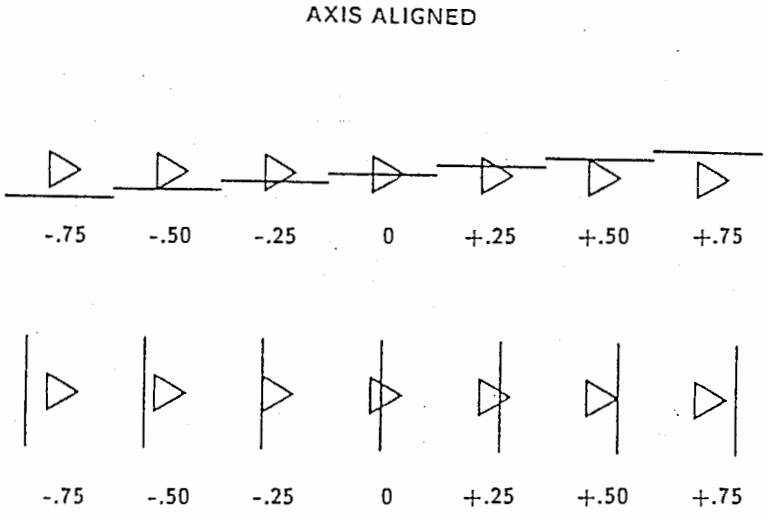

Figure 14. Example stimuli from Experiment 4 (Line Position). Lateral displacement of a line segment preserves symmetry in the base-aligned conditions, but breaks symmetry in axis-aligned conditions.

Fig. 44

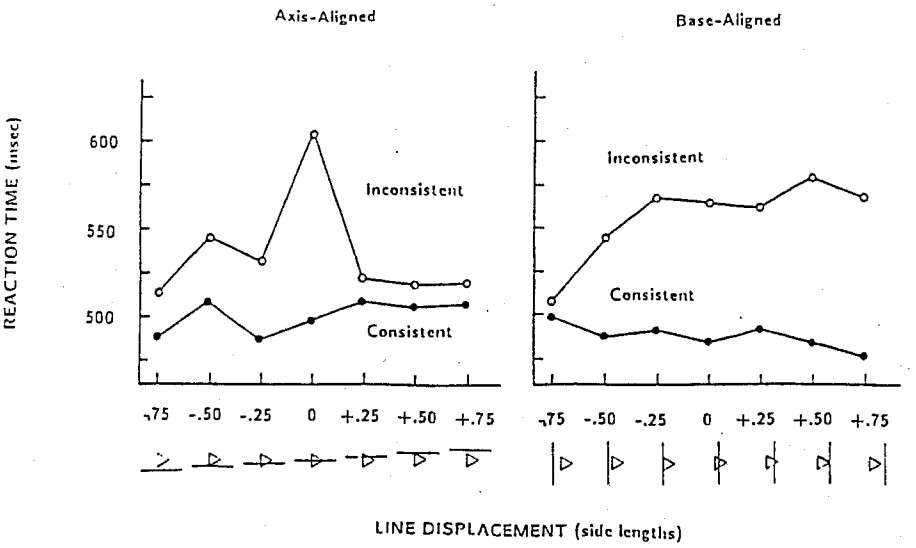

Figure 15. Results of Experiment 4 (Line Position). Displacing the line segment even slightly from a central position reduces the bias effect for axis-aligned conditions, whereas comparable displacements scarcely change the bias effect for base-aligned conditions.

Fig. 45

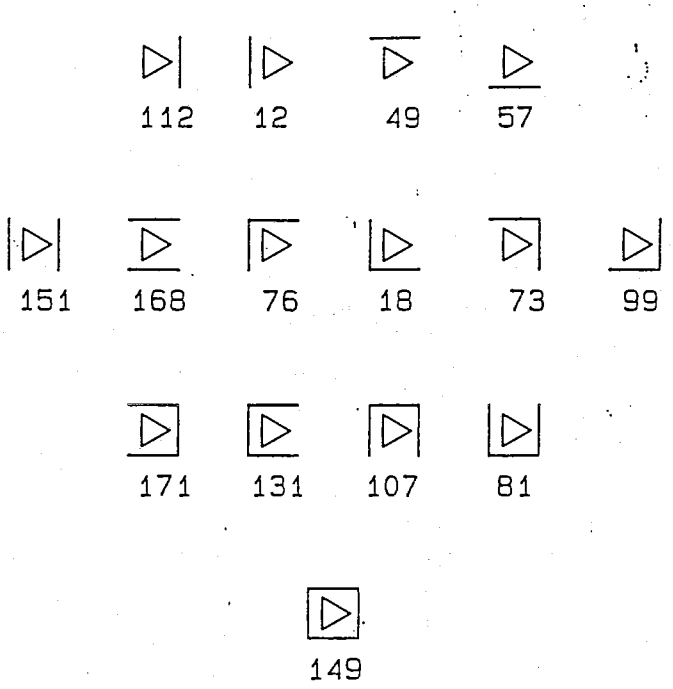

Figure 16. Examples stimuli and results of Experiment 5 (Parts of a Frame). All possible combinations of sides of a square frame were measured for the amount of intereference they produced. Numbers below each stimulus show the results: inconsistent RT - consistent RT = interference (in msec.).

Fig. 46

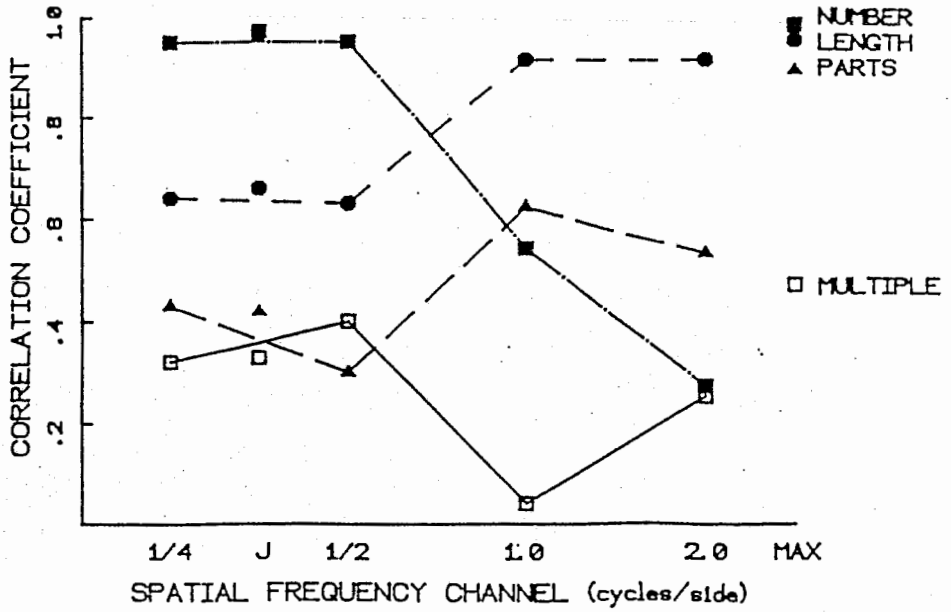

Figure 18. Fits of Janez's dominence ratio model to the results of four experiments. Correlations between measured interference scores and the dominance ratio are plotted for individual spatial frequency channels (filled circles), Janez's original formulation, including just the .25 and .50 cycles/side channels (open triangles), and the optimal linear combination of dominance ratios over all channels.

Fig. 47

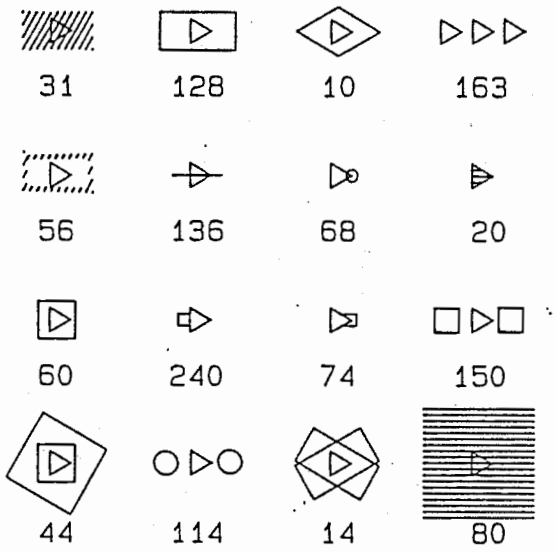

Figure 19. Example stimuli and results of Experiment 6 (Multiple Contexts). Sixteen patterns were measured for the amount of interference they produced. Numbers below each stimulus indicate interference (in msec.) = inconsistent RT - consistent RT.

Fig. 48

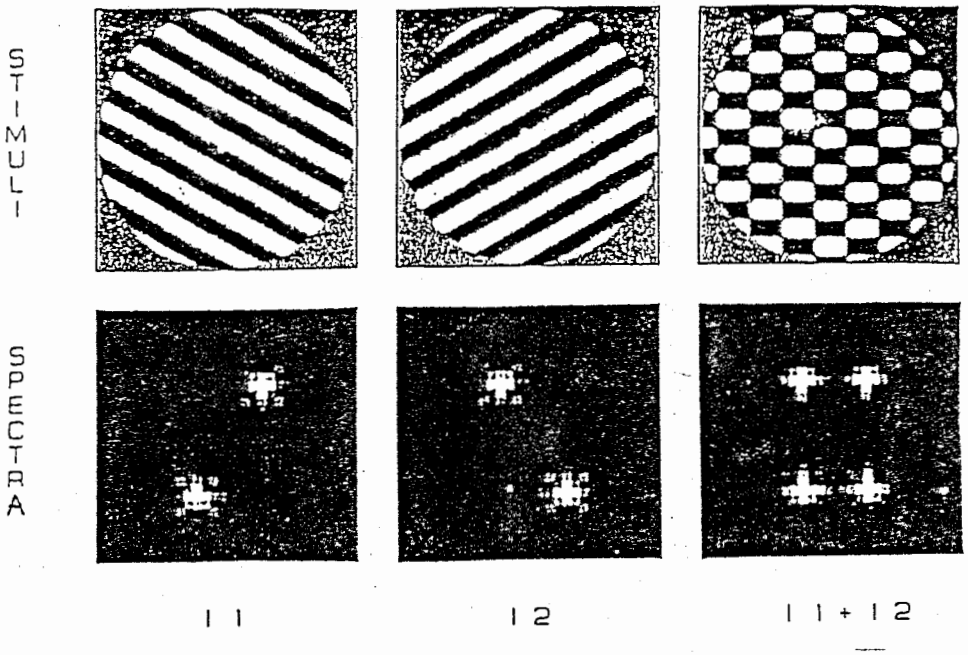

Figure 20. Examples of the experimental stimuli from Experiment 7. Two inconsistent single gratings are shown on the left and the double grating that results from adding them together is shown at right. Below each image is shown an enlarged image of the low-frequency region of its amplitude spectrum.

Fig. 49

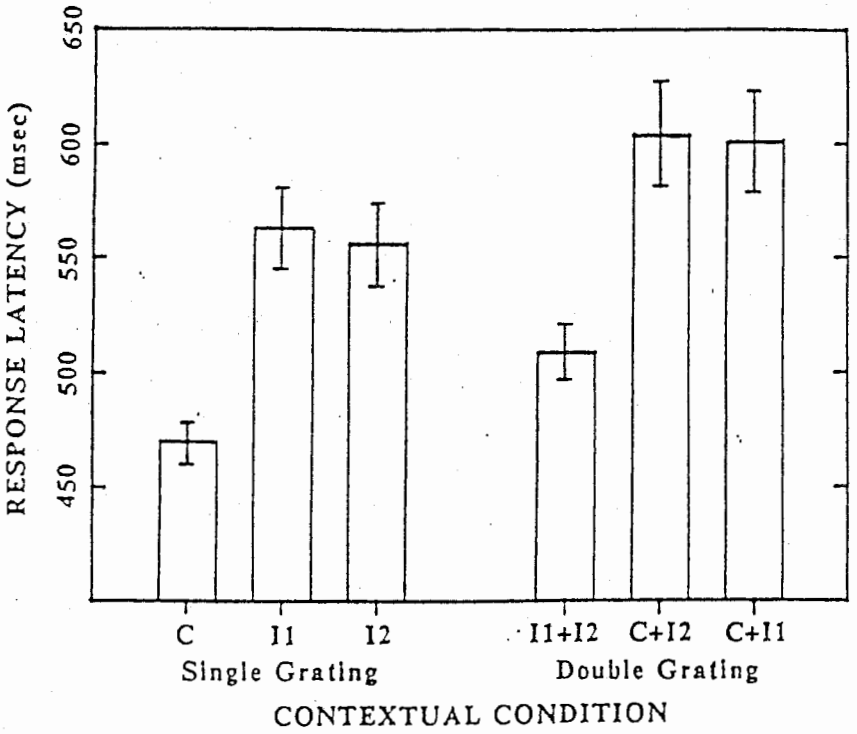

Figure 21. Results of Experiment 7 (Symmetry vs Spectral Power). Mean RTs for single and double gratings indicate that double gratings produce the pattern of results predicted by the symmetry analysis and not by the spatial frequency analysis.

Fig. 50

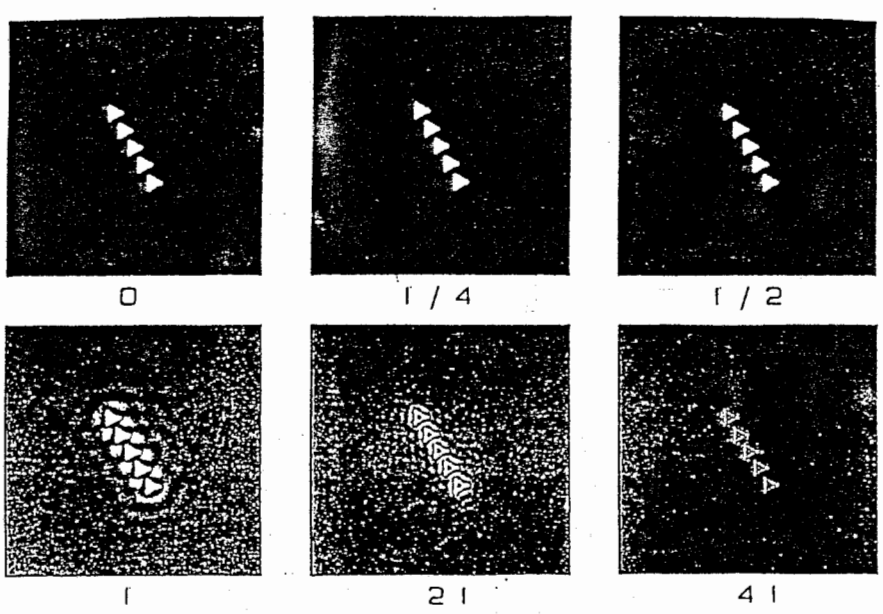

Figure 22. Examples of low-pass filtered configurations of triangles. All spatial frequencies below the specified cutoff frequency (in cycles/side) have been removed from the spectrum before resynthesizing these images.

Fig. 51

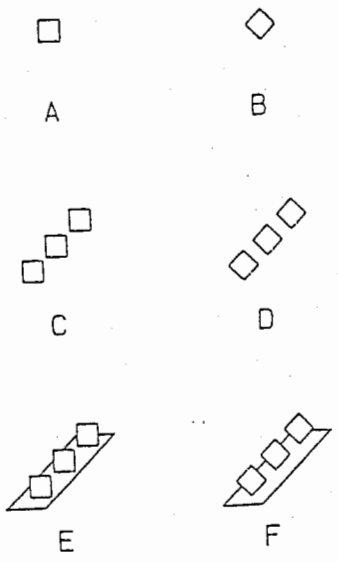

Figure 1. The ambiguous square/diamond in different orientations and contexts.

Fig 52

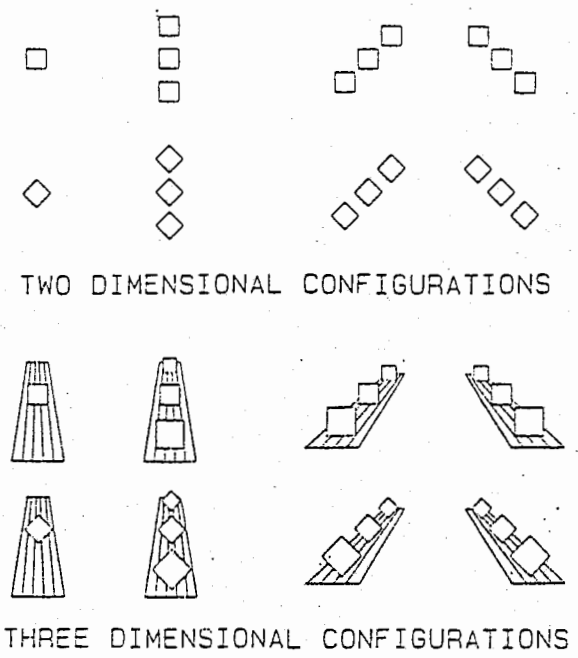

Figure 2. Stimuli for Experiment 1: Configurations of squares/diamonds in the 2-D and 3-D conditions.

Fig. 53

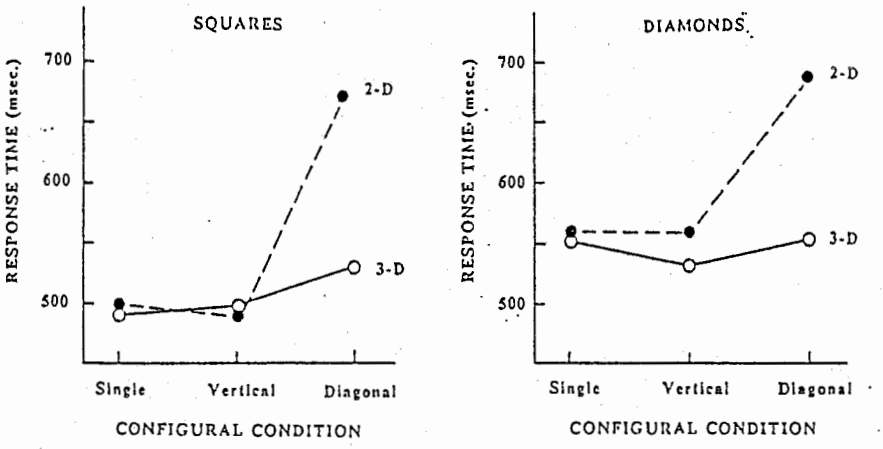

Figure 3. Results of Experiment 1: Mean RTs as a function of configural condition for squares and diamonds in 2-D and 3-D depth conditions.

Fig. 54

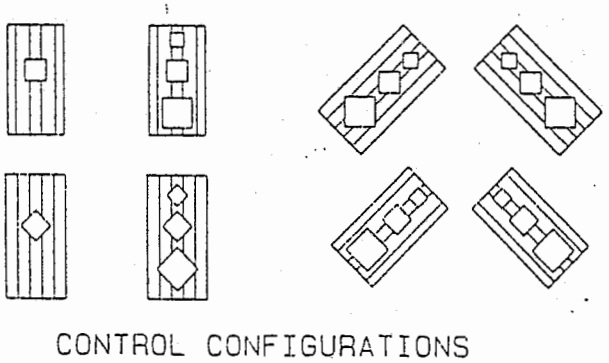

Figure 4. Stimuli for Experiment 2: Configurations of squares/diamonds in the "control" condition for depth information from relative size, occlusion, and height in the picture plane.

Fig. 55

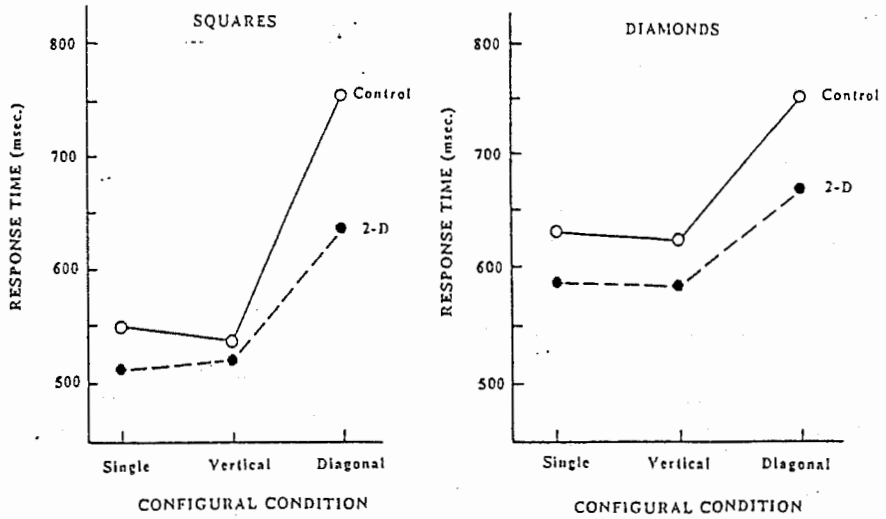

Figure 5. Results of Experiment 2: Mean RTs as a function of configural condition for squares and diamonds in the 2-D and control conditions.

Fig. 56

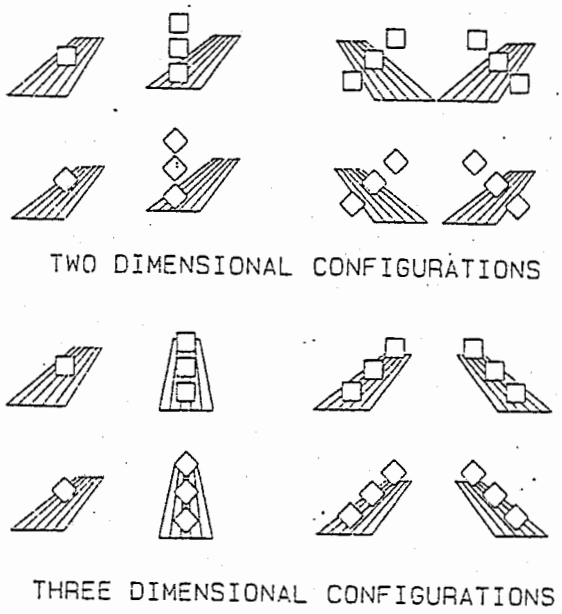

Figure 6. Stimuli for Experiment 3: Configurations of squares/diamonds in the 2-D and 3-D conditions.

Fig. 57

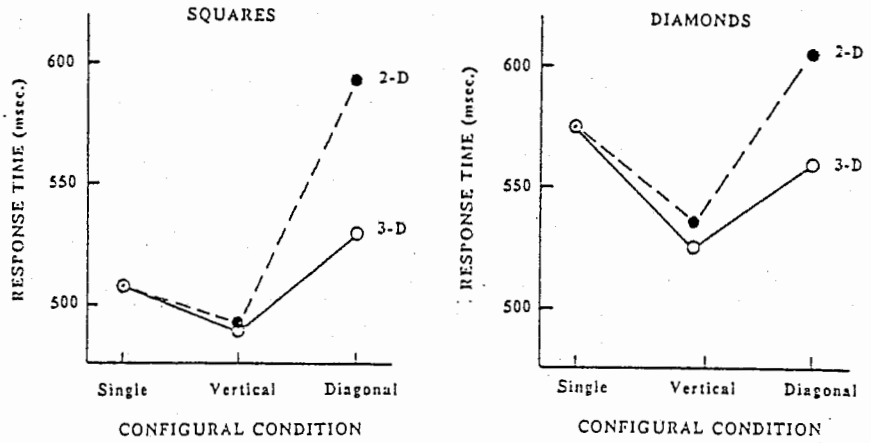

Figure 7. Results of Experiment 3: Mean RTs as a function of configural condition for squares and diamonds in the 2-D and 3-D conditions.

Fig. 58

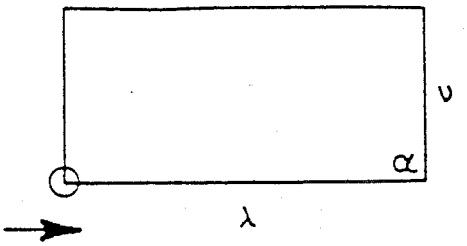

Figure 9. A rectangle and possible code elements.

Fig. 59

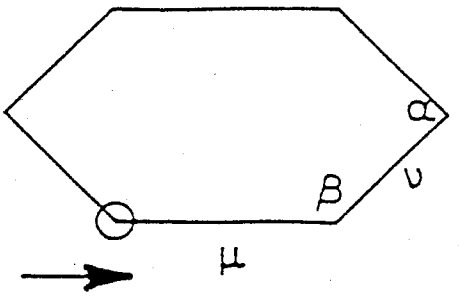

Figure 10. A lozenge with angles and line lengths.

Fig. 60

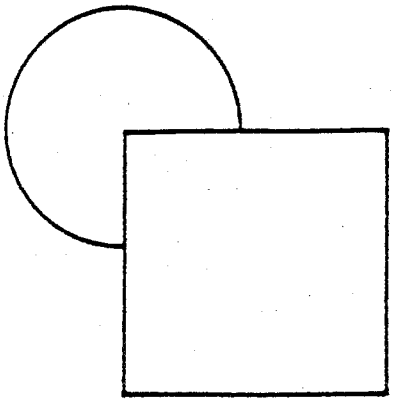

Figure 1. An example of figural completion—most observers "see" the circle completed behind the square.

Fig. 61

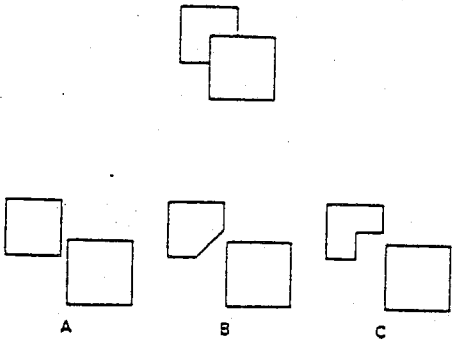

Fig. 62

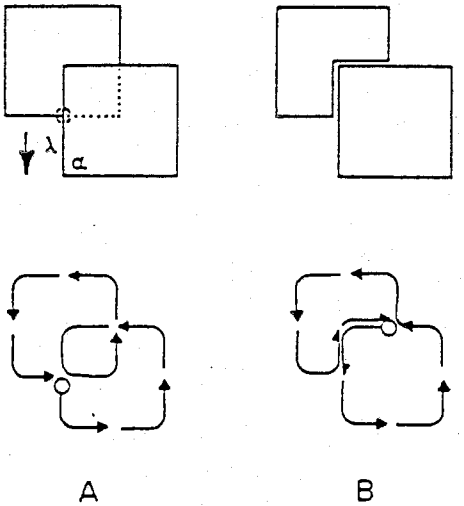

Figure 15. Two possible interpretations of a simple figure completion display, with coding paths indicated.

Fig. 63

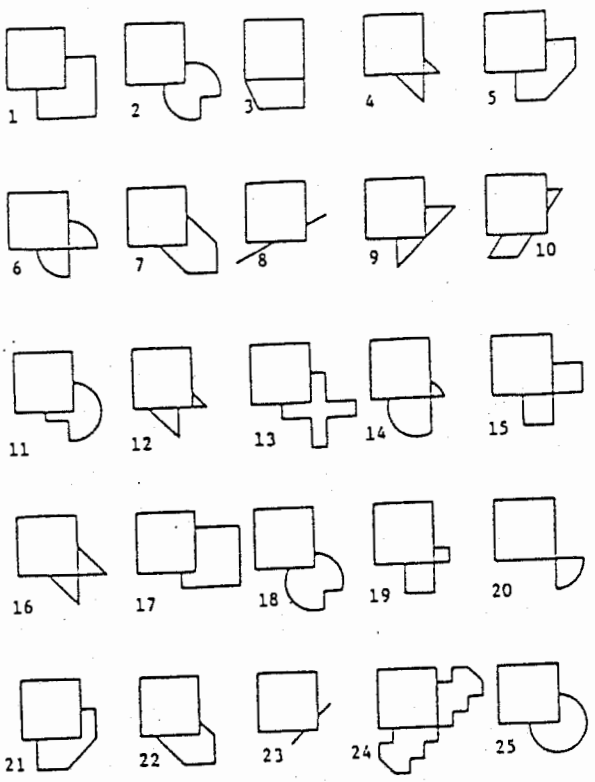

Figure 16. Figures used in experiments, as arranged on test sheet.

Fig. 64

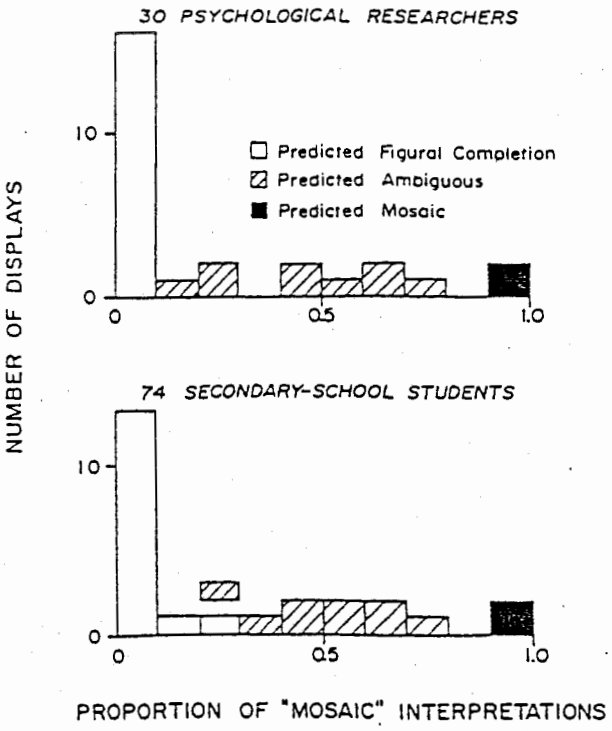

Figure 17. Summary distributions showing that in both experiments, displays predicted to produce figural completions almost always did so, figures predicted to produce mosaic interpretations almost all showed such interpretations, and figures predicted to be ambiguous between completion and mosaic were distributed between, centering near 50–50 choices.

Fig. 65

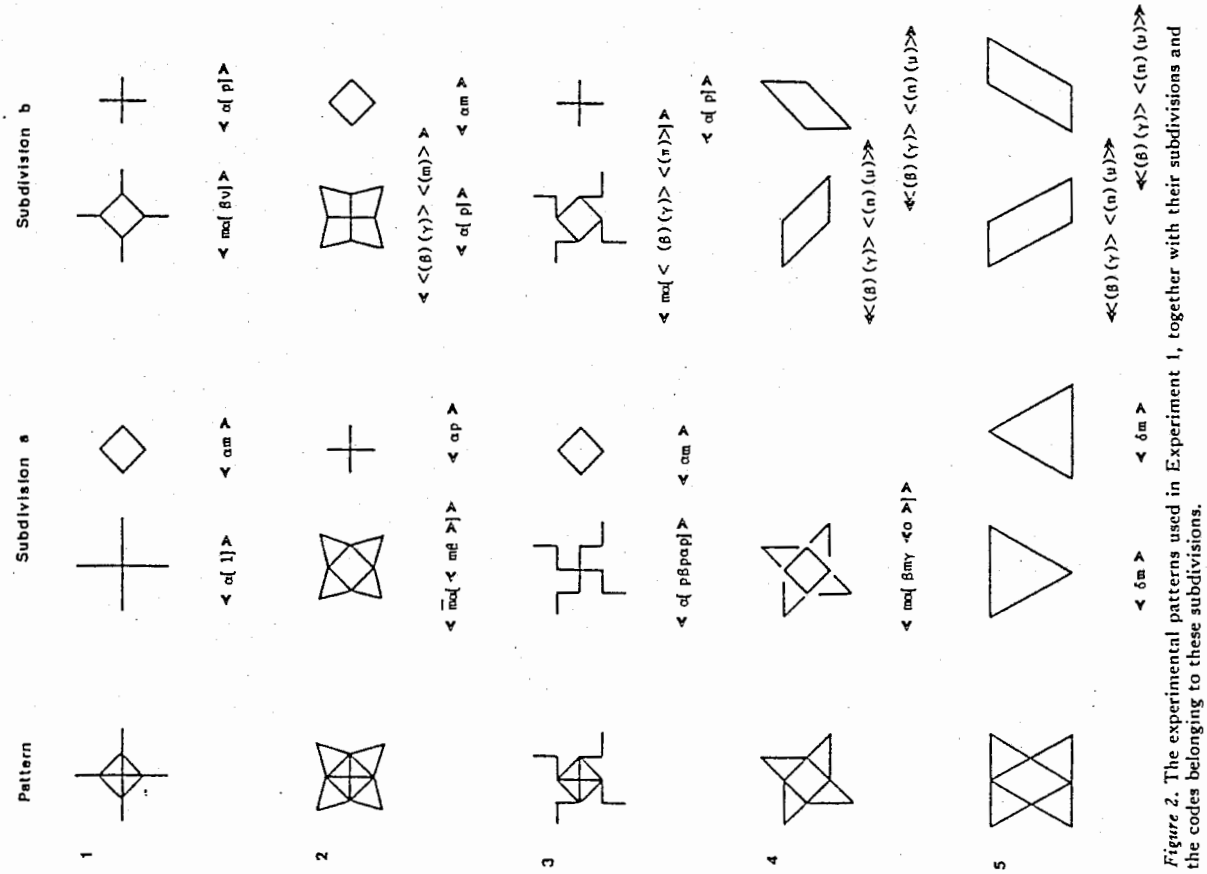

Figure 2. The experimental patterns used in Experiment 1, together with their subdivisions and the codes belonging to these subdivisions.

Fig. 66

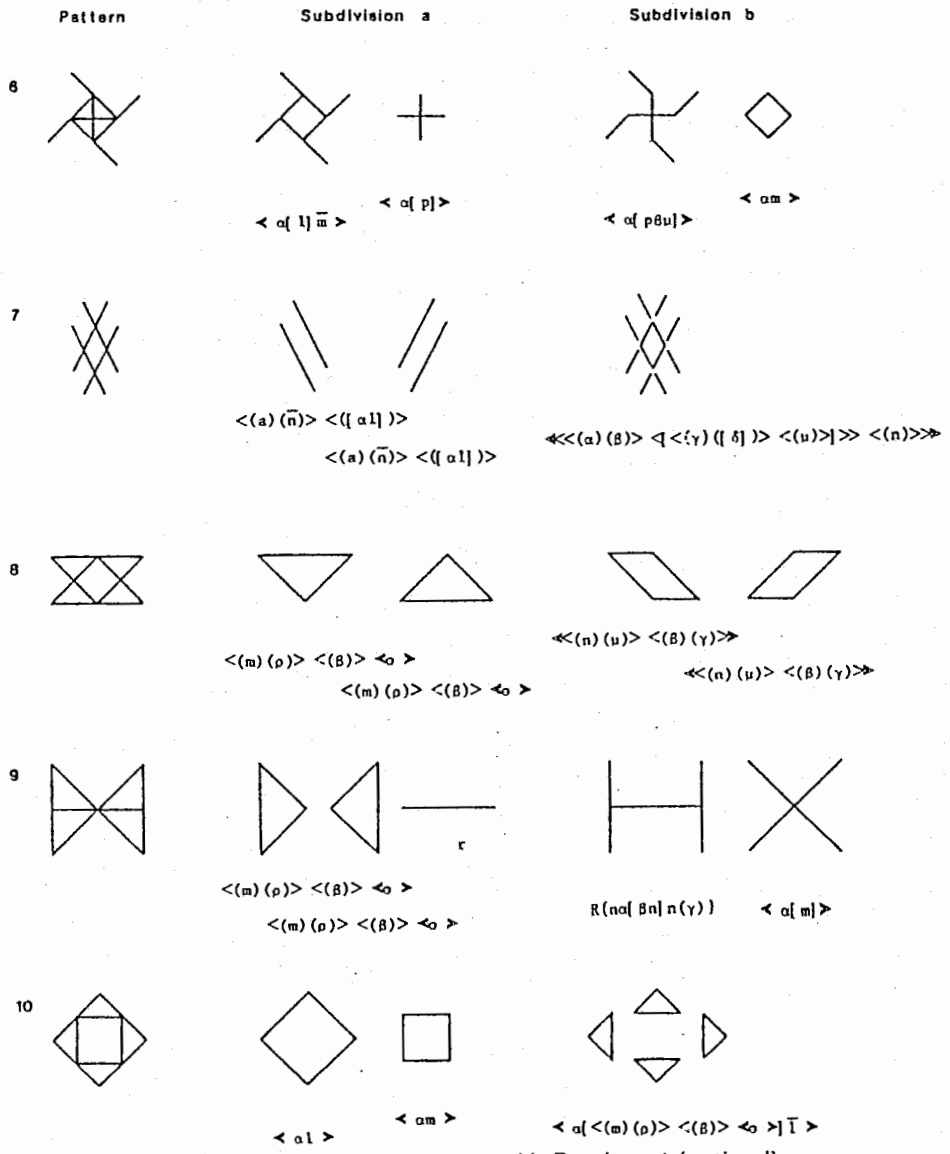

Figure 3. The experimental patterns used in Experiment 1 (continued).

Fig. 67

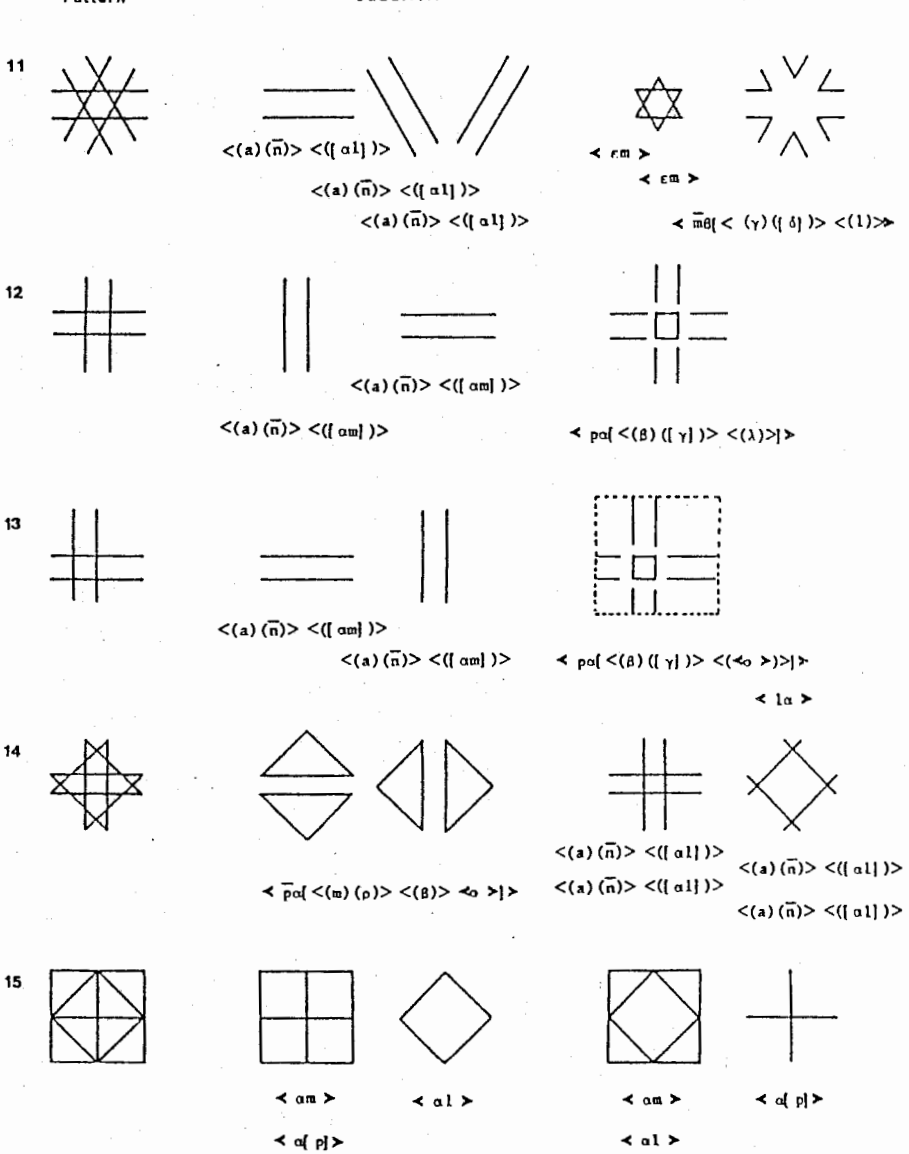

Figure 4. The experimental patterns used in Experiment 1 (continued).

Fig. 68

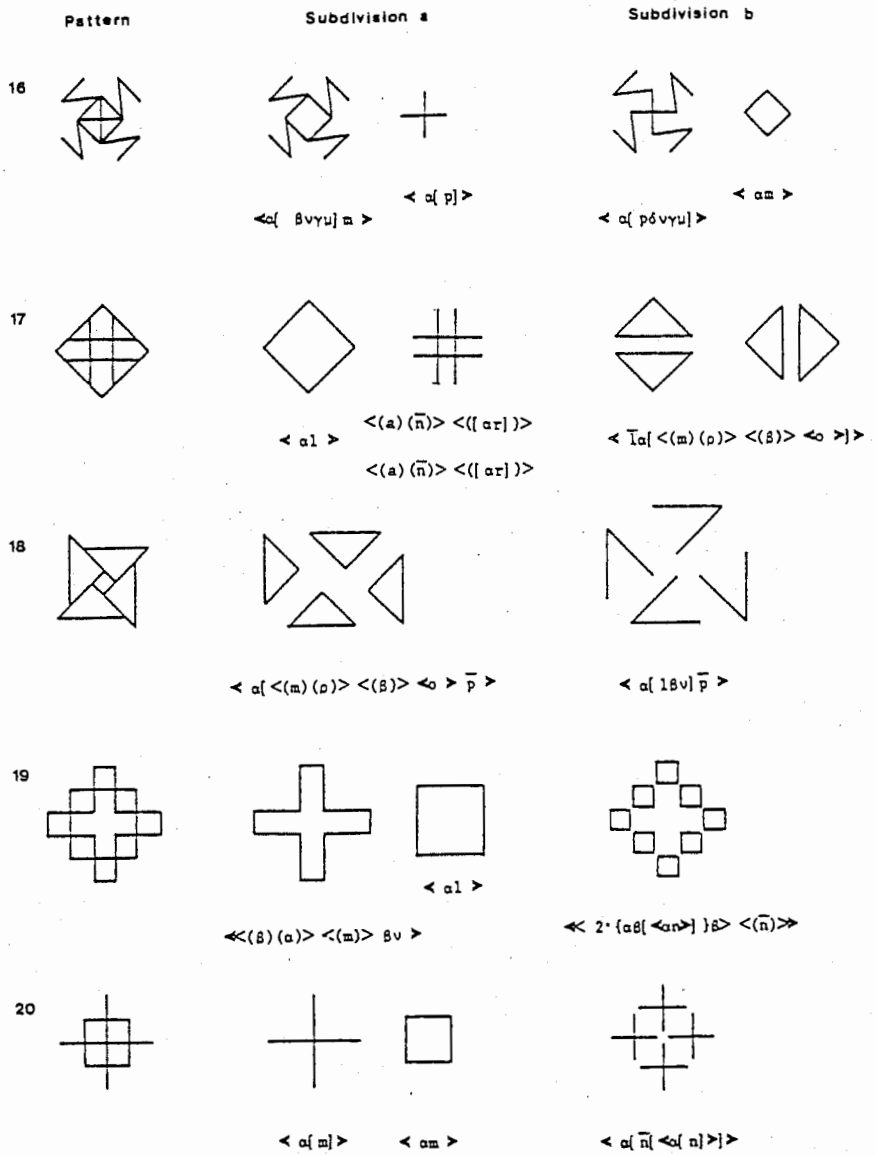

Figure 5. The experimental patterns used in Experiment 1 (continued).

Fig. 69

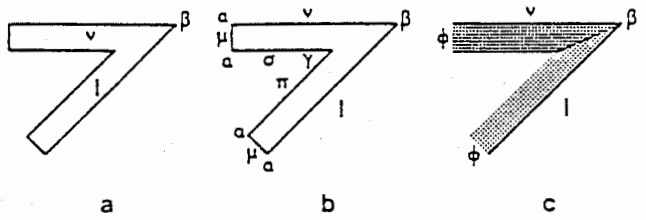

Figure 6. (a) The elements of the hook (i.e., two legs and one angle) are each represented by a code element. (b) Every contour element of the hook is represented by a code element. (c) The contour elements of the hook are coded indirectly by coding the surface of the hook.

Fig. 70

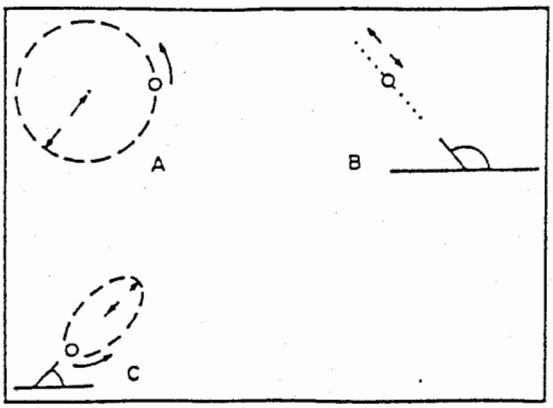

Figure 1. Parameters of motions analyzed in the coding model. (A: standard circular motion, in counterclockwise direction; B: linear motion represented as a circle tilted 90° relative to the presentation plane, orientation (β) = 135°; C: elliptical motion, a tilt of 60° with respect to the plane of project yields an ellipse with minor axis half as long as the major axis, and β = 45°.)

Fig. 71

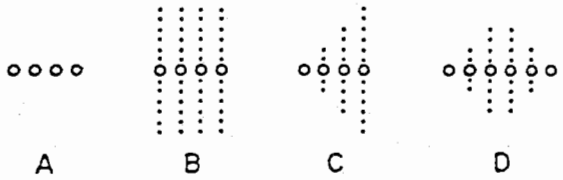

Figure 2. Motion patterns in Johansson's (1950) Experiments 1 (Displays A and B), 2 (Display C), and 3 (Display D). (The degree to which dots are seen as forming a unified whole increases from A to D.)

Fig. 72

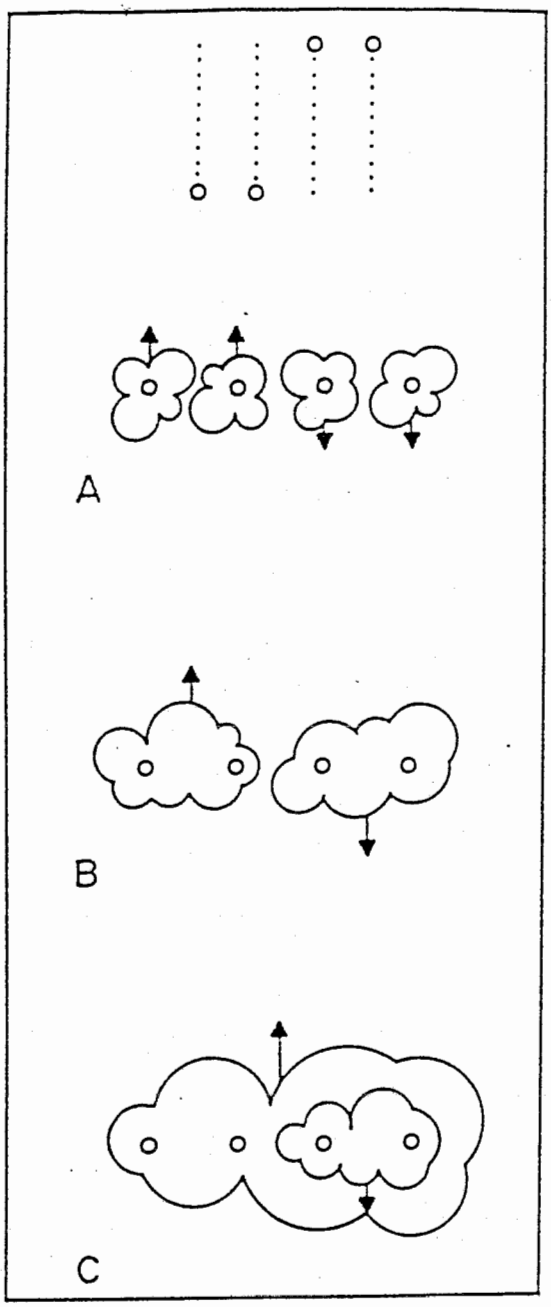

Figure 3. Motion pattern and three interpretations of Johansson's (1950) Experiment 5. {Interpretation A has code $M_{\bullet\bullet\lambda\beta r}(a) + M(b) + M(c) + M(d)$, I = 20. Interpretation B has code $M_{\bullet\bullet\lambda\beta r}(ab) + M_{\bullet\bullet\lambda\beta r}(cd)$, I = 10. Interpretation C has code $M_{\bullet\bullet\lambda\beta r}$ (system) $[M_{\bullet\ldots\beta}.(cd)]$ or $M(M_{\bullet\ldots\beta}.)$, I = 7. Most subjects report subunits of (ab) and (cd) and see the two subunits as related.}

Fig. 73

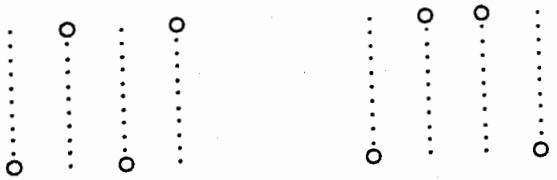

Figure 4. Motion patterns for Johansson's (1950) Experiments 6 and 7. (In both experiments, points moving in the same direction are grouped together, and the groups are seen as related.)

Fig. 74

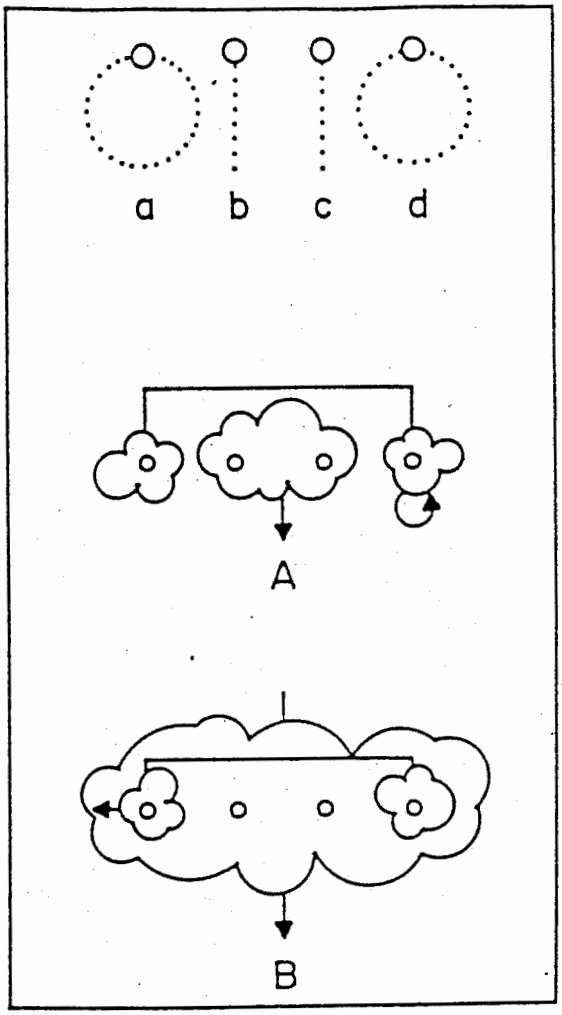

Figure 6. Motion pattern and two interpretations of Johansson's (1950) Experiment 18, in which the circular motion is analyzed into two out-of-phase linear components. (The figure shows that there is no general preference for circular motions, since observers' reports agree with Interpretation B. Codes are A: M(ad) + M(bc), $I = 10$ and B: M(system)[$M_{\omega\phi \cdot \beta}$.(ad)], $I = 8$.)

Fig. 76

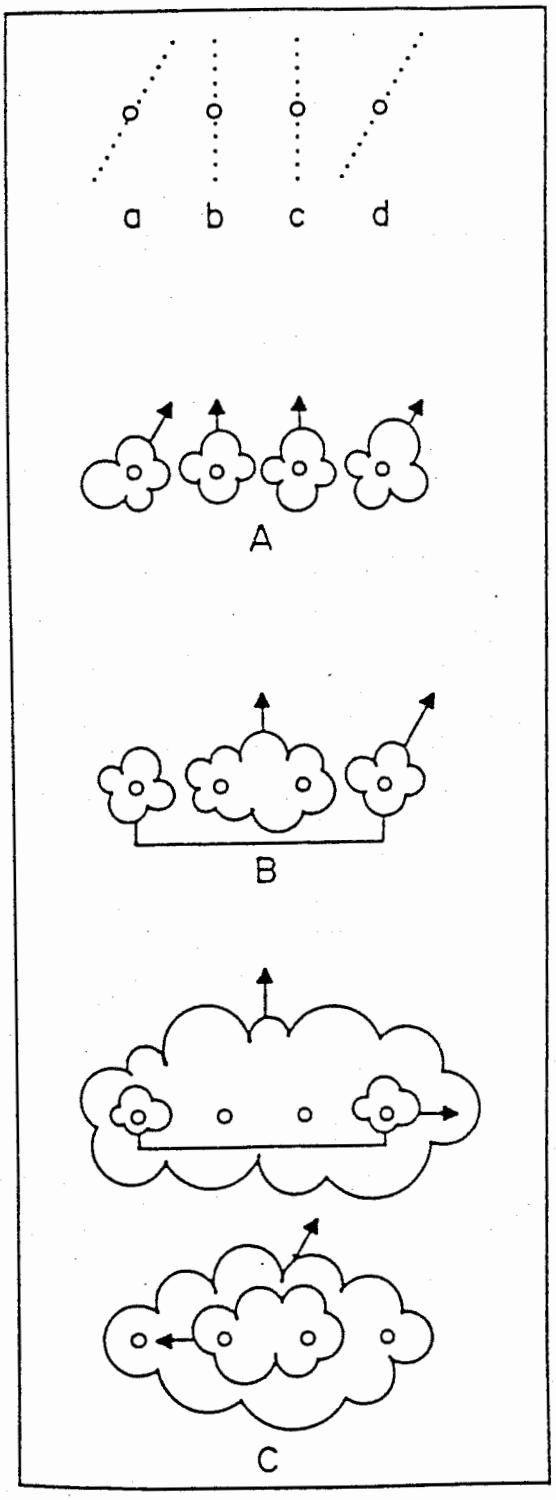

Figure 5. Motion pattern and interpretations of Johansson's (1950) Experiment 17, showing grouping and also analysis of a sloping motion into vertical and lateral components. (Codes are A: M(a) + M(b) + M(c) + M(d), $I = 20$; B: M(ad) + M(bc), $I = 10$; and C: M (system)[$M_{\omega \ldots \beta}$.(ad)], $I = 7$. The two versions of Interpretation C are seen by observers.)

Fig. 75

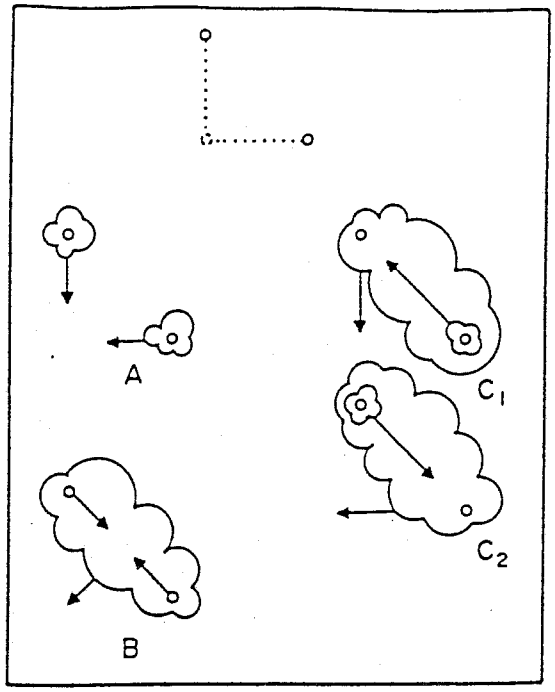

Figure 7. Analysis of horizontal and vertical components into sloping components—either two sloping components (Interpretation B) or one sloping and one vertical or horizontal component (Interpretation C). (Codes are A: M(a) + M(b), $I = 10$; B: M(system)[$M_{\alpha\ldots\beta}$.(distance a, b)], $I = 7$; C_1: M(system)[$M_{\alpha\ldots\beta}$.(b)]; and C_2: M(system)[$M_{\alpha\ldots\beta}$.(a)], $I = 7$. This result shows that subjects do not have a general preference for horizontal or vertical orientations.)

Fig. 77

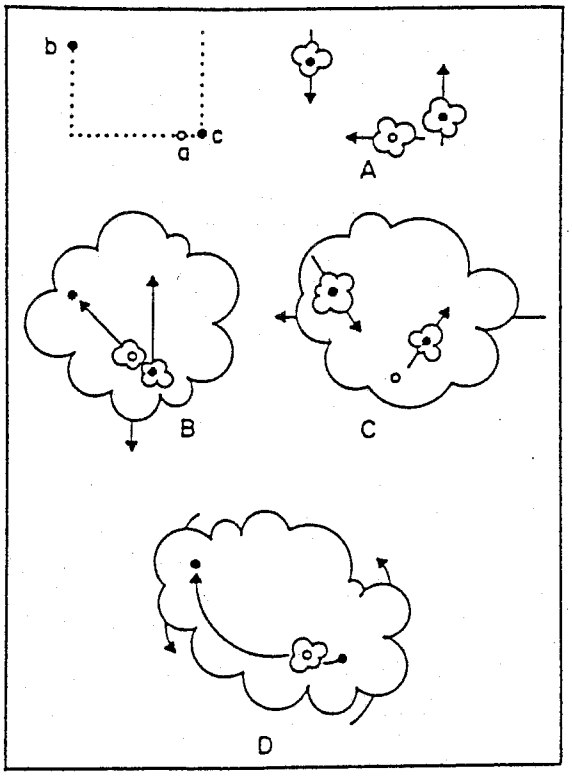

Figure 8. Gogel's (1974) display with four interpretations. (Codes are A: M(a) + M(b) + M(c), $I = 15$; B: M(system)[$M_{\alpha\ldots\beta}$.(c)], $I = 9$; and C: M(system: × [$M_{\alpha\ldots\beta}$.(b) + $M_{\alpha\ldots\beta}$.(c)], $I = 9$. D: Since Interpretation D involves a curved path and a rocking motion, it has no code in this system.)

Fig. 78

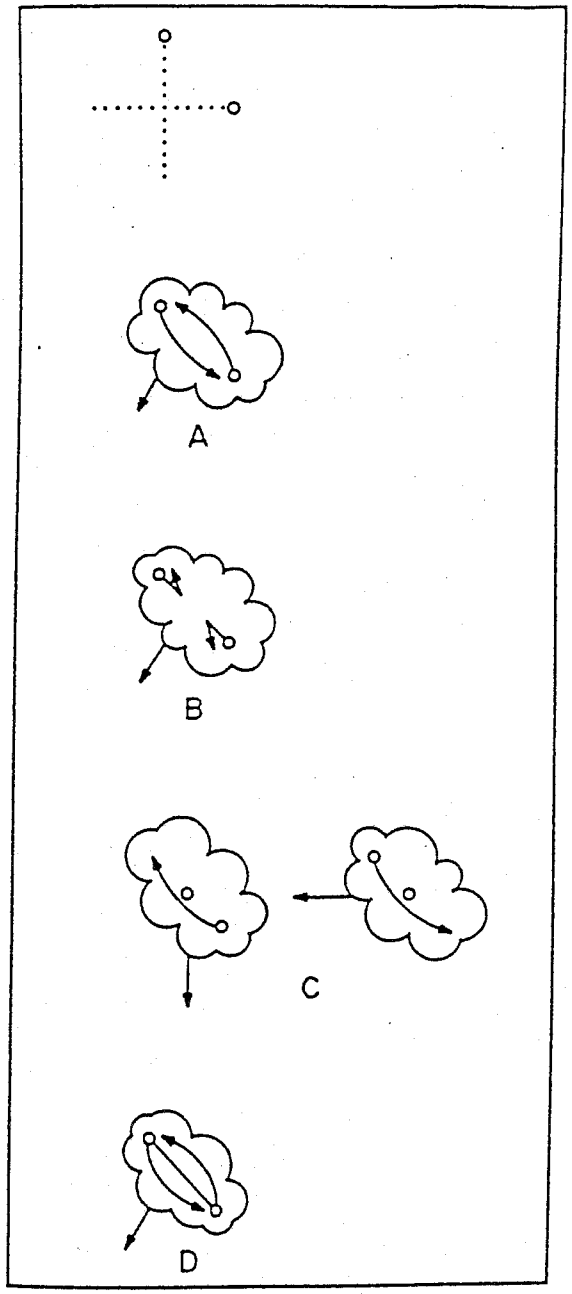

Figure 9. Johansson's (1950) Experiment 20, in which paths intersect; notice the variety of interpretations, all of which can be seen. (Codes are A: M(ab)[$M_{\alpha\ldots\beta}$.(a) + M..$_{\beta}$..(b)], $I = 8$; B: M(ab)[$M_{\alpha\ldots\beta}$. (distance a to b)] + collision, $I = 7$ or 8; C: M(system)[$M_{\alpha\ldots\beta}$.(a)], $I = 7$; and D: M(system)[$M_{\alpha\ldots\beta}$.(ab)]. in third dimension, $I = 7$.)

Fig. 79

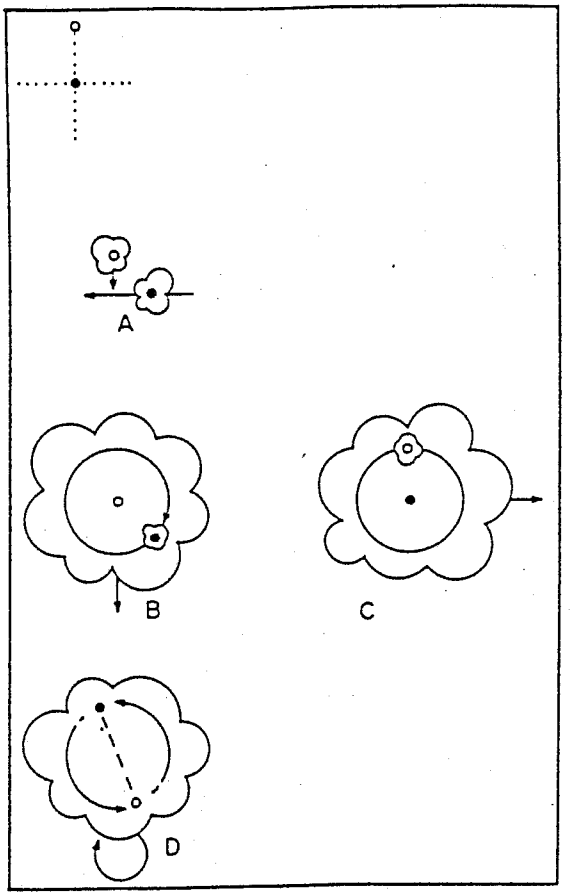

Figure 10. Motion paths in Johansson's (1950) Experiment 21. {The points are 90° out of phase, and as a result remain always the same distance apart. In this case, two straight-line motions are synthesized into one (Interpretations B and C) or two (Interpretation D) circular apparent motions. This result shows that straight line motions are not preferred over circles. Codes are A: M(a) + M(b), $I = 10$; B: M(system) × [$M_{\alpha} \ldots_{\beta,\gamma}$(a)], $I = 8$; C: M(system)[$M_{\alpha} \ldots_{\beta,\gamma}$(b)], $I = 8$; and D: M(system)[$M_{\alpha} \ldots_{\beta,\gamma}$(ab)].}

Fig. 80

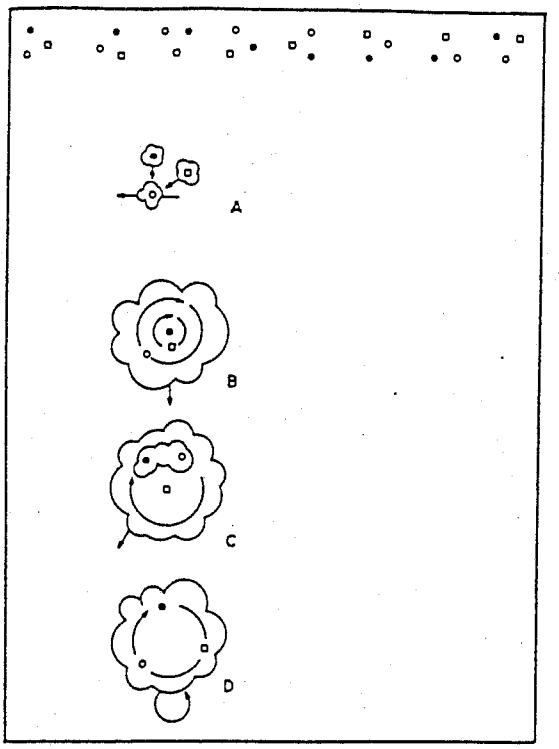

Figure 11. Johansson's (1950) Experiment 24 with three points in linear paths, out of phase. {The relative positions of the three points are constant, and the points could be lights on the rim of a wheel that rotates within a hoop. Codes are A: M(a) + M(b) + M(c), $I = 15$; B: M(system)[$M_{\alpha\phi} \ldots_{\gamma}$(b) + $M_{\alpha\phi} \ldots_{\gamma}$(c)], $I = 11$; C: M(system)[$M_{\alpha\phi} \ldots_{\gamma}$(a, c)], $I = 8$; and D: M(system)[$M_{\alpha\phi} \ldots_{\gamma}$(wheel)], $I = 8$.}

Fig. 81

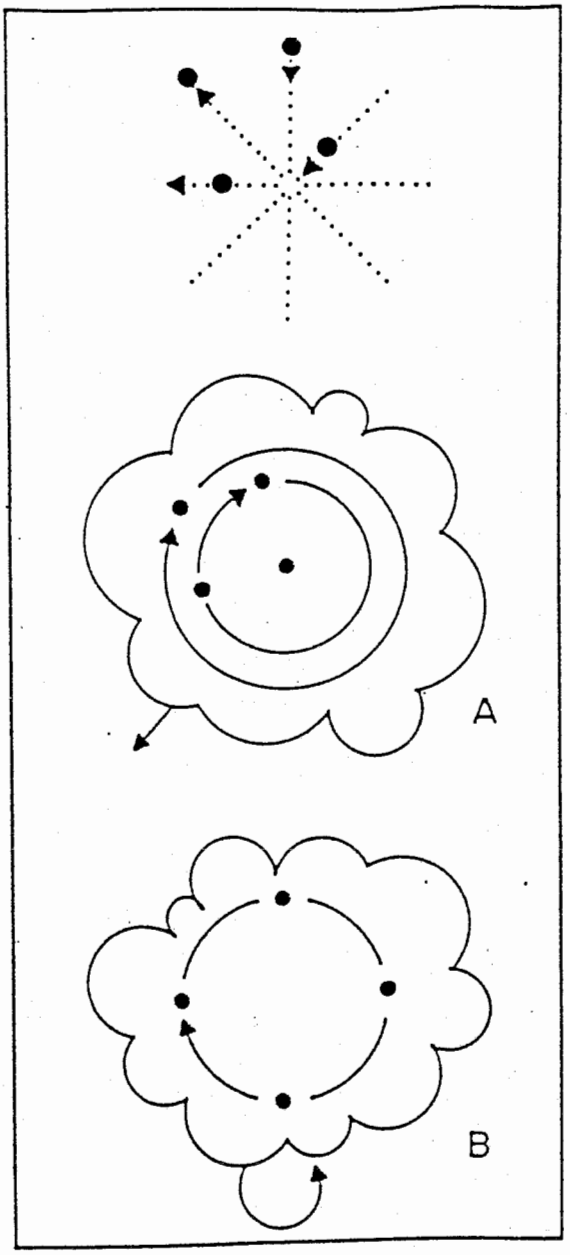

Figure 12. New experiment by the author, using four points at angles and phases of 0°, 45°, 90°, and 135°. (Interpretation B, the wheel within a hoop, is dominant; it has code M(system)[$M_{\alpha\ldots\beta,\gamma}$(wheel)], though it is possible to see something like Interpretation A with code M(system)[$M_{\alpha\ldots\gamma}$(a, c) + $M_{\alpha\ldots\gamma}$(d)] by fixating one dot. However, one does not see the orbits of nonfixated points as independent, but instead one sees a square rotating around the fixated corner.)

Fig. 82

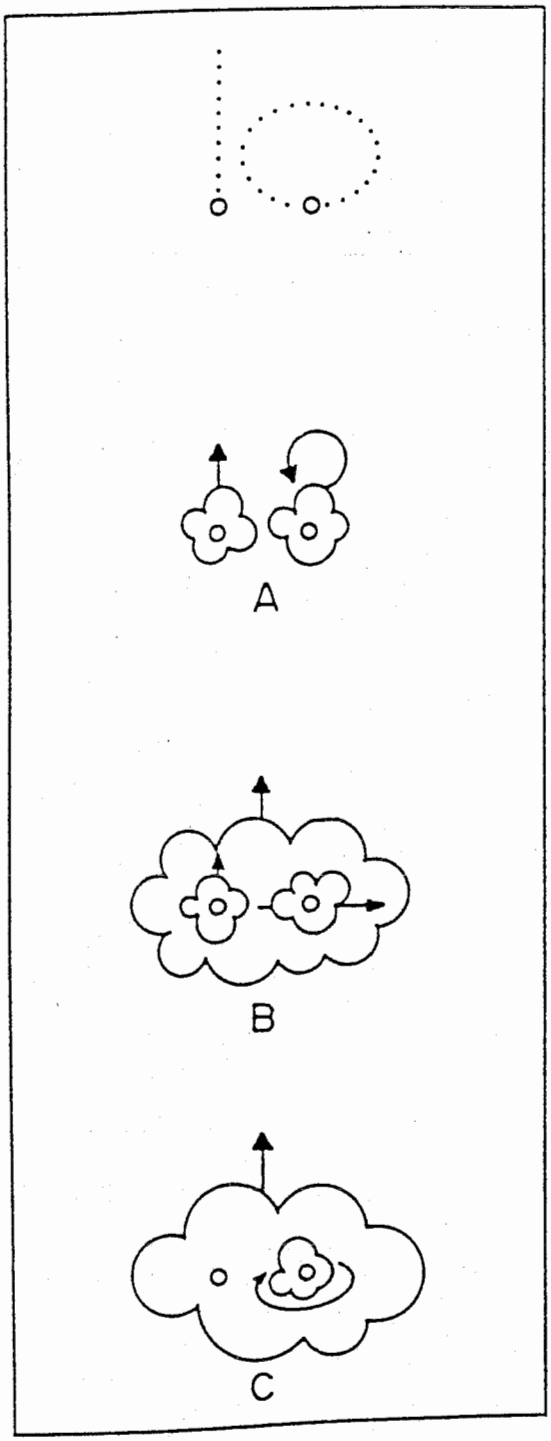

Figure 13. Motion analysis when there is no common vector that exhausts a given direction. (The code of A is M(a) + M(b), $I = 10$. Interpretation B, with three motions, has code M(system)[$M_{\alpha\ldots}$(a) + $M_{\alpha\alpha\cdot\beta\cdot}$(b)], $I = 9$ and is reported by Johansson (1950). Interpretation C, which should be equally apparent, is not seen; the code of C is M(system)[$M_{\alpha\alpha\cdot\beta,\gamma}$(b)], $I = 9$.)

Fig. 83

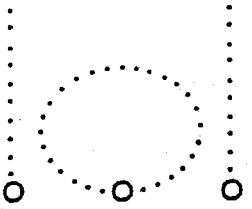

Figure 14. Variant of Johansson's (1950) Experiment 28 devised by the author, which generates a clockwise (retrograde) elliptical path for point b. (This corresponds to the "missing" Interpretation C in Figure 13.)

Fig. 84

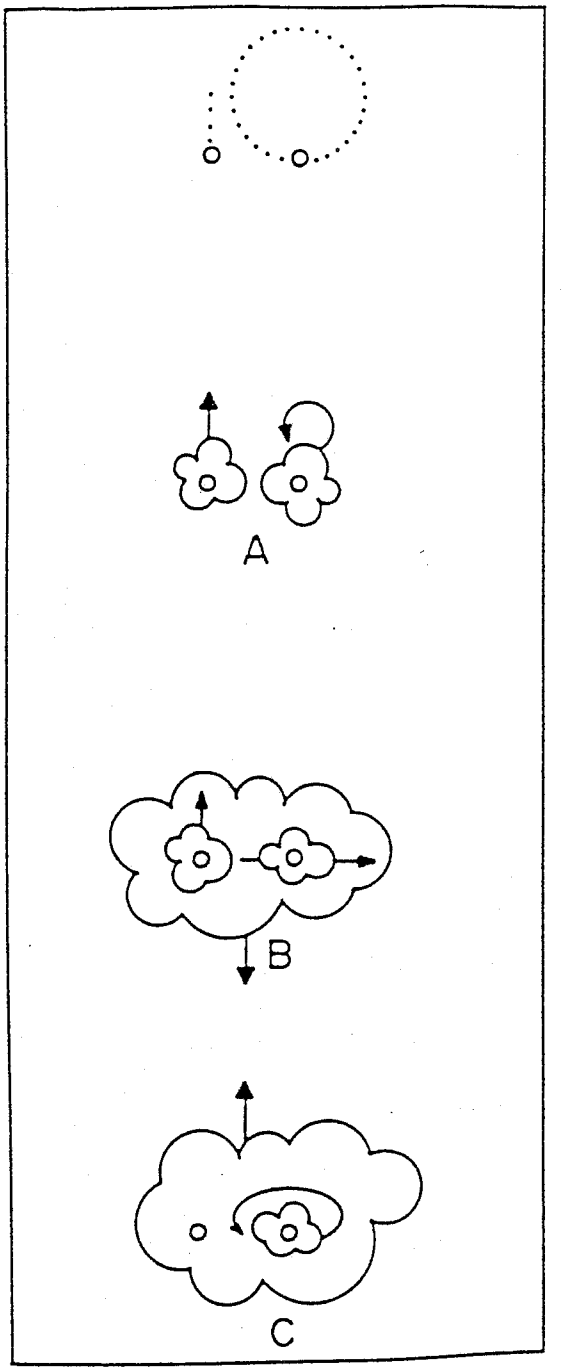

Figure 15. Johansson's (1950) Experiment 29, which again demonstrates motion analysis without common vectors. (This also results in an elliptical motion (Interpretation C) being seen, as a product of a linear and a circular motion. In combination with Figures 6, 7, and 9, this figure establishes that circular, linear, and elliptical paths are equally seen, and orientation as well as shape of path is unimportant. What is consistent is that subjects prefer to see the motion configuration with the minimum information load. The code of A is M(a) + M(b), $I = 10$; the code of B is M(system)[$M_{\bullet\ldots\beta}$.(a) + $M_{\bullet\bullet\ldots\beta}$.(b)], $I = 10$; and the code of C is M(system)[$M_{\bullet\bullet\ldots\beta r}$(b)], $I = 9$.)

Fig. 85

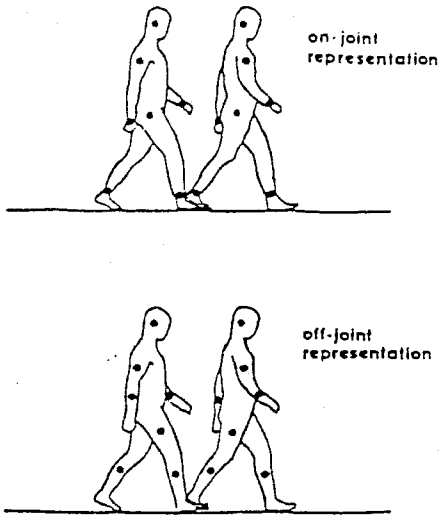

Figure 1. Schematic representations of a male walker. (In the upper panel, lights are mounted on the head, on the right shoulder and hip, and on the right and left wrists and ankles. In the dynamic displays only the lights are seen. This is called an *on-joint* representation of a walker. In the lower panel, lights are mounted on the head, on the upper right arm and leg, and on the lower right and left arms and legs. These lights are halfway between major joints, and the configuration is called an *off-joint* representation of a walker. Notice that the two types of stimuli have the same number of lights.)

Fig. 86

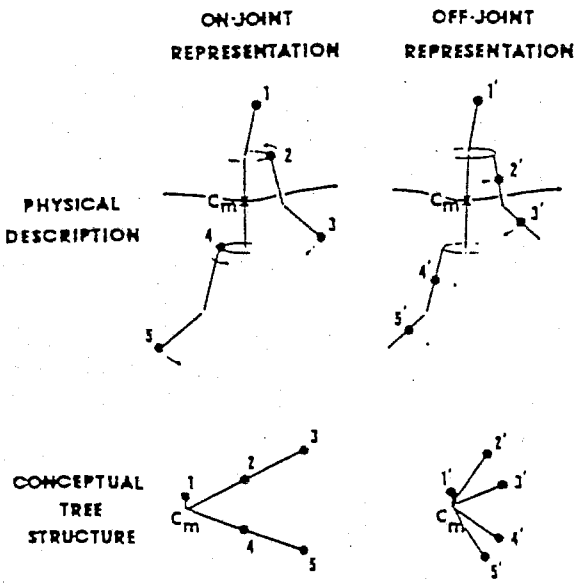

Figure 2. In the upper panels are the physical, vectorlike descriptions of the on- and off-joint walkers, considering only the right side of the body; below these are conceptual tree structures representing the nesting of movements. (Notice that both figures have centers of moment.)

Fig. 87

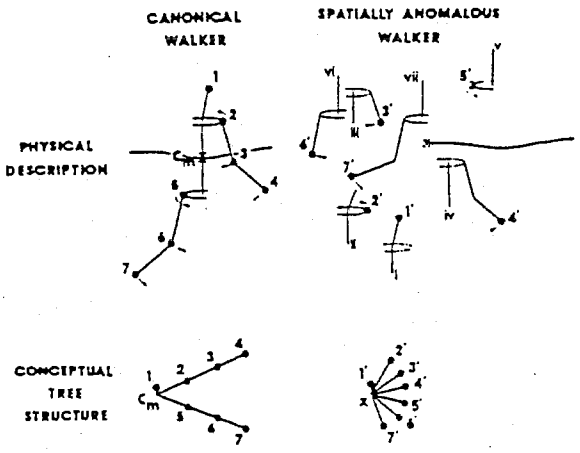

Figure 3. In the upper panels are the physical, vectorlike descriptions of a canonical walker and a spatially anomalous walker, one whose particular spatial relations among lights has been markedly perturbed; below these are conceptual tree structures of the nested movements around their generating centers. (Notice that only the canonical walker has a true center of moment; that for the anomalous walker is indeterminate in location.)

Fig. 88

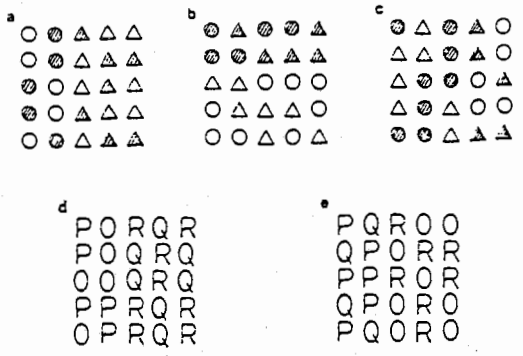

FIG. 1. Examples of easy and of difficult texture segregation: (a) salient vertical boundary between circles (curved shapes) on left and triangles (straight and angular shapes) on right; (b) salient horizontal boundary between red shapes above and green shapes below; (c) no salient boundary between conjunctions of green triangles and red circles on left and green circles and red triangles on right; (d) salient vertical boundary between letters without diagonal line on left and letters with diagonal line on right; (e) no salient boundary between *P*s and *Q*s on left and *R*s and *O*s on right.

Fig. 89

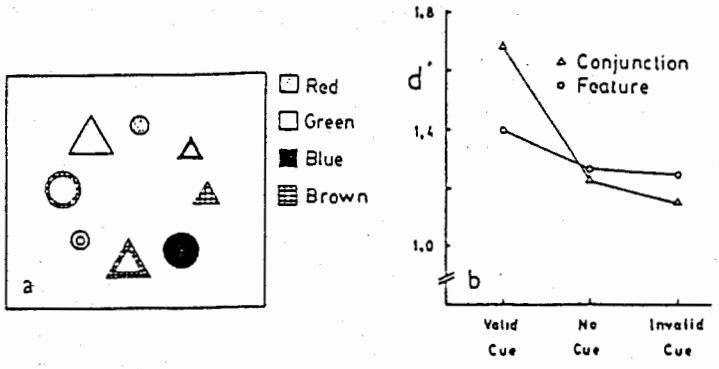

FIG. 4. (a) Example of a display of multi-dimensional stimuli used either for feature search or for conjunction search. The feature target for this display might be a red item and the conjunction target might be a large brown outline triangle. An advance cue, consisting of a bar marker outside the display pointing at the location to be occupied by one of the eight items, was given on most trials. (b) Mean accuracy (expressed as the signal detection measure *d'*) in the different cue conditions for feature and for conjunction targets.

Fig. 90

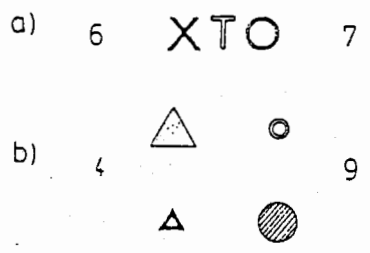

FIG. 5. (a) Example of displays used to demonstrate the occurrence of illusory conjunctions when attention cannot be focused on each letter in turn. If solid letters were blue, outline letters green and speckled red, then subjects, given this display, might report, for example, a blue *T* or a red *X*. (b) Example of displays used to investigate possible similarity constraints on illusory conjunctions. Subjects were as likely to attribute the color of the large filled triangle to the small outline circle as to attribute to it the color of the small outline triangle (or even of another small outline circle, when two were included in the display).

Fig. 91

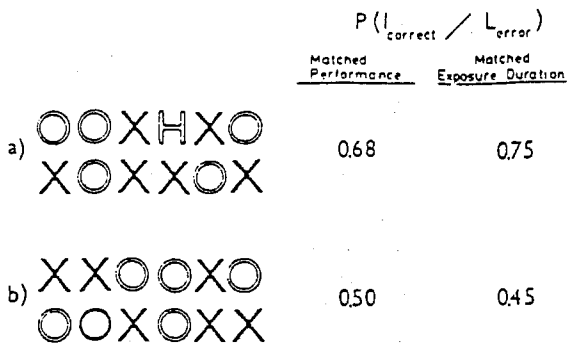

FIG. 6. Examples of displays used to investigate the dependence of accurate identification on accurate localization. (a) The target was either an *H* or an orange letter (among red and blue distractors). Forced choice identification was significantly better than chance even when the target was mislocalized by more than one position in any direction. (b) The target was either a red *O* or a blue *X* (among blue *O* and red *X* distractors). These targets differ from the distractors only in the way their properties are conjoined. Forced choice identification was at chance when localization was incorrect.

Fig. 92

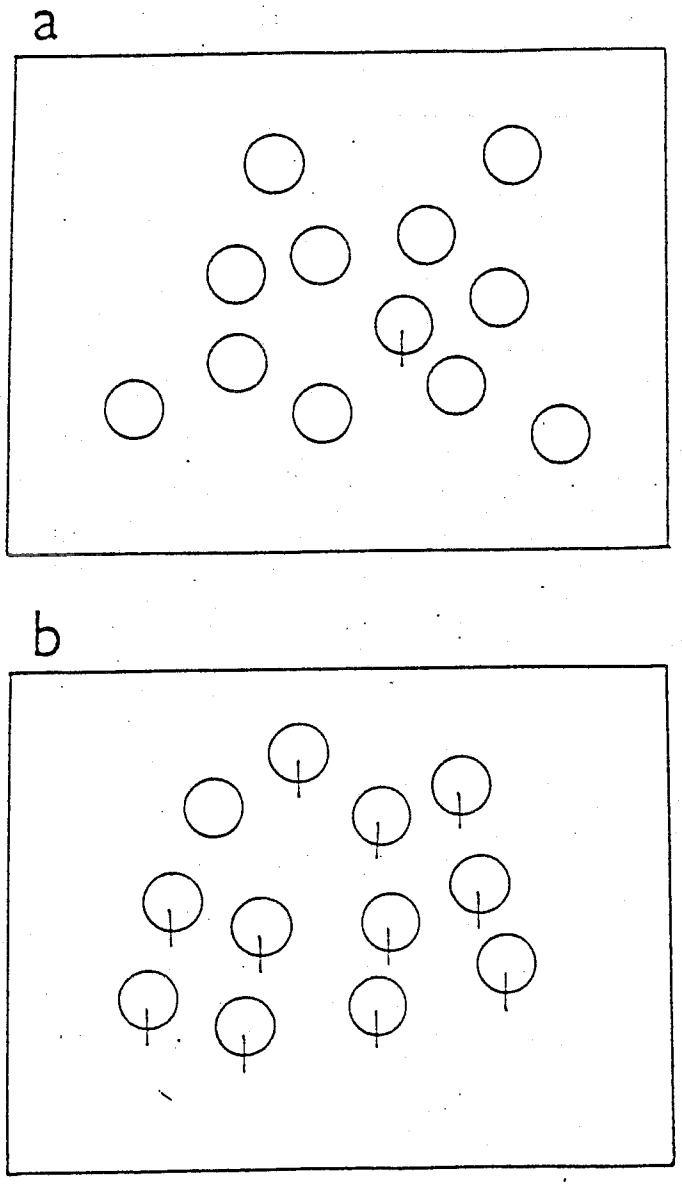

Figure 1. Examples of displays of 12 items with target present for each type of target.

Fig. 93

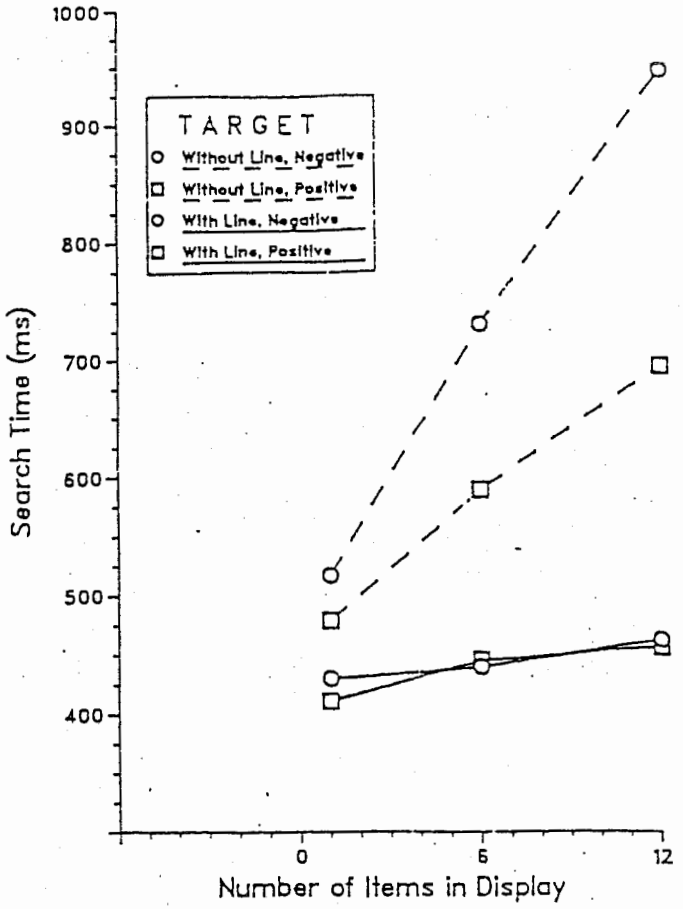

Figure 2. Search times in the different conditions of Experiment 1.

Fig. 94

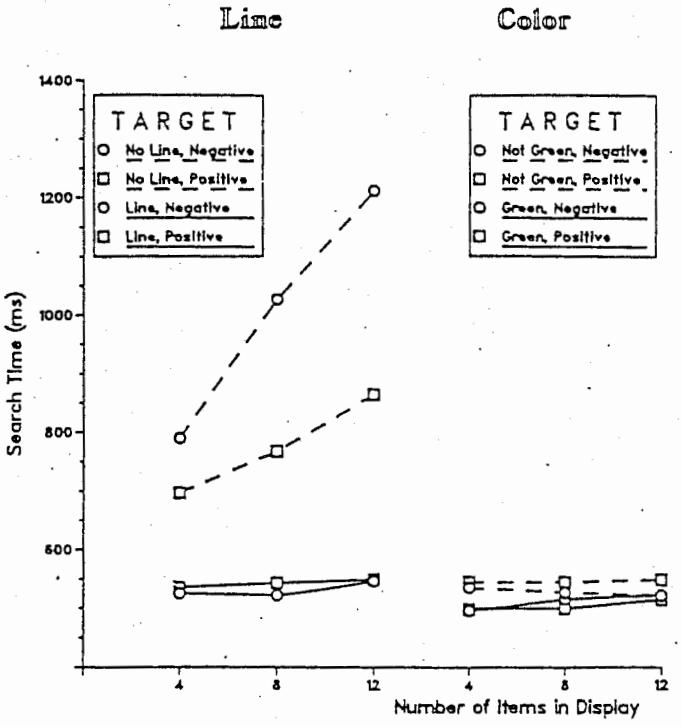

Figure 3. Search times in the different conditions of Experiment 2.

Fig. 95

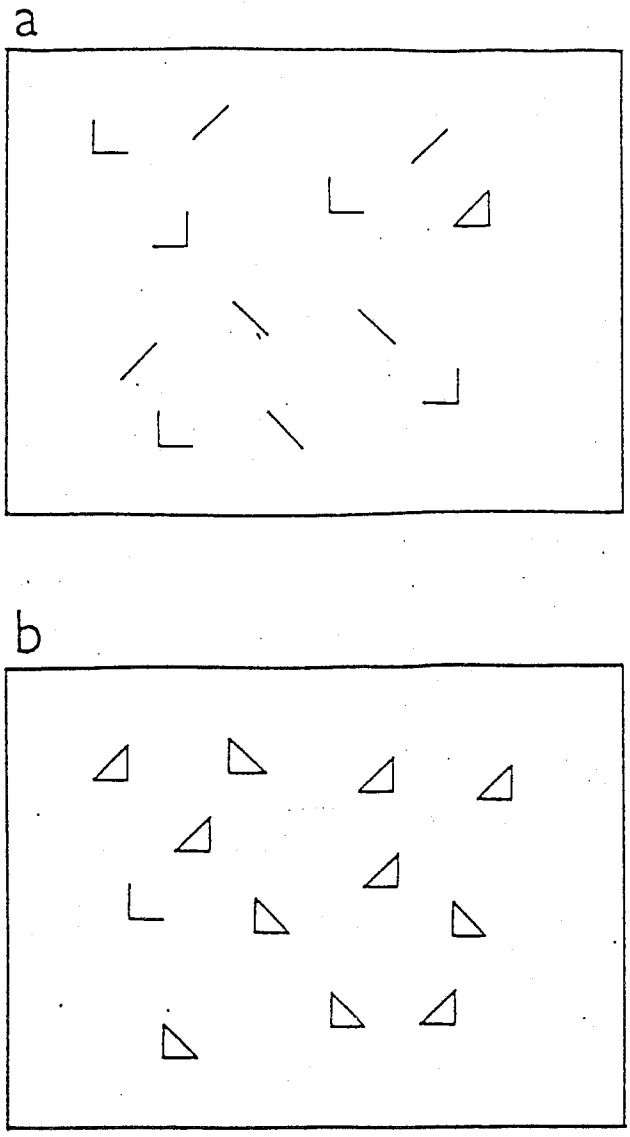

Figure 4. Examples of displays in the triangle presence and absence conditions of Experiment 3.

Fig. 96

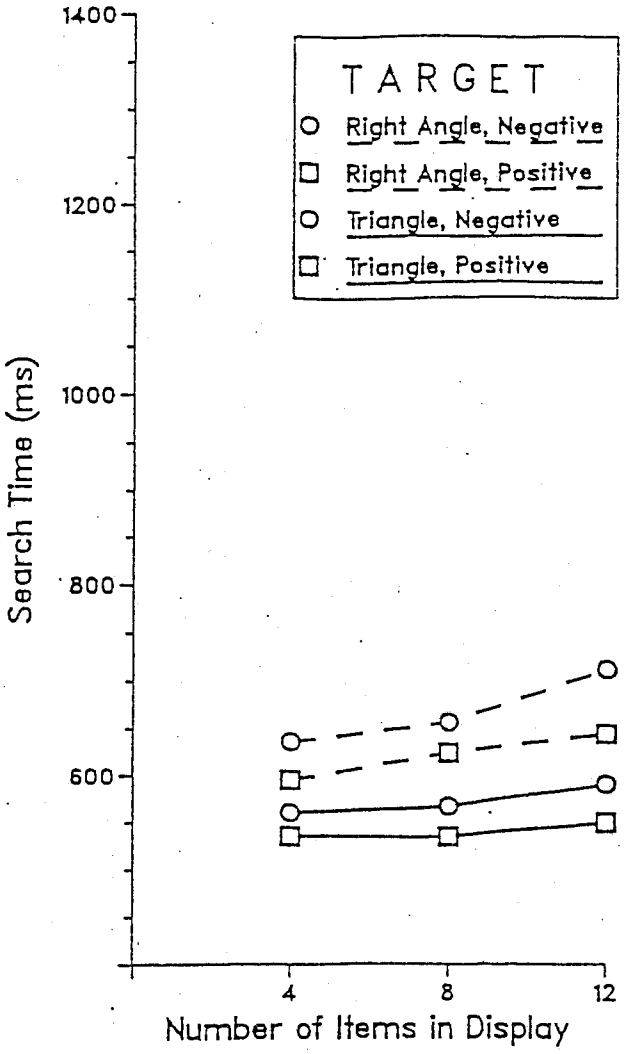

Figure 5. Search times in Experiment 3.

Fig. 97

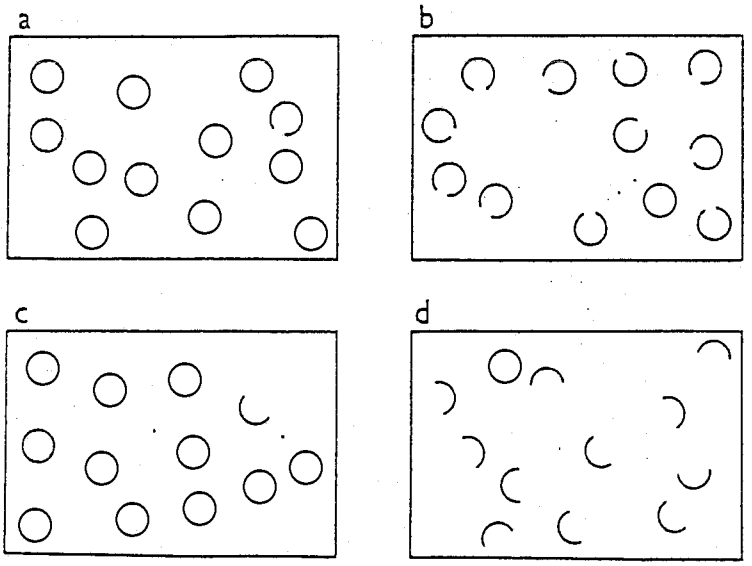

Figure 6. Examples of displays with target circles, and target circles with gaps at the largest and smallest gap sizes in Experiment 4.

Fig. 98

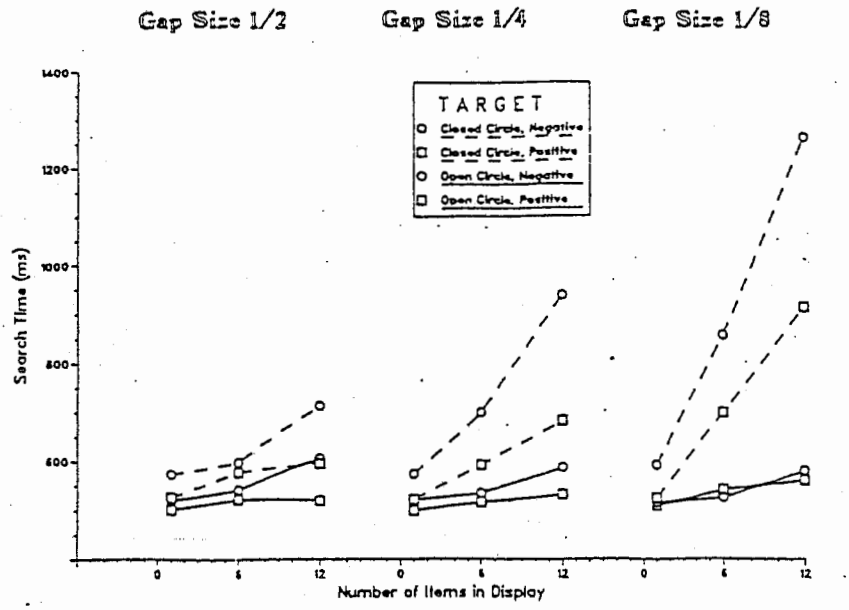

Figure 7. Search times in the different conditions of Experiment 4.

Fig. 99

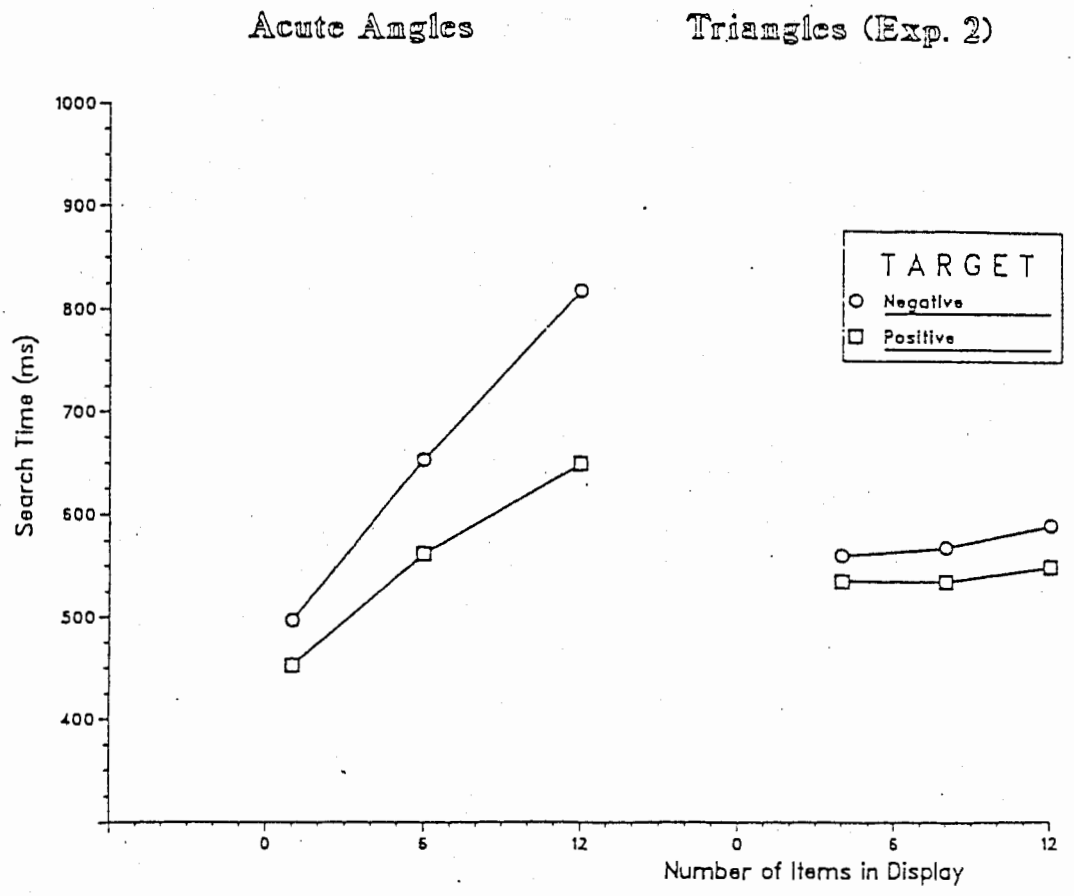

Figure 8. Search times in the different conditions of Experiment 5. (Exp. = Experiment)

Fig. 100

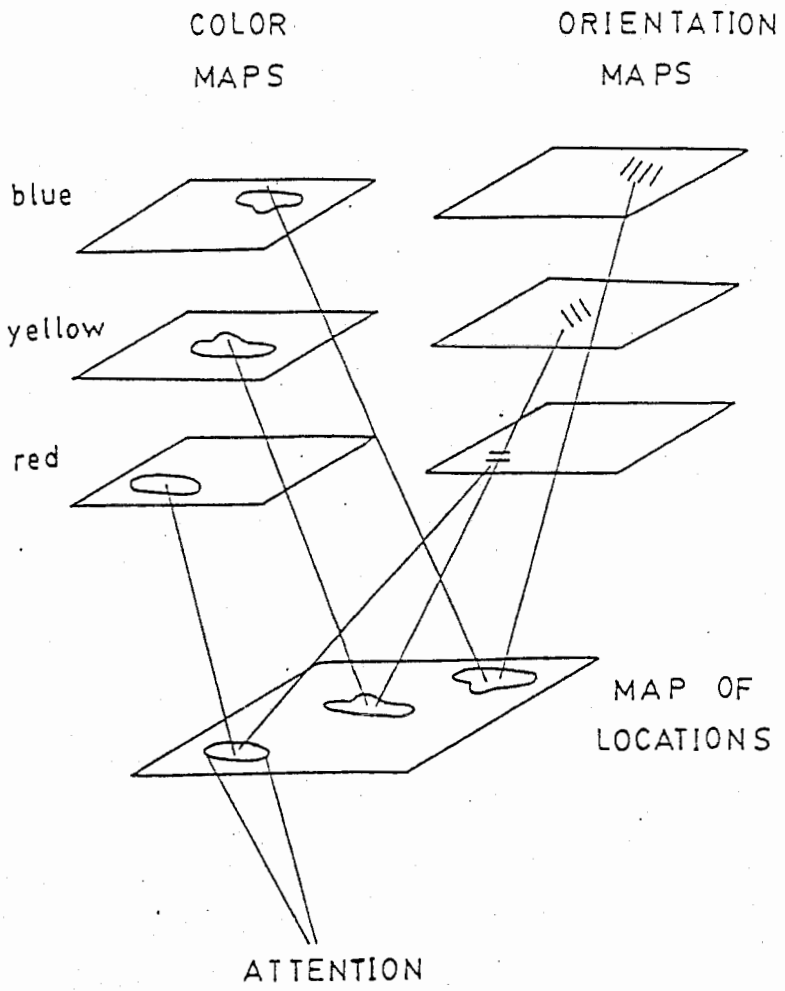

Figure 9. Schematic diagram suggesting the functional arrangement of feature maps and master location map through which attention links features to form objects.

Fig. 101

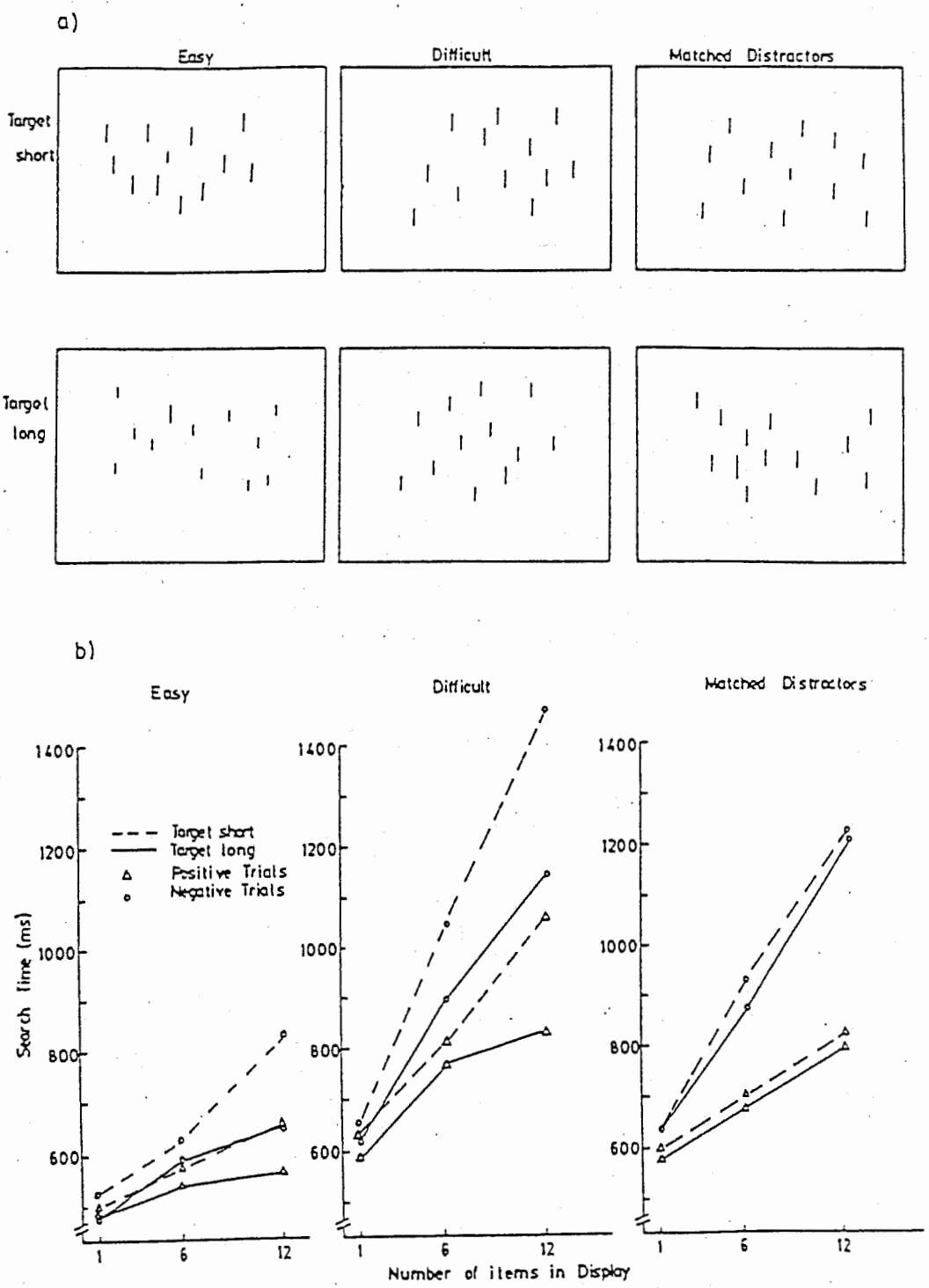

Figure 2. (a) Examples of displays testing search for targets defined by differences in line length and (b) search latencies in Experiments 1 and 1a—line length.

Fig. 102

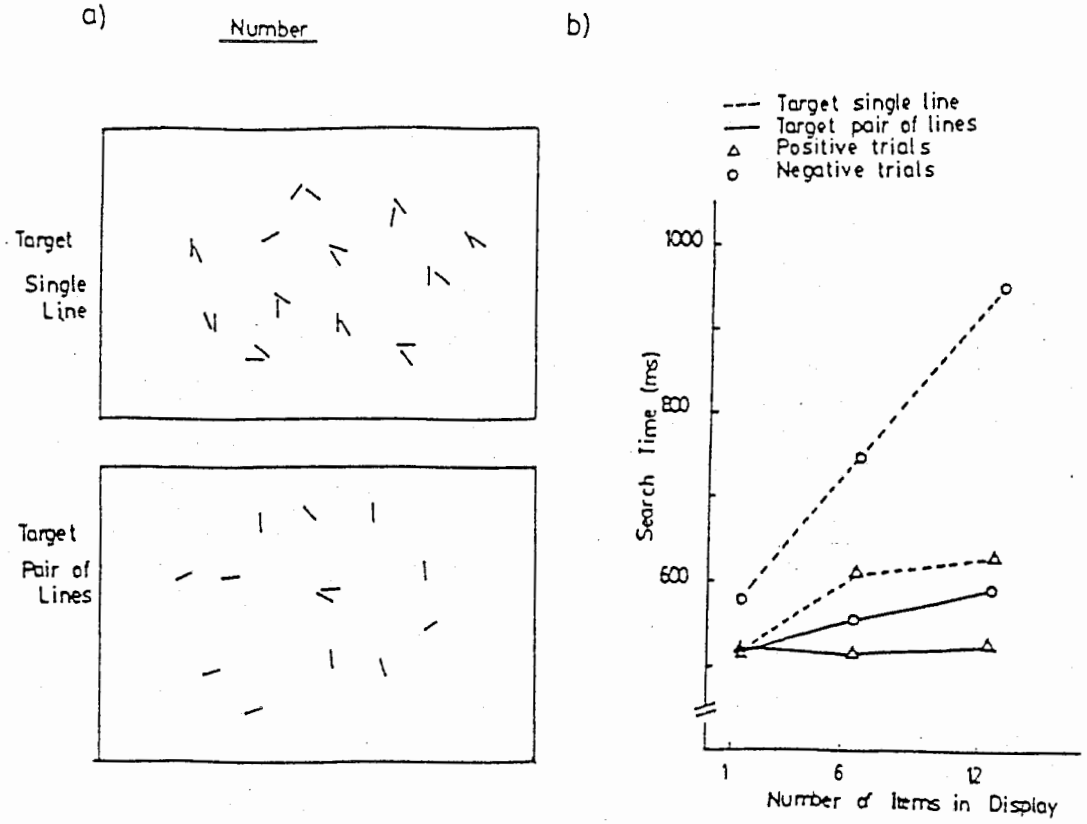

Figure 3. (a) Examples of displays testing search for targets defined by number (two vs. one) and (b) search latencies in Experiment 2—number.

Fig. 103

↑
3

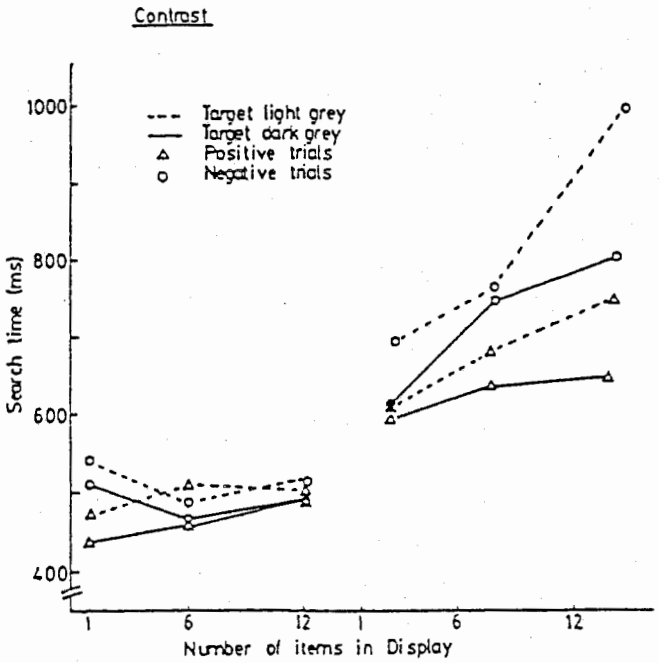

Figure 4. Search latencies in Experiment 3—contrast. (More discriminable greys on left and less discriminable greys on right.)

Fig. 104

↑
2

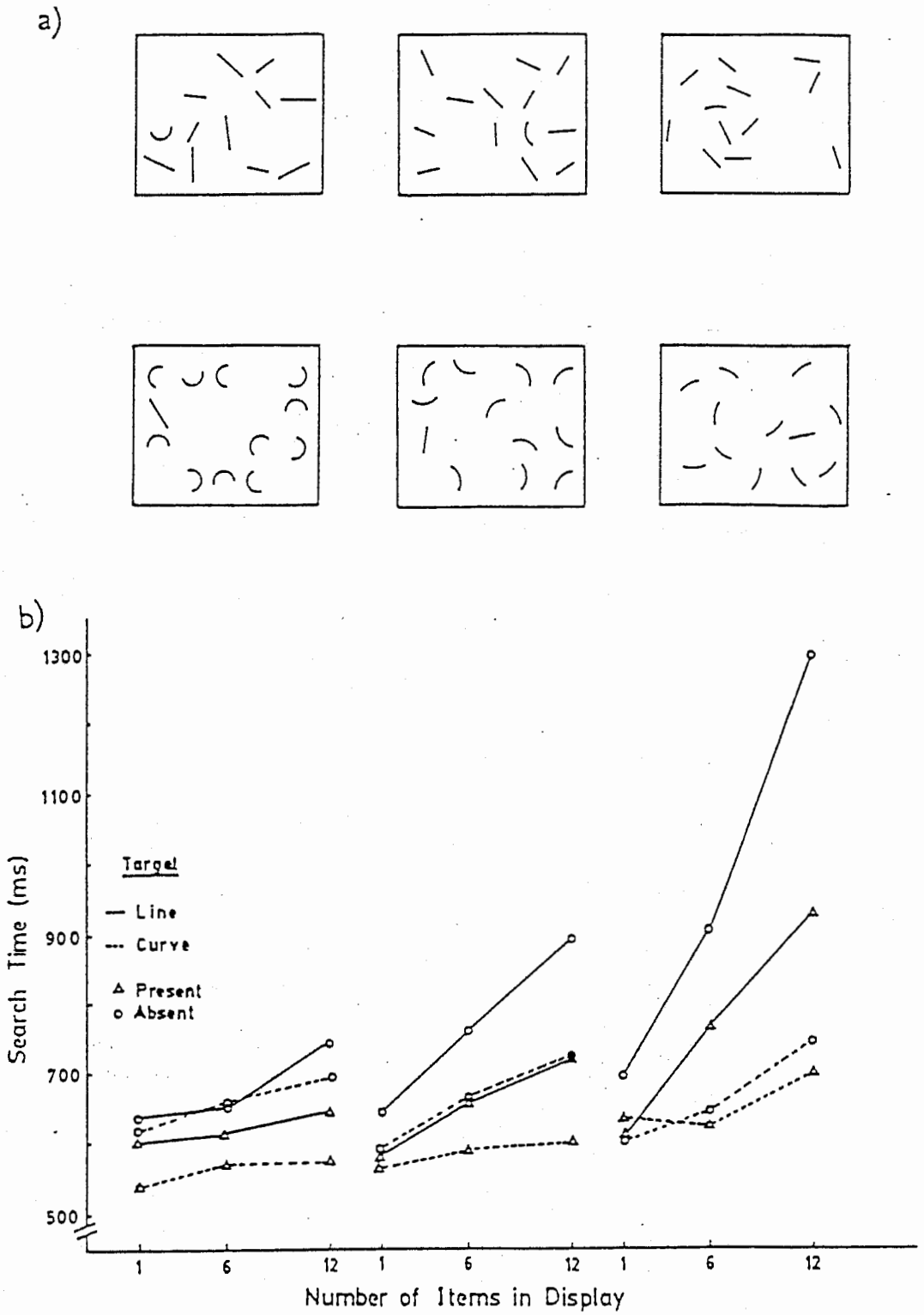

Figure 5. (a) Examples of displays testing search for targets defined by curvature or straightness and (b) search latencies in Experiment 4—curvature.

Fig. 105

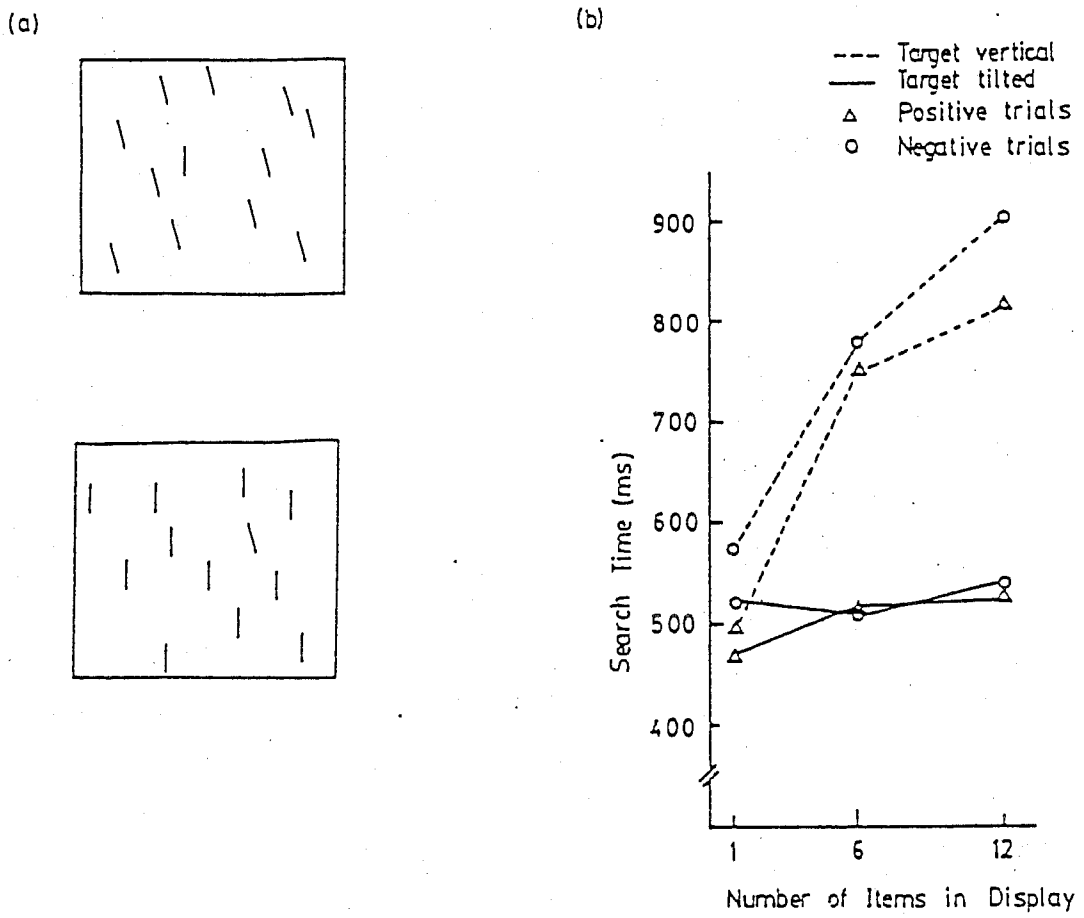

Figure 6. (a) Examples of displays testing search for targets defined by line orientation and (b) search latencies in Experiment 5—orientation.

Fig. 106

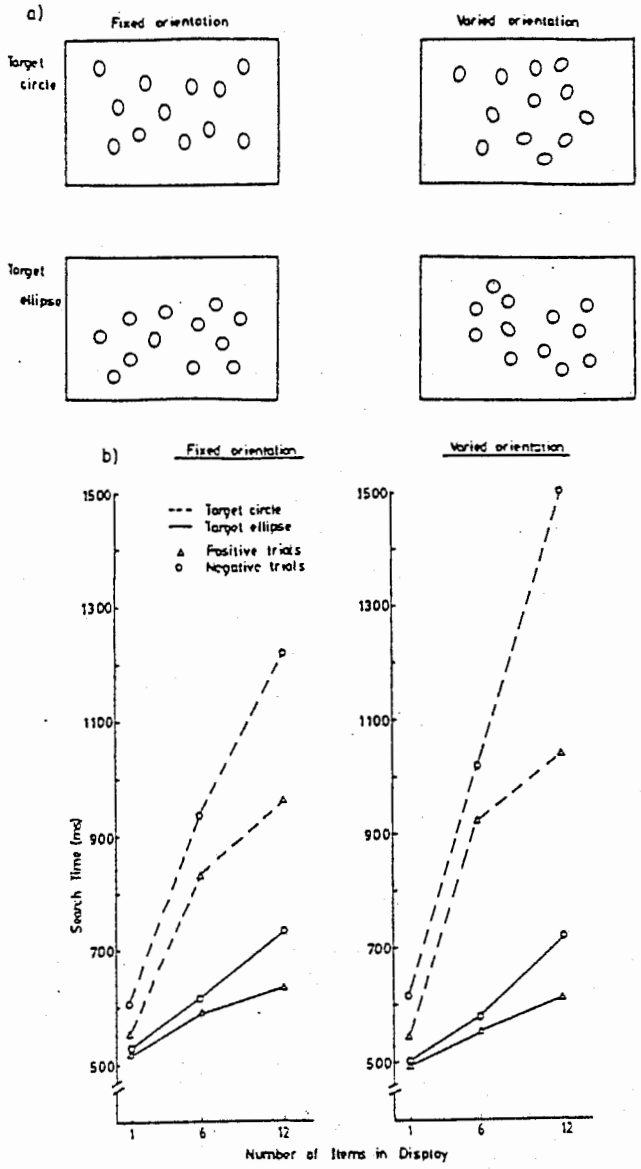

Figure 7. (a) Examples of displays testing search for circles and ellipses and (b) search latencies in Experiment 7—circles and ellipses.

Fig. 107

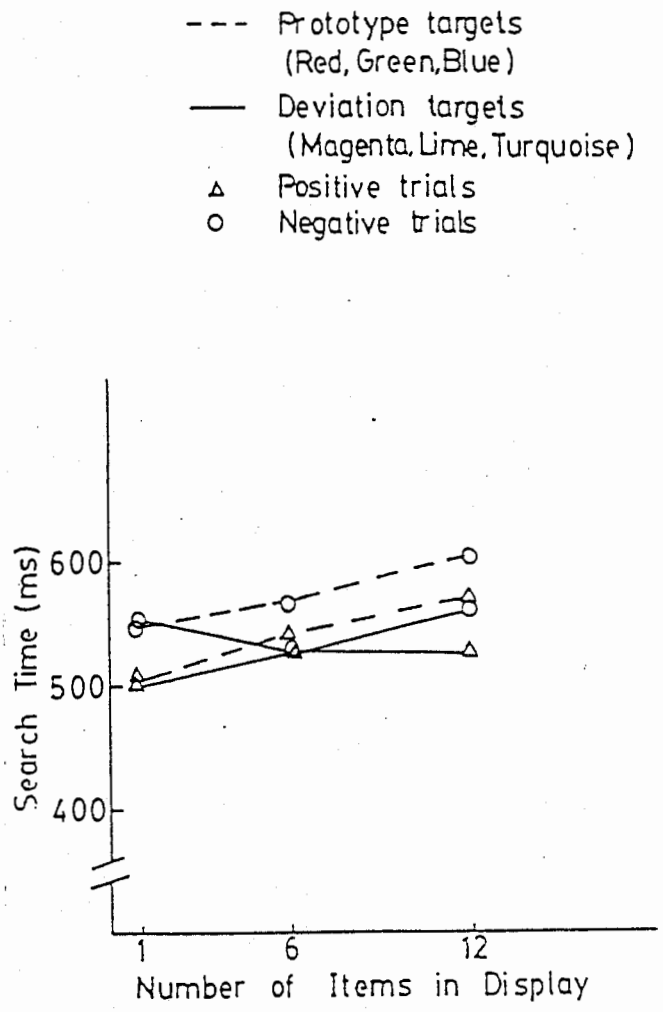

Figure 8. Search latencies in Experiment 6—color.

Fig. 108

a)

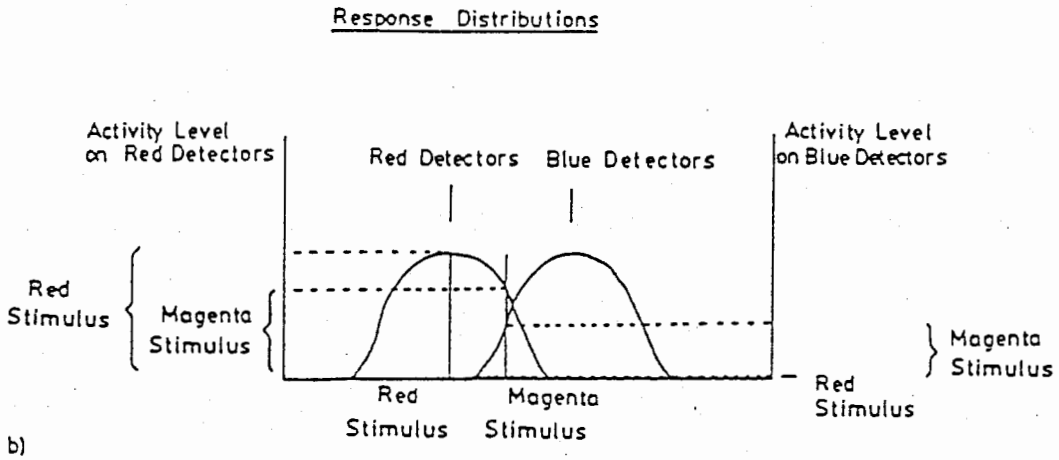

b)

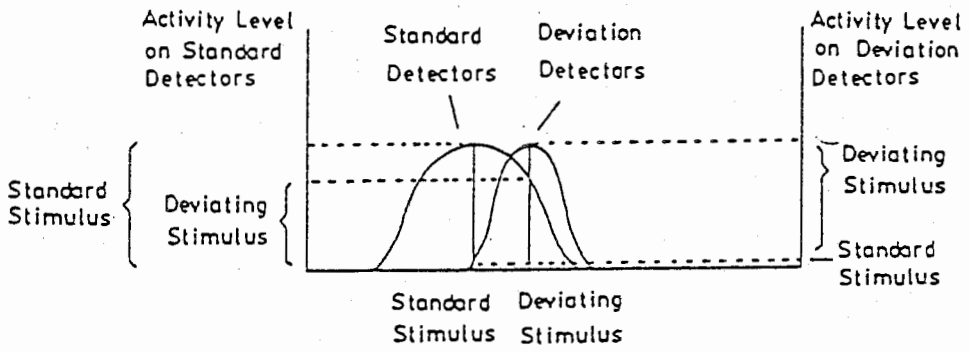

c)

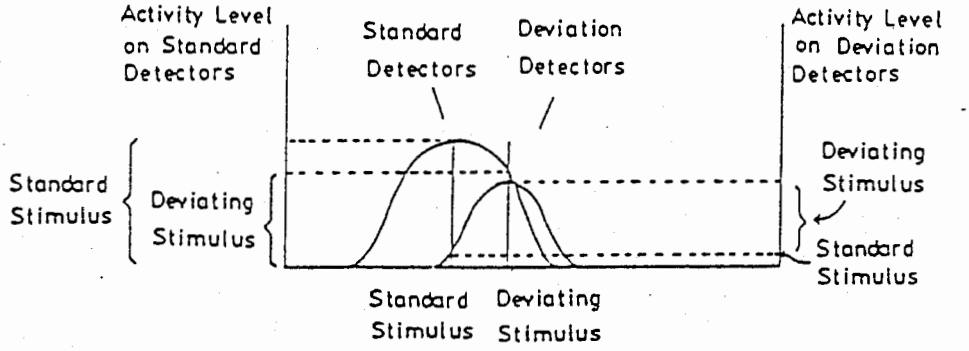

Figure 9. Possible models for distributions of feature activity in detectors for standard and for deviating values: (a) widely spaced broadly tuned channels, (b) closely spaced detectors with broader tuning for standard than for deviating values, and (c) closely spaced detectors with asymmetric inhibition.

Fig. 109

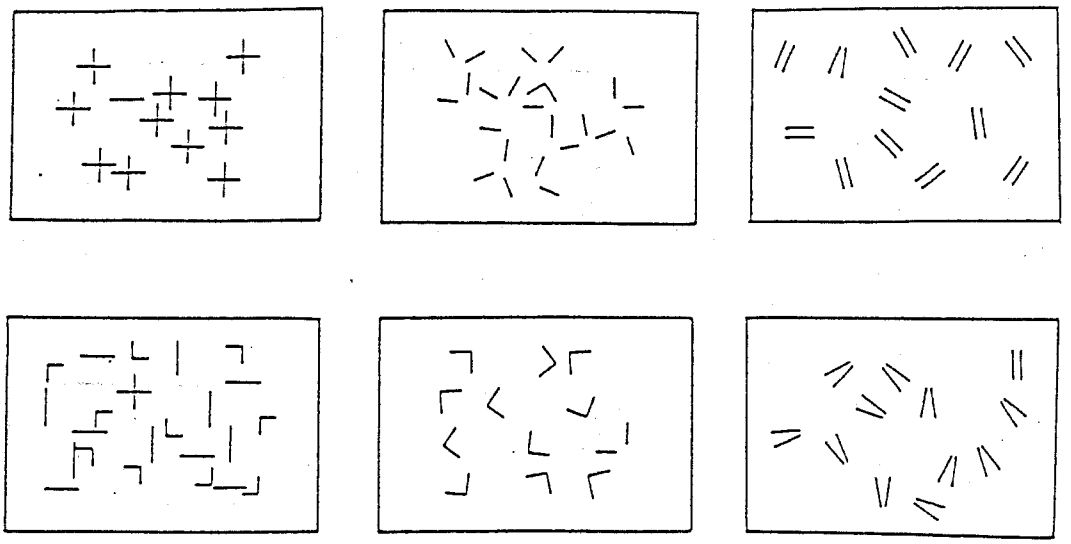

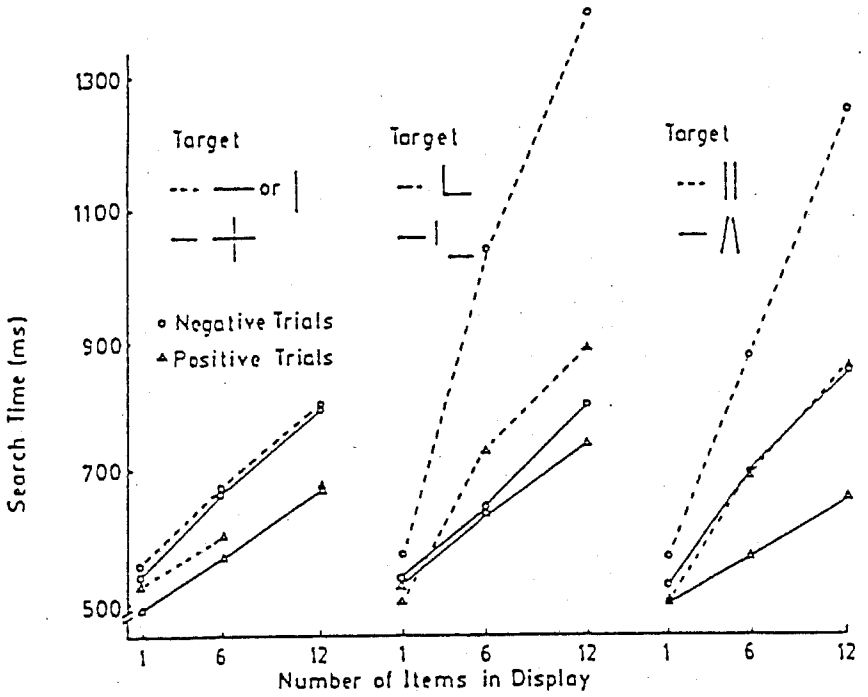

Figure 10. (a) Examples of displays testing search for line arrangements and(b) search latencies in Experiments 8, 9, and 10—intersection, juncture, and convergence.

Fig. 110

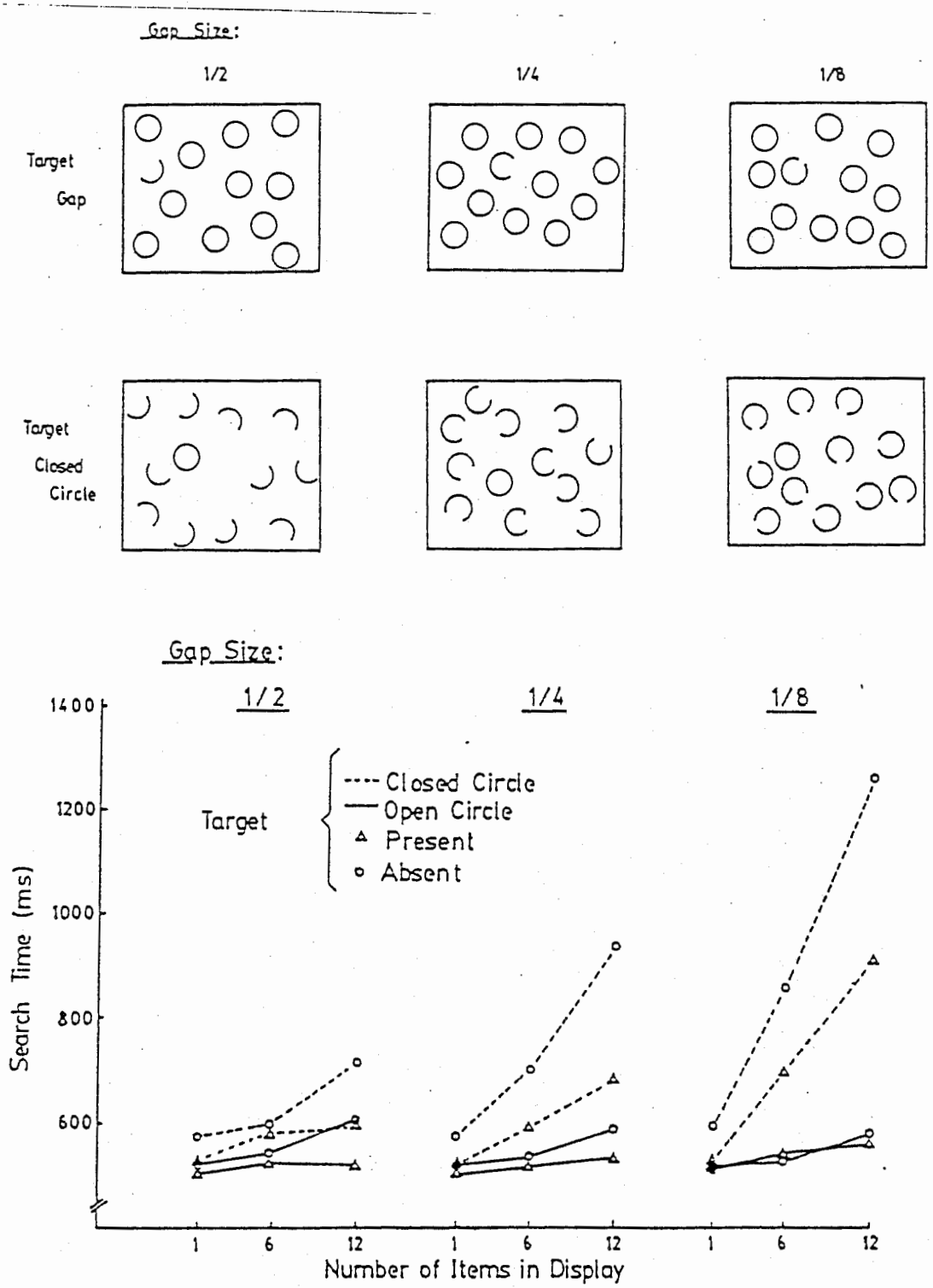

Figure 11. (a) Examples of displays testing search for closed circle or circle with gap and (b) search latencies in Experiment 2—connectedness and terminators.

Fig. 11

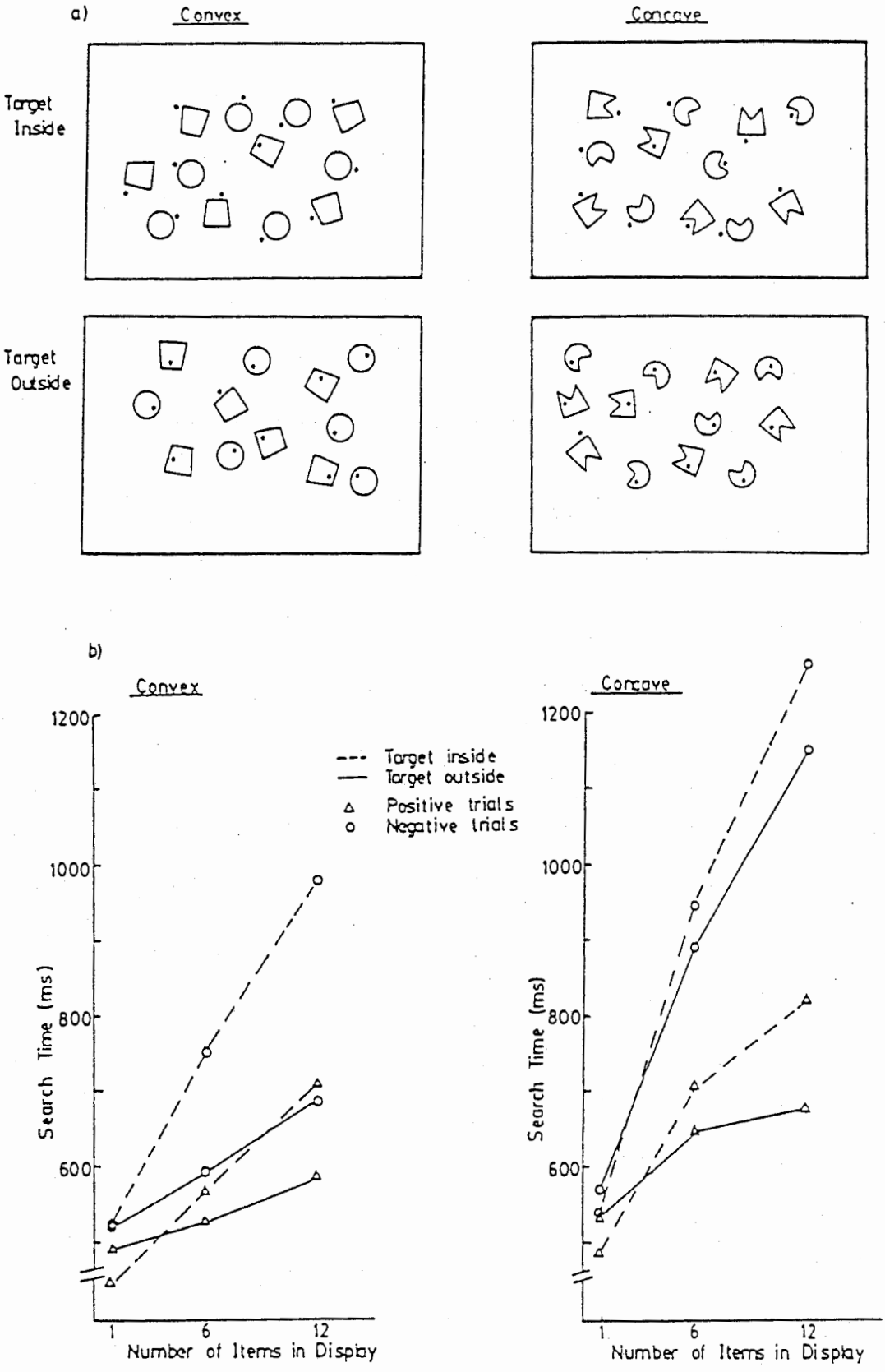

Figure 12. (a) Examples of displays testing search for inside or outside dots and (b) search latencies in Experiment 12—containment.

Fig. 112

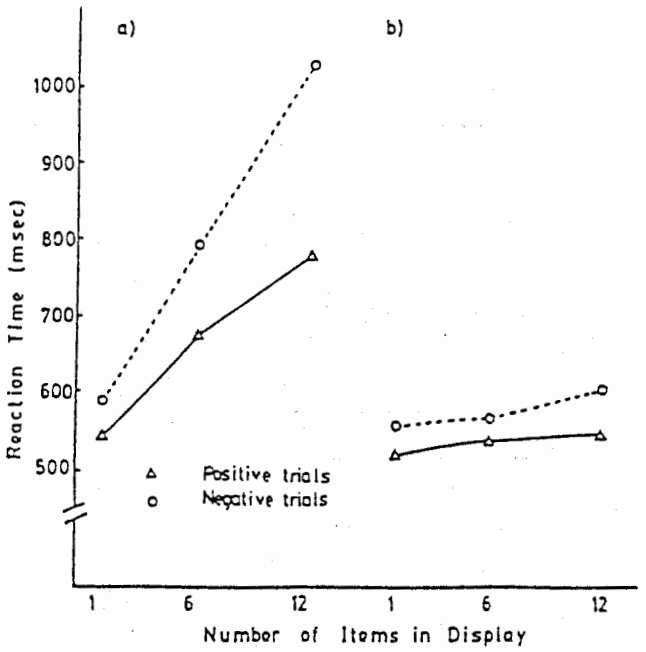

Figure 13. (a) Mean search latencies in 37 conditions giving slopes above 10 ms per item. (b) Mean search latencies in 17 conditions giving slopes of less than 10 ms per item.

Fig. 113

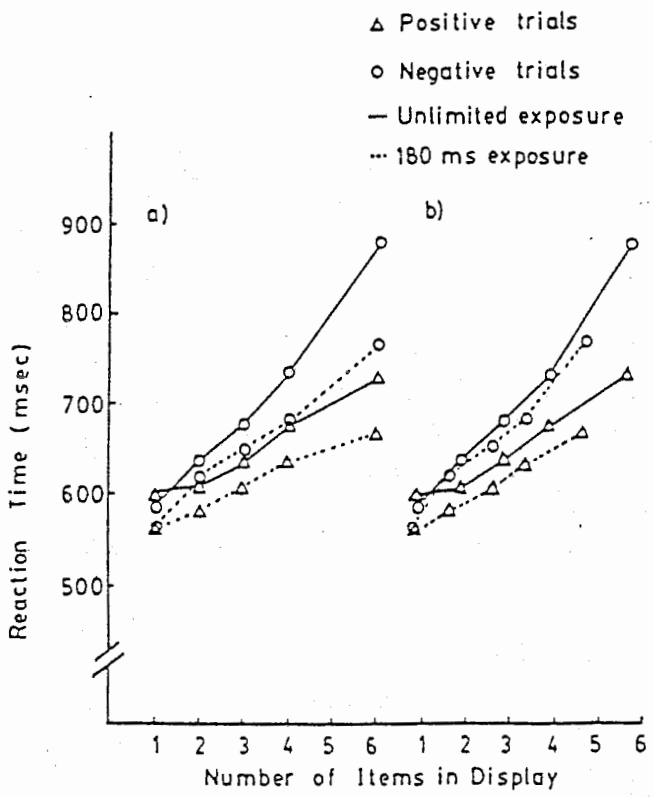

Figure 14. (a) Mean search latencies for line length targets in experiments with brief exposures and with response-terminated exposures and (b) same latencies as a function of corrected display sizes.

Fig. 114